

# THE ROLE OF *Repin1* IN ADIPOSE TISSUE

Die Rolle von *Repin1* im Fettgewebe

Der Fakultät für Biowissenschaften, Pharmazie und Psychologie  
der Universität Leipzig  
eingereichte

DISSERTATION

zur Erlangung des akademischen Grades  
Doctor rerum naturalium  
Dr. rer. nat.

vorgelegt von  
M. Sc. Nico Hesselbarth

geboren am 29. November 1984 in Leipzig

LEIPZIG, DEN 23.05.2017

---

## BIBLIOGRAPHY

Nico Hesselbarth

The Role of *Repin1* in Adipose Tissue

University of Leipzig, Faculty of Biology, Pharmacy and Psychology

Dissertation

Pages: 192, References: 276, Tables: 10, Figures: 17

---

Since 1980 worldwide obesity has doubled in incidence to 52 % of people being overweight or obese. Obesity causes various comorbidities such as cardiovascular diseases, type II diabetes, dyslipidemia and several cancer types, making it one of the biggest challenges in worldwide health care systems. It is well known that obesity is highly heritable by either monogenetic causes or multifactorial interactions of different genes that superimpose on environmental factors and behavior. To answer questions in understanding mechanisms of obesity and/or associated metabolic pathways, mouse models have been a powerful tool. Several approaches in characterizing genes involved in obesity development through mouse engineering have been implemented, with the Cre/*loxP* system emerging as one of the most informative and widespread techniques. Using this approach, promoter-dependent temporal and tissue-specific regulated recombination can be achieved by Tamoxifen administration. To investigate effects of Tamoxifen on adipocyte biology *in vivo*, we characterized 12 weeks old male C57BL/6NTac mice after Tamoxifen treatment. We found that Tamoxifen treatment caused transient body composition changes, increased HbA<sub>1c</sub>, triglyceride and free fatty acid serum concentrations as well as smaller adipocytes in combination with browning of subcutaneous adipose tissue. Therefore, we suggest considering these effects when using Tamoxifen as a tool to induce conditional transgenic mouse models and to treat control mice in parallel. Another methodology used to identify genes involved in obesity related traits is QTL mapping in combination with congenic and subcongenic strains of mice or rats. One candidate gene that was previously identified on rat chromosome 4 is replication initia-

tor 1 (*Repin1*). This gene was first described as a 60 kDa zinc finger protein involved in replication activation of the Chinese hamster dihydrofolate reductase (*dhfr*) gene. Moreover, a triplet repeat (TTT) in the 3'UTR is associated with facets of the metabolic syndrome, including body weight, serum insulin, cholesterol and triglyceride levels. *In vitro* studies in 3T3-L1 cells revealed that Repin1 regulates adipocyte size, glucose transport and lipid metabolism. In this thesis functional analyses of Repin1 were performed using different Repin1 deficient mouse models. In the first study we generated a whole body Repin1 deficient *db/db* double knockout mouse ( $\text{Rep1}^{-/-}$ -x *db/db*) and systematically characterized the consequences of Repin1 deficiency. Our study provided evidence that loss of Repin1 in *db/db* mice improves insulin sensitivity and reduces chronic hyperglycemia most likely by reducing fat mass and adipose tissue inflammation. We next generated a liver-specific Repin1 knockout mouse ( $\text{LRep1}^{-/-}$ ) and could show that loss of Repin1 in liver leads to reduced body weight gain in combination with lower fat mass. Liver specific Repin1 deficient mice also show lower triglyceride content in the liver, improved insulin sensitivity and altered gene expression of genes involved in lipid and glucose metabolism. Finally, we inactivated the *Repin1* gene in adipose tissue ( $\text{iAREp}^{-/-}$ ) at an age of four weeks using Tamoxifen-inducible gene targeting strategies on a background of C57BL/6NTac mice. Mice lacking Repin1 in adipose tissue showed reduced body weight gain, decreased fat mass with smaller adipocytes, improved insulin sensitivity, lower LDL-, HDL- and total cholesterol serum concentrations and reduced expression of genes involved in lipid metabolism (*Cd36* and *Lcn2*). In conclusion, the thesis presented here provides novel insights into Repin1 function. Moreover, the data clearly indicate that Repin1 plays a role in insulin sensitivity and lipid metabolism by regulating key genes involved in those pathways.

## List of Abbreviations

18Sr	18S ribosomal RNA
3T3-L1	fibroblast-like cell line derived from mouse
ACC	acetyl-CoA carboxylase
Adipoq-Cre	adiponectin promoted Cre recombinase mouse
Akt	protein kinase B
AlbCre	Cre recombinase under control of albumin promoter
ALT	alanine transaminase
ANOVA	analysis of variance
aP2	adipocyte protein 2
Ap3m2	adaptor-related protein complex 3, mu 2 subunit
AST	aspartate aminotransferase
AT	adipose tissue
Atgl	adipose triglyceride lipase
BAT	brown adipose tissue
BB/OK	BioBreeding/OttawaKarlsburg
BMI	body mass index
bp	base pair
C57BL/6NTac	inbred mouse strain from taconic laboratories
Cd36	platelet glycoprotein 4
CLS	crown like structure
CMV	human cytomegalovirus
CO <sub>2</sub>	carbon dioxide
Cre	Cre recombinase
CreER(T) <sup>2</sup>	CreER tamoxifen induced system
Ctp1	citrate transport protein 1
Ctp2	citrate transport protein 2
D20%	exogenous glucose
db/db	leptin-receptor-deficient obese mouse
dhfr	dihydrofolate reductase gene
DNA	deoxyribonucleic acid
ELISA	enzyme-linked immunosorbent assay

---

epi	epigonadal
epiAT	epigonadal adipose tissue
ER	estrogen receptor
ER $\alpha$	estrogen receptor alpha
Esr1	estrogen receptor alpha gene
Esr2	estrogen receptor beta gene
Esr $\alpha$	estrogen receptor alpha
Esr $\beta$	estrogen receptor beta
F4/80	marker of murine macrophage populations
Fabp4	fatty acid binding protein 4
fa/fa	Zucker obese rat
Fasn	fatty Acid Synthase
Fatp 1	fatty acid transport protein 1
Fatp 2	fatty acid transport protein 2
Fatp 4	fatty acid transport protein 4
FFA	free fatty acid
FIRKO	fat specific insulin receptor deficient mouse
Frt	flippase recognition target
FTO	fat mass and obesity-associated gene/protein
GAPDH	glyceraldehyde 3-phosphate dehydrogenase
GIR	glucose infusion rate
GLDH	glutamate dehydrogenase
Glut2	glucose transporter 2
GTT	glucose tolerance test
GWAS	genome wide association study
HbA <sub>1c</sub>	glycated hemoglobin A1C
HDL	high-density lipoprotein
HE	hematoxylin and eosin stain
HFD	high fat diet
iARep <sup>-/-</sup>	inducible adipose tissue specific Repin1 deficient mouse
Hsl	hormonsensitive lipase
Ifn- $\gamma$	interferon gamma
IRS-1	insulin receptor substrate 1

---

ITT	insulin tolerance test
Ki67	proliferation gene/protein
L19	ribosomal protein L19
LBD	ligand binding domain
Lcn2	lipocalin 2
LDL	low-density lipoprotein
LEP	leptin
LEPR	leptin-receptor
LIRKO	Liver-specific insulin receptor knockout mouse
loxP	Cre recombinase recognition sites
Lpl	lipoprotein lipase
LRep1 <sup>-/-</sup>	liver specific Repin1 deficient mouse
MC4R	melanocortin-4 receptor
Mcp1	monocyte chemotactic protein
MPI CBG	Max Planck Institute of Molecular Cell Biology and Genetics
mRNA	messenger ribonucleic acid
Mt1	metallothionein 1
Mt2	metallothionein 2
Myf5	myogenic factor 5
NAFLD	non-alcoholic fatty liver disease
NIH	National Institute of Health
NPY	neuropeptide Y
O <sub>2</sub>	oxygen
ob/ob	leptin-deficient obese mouse
pACC	phosphorylated acetyl-CoA carboxylase
pAKT	phosphorylated protein kinase B
PCR	polymerase chain reaction
pIRS-1	phosphorylated insulin receptor substrate 1
POMC	proopimelanocartin
Ppar $\gamma$	peroxisome proliferator-activated receptor gamma
Prdm16	PR domain containing 16
qPCR	real time quantitative PCR

---

QTL	quantitative trait locus
Rarres2	retinoic acid receptor responder protein 2
Rep1 <sup>-/-</sup> x <i>db/db</i>	Repin1-deficient double knockout mouse
Repin1	replication initiator 1
RIP60	replication initiator 1
RNA	ribonucleic acid
rRNA	ribosomal ribonucleic acid
RT-PCR	reverse transcription polymerase chain reaction
sc	subcutaneous
scAT	subcutaneous adipose tissue
Scd1	stearoyl-CoA desaturase 1
Scd2	stearoyl-CoA desaturase 2
SEM	standard error of the mean
SERM	selective estrogen receptor modulator
SHR	Spontaneous Hypertensive Rat
siRNA	small interfering ribonucleic acid
SMA-1	growth hormone receptor
Snap23	synaptosomal-associated protein 23
SNP	single nucleotide polymorphism
SVF	stroma-vascular fraction
TAG	triacylglyceride
Tam	tamoxifen
Tnf $\alpha$	tumor necrosis factor alpha
TG	triglyceride
UCP1	uncoupling protein 1
Vamp4	vesicle-associated membrane protein 4
visAT	visceral adipose tissue
VLDL	very low density lipoprotein
WAT	white adipose tissue
WHO	World Health Organisation
WOKW	Wistar Ottawa Karlsburg RT1 <sup>u</sup> rats
WT	wildtype

# Contents

Bibliography . . . . .	i
List of Abbreviations . . . . .	iii
Summary . . . . .	xiii
Zusammenfassung . . . . .	xviii

## 1 Chapter 1

<i>Introduction</i> . . . . .	1
1.1 Obesity . . . . .	2
1.2 Adipose Tissue . . . . .	3
1.3 Genetics of Obesity . . . . .	4
1.4 Animal Models in Obesity . . . . .	7
1.4.1 Cre loxP System . . . . .	8
1.4.2 Tamoxifen . . . . .	10
1.4.3 Estrogen pathway . . . . .	10
1.5 Identification of target genes protecting against obesity using QTL mapping . . . . .	11
1.6 Repin1 . . . . .	13
1.6.1 Zinc finger proteins . . . . .	14
1.6.2 Lipid metabolism and insulin action on adipose tissue .	15
1.7 Aims and Hypothesis . . . . .	18
1.8 References . . . . .	19

## 2 Chapter 2



<i>Tamoxifen affects glucose and lipid metabolism parameters, causes browning of subcutaneous adipose tissue and transient body composition changes in C57BL/6NTac mice</i>	41
2.1 Abstract . . . . .	43
2.2 Introduction . . . . .	43
2.3 Material and methods . . . . .	44
2.3.1 Animals . . . . .	44
2.3.2 Phenotypic characterization . . . . .	44
2.3.3 Analytical procedures . . . . .	45
2.3.4 Adipocyte size and AT histology . . . . .	45
2.3.5 mRNA expression . . . . .	46
2.3.6 Western blot analyses . . . . .	46
2.3.7 Statistical analyses . . . . .	46
2.4 Results . . . . .	46
2.4.1 Tamoxifen administration transiently affects body composition . . . . .	46
2.4.2 Tamoxifen administration induces browning and adipocyte proliferation in subcutaneous AT . . . . .	47
2.4.3 Tamoxifen administration induces changes in glucose and lipid metabolism . . . . .	48
2.5 Discussion . . . . .	53
2.6 Contribution statement . . . . .	54
2.7 Duality of interest . . . . .	54
2.8 Acknowledgments . . . . .	54
2.9 Transparency document . . . . .	55
2.10 References . . . . .	55

### 3 Chapter 3

<i>Repin1 deficiency improves insulin sensitivity and glucose metabolism in db/db mice by reducing adipose tissue mass and inflammation</i>	58
3.1 Abstract . . . . .	60
3.2 Introduction . . . . .	60

3.3	Material and methods . . . . .	61
3.3.1	Animals . . . . .	61
3.3.2	Generation of whole body Repin1 (Rep1 <sup>-/-</sup> ) deficiency in <i>db/db</i> knockout mice . . . . .	61
3.3.3	Phenotypic characterization . . . . .	62
3.3.4	Hyperinsulinemic-euglycemic clamp studies . . . . .	62
3.3.5	Histology and immunohistochemistry . . . . .	62
3.3.6	Statistical analysis . . . . .	63
3.4	Results . . . . .	63
3.4.1	Generation of whole body deletion of Repin1 in <i>db/db</i> mice (Rep1 <sup>-/-</sup> × <i>db/db</i> ) . . . . .	63
3.4.2	Growth, fat mass and tissue mass of double knockouts (Rep1 <sup>-/-</sup> × <i>db/db</i> ) . . . . .	64
3.4.3	Repin1 deficiency improves insulin sensitivity . . . . .	64
3.4.4	Repin1 deficiency causes reduced inflammatory infil- trates in AT . . . . .	64
3.5	Discussion . . . . .	67
3.6	Funding . . . . .	67
3.7	Conflict of interest . . . . .	67
3.8	Contribution statement . . . . .	67
3.9	Duality of interest . . . . .	68
3.10	Acknowledgements . . . . .	68
3.11	Transparency document . . . . .	68
3.12	References . . . . .	68

## 4 Chapter 4

*Liver-Restricted Repin1 Deficiency Improves Whole-Body Insulin Sensitivity, Alters Lipid Metabolism, and Causes Secondary Changes in Adipose Tissue in Mice* **71**

4.1	Abstract . . . . .	73
4.2	Introduction . . . . .	73
4.3	Research Design and Methods . . . . .	74

---

4.3.1	Animal Studies . . . . .	74
4.3.2	Generation of LRep1 <sup>-/-</sup> Mice . . . . .	75
4.3.3	Vector Construction ET (SIS17) . . . . .	75
4.3.4	Molecular Characterization and Genotyping of LRep1 <sup>AlbCre</sup> Mice . . . . .	76
4.3.5	Phenotypic Characterization . . . . .	76
4.3.6	Analytical Procedures . . . . .	77
4.3.7	Hyperinsulinemic-Euglycemic Clamp Studies . . . . .	78
4.3.8	Liver Lipidomics . . . . .	78
4.3.9	RNA Isolation and Quantitative Real-Time PCR Anal- ysis . . . . .	78
4.3.10	<i>In Vivo</i> Lipogenesis in Liver, <i>In Vivo</i> VLDL TG Pro- duction, and Fat Load Test . . . . .	79
4.3.11	<i>Ex Vivo</i> Glucose Transport, <i>Ex Vivo</i> Lipolysis, and Palmitate Uptake Into Adipocytes . . . . .	79
4.3.12	Western Blot Analysis . . . . .	79
4.3.13	Insulin Signaling . . . . .	80
4.3.14	Liver Affymetrix GeneChip Analysis . . . . .	80
4.3.15	Histology and Immunohistochemistry . . . . .	80
4.3.16	Statistical Analysis . . . . .	80
4.4	Results . . . . .	81
4.4.1	Generation of LRep1 <sup>-/-</sup> Mice . . . . .	81
4.4.2	Growth, Tissue Mass, and Energy Expenditure of LRep1 <sup>-/-</sup> Mice . . . . .	81
4.4.3	Repin1 Deficiency in Liver Improves Insulin Sensitivity	82
4.4.4	Repin1 Affects Insulin Signaling in the Liver . . . . .	83
4.4.5	Liver-Specific Repin1 Deficiency Leads to Dyslipidemia, Altered Liver Lipid Transport/Storage, and Liver Lipidomic Profile . . . . .	83
4.4.6	LRep1 <sup>-/-</sup> Mice Are Protected Against Development of HFD-Induced Adipocyte Hypertrophy . . . . .	84
4.4.7	Target Genes of Repin1 . . . . .	85

---

4.4.8	Altered Expression of Genes Involved in Accumulation of Cytosolic Lipids and Lipid Droplet Fusion in Liver . . .	86
4.4.9	Model for the Role of Repin1 in Insulin Sensitivity . . .	86
4.5	Discussion . . . . .	98
4.6	Acknowledgments . . . . .	103
4.7	Funding . . . . .	103
4.8	Duality of Interest . . . . .	104
4.9	Author Contributions . . . . .	104
4.10	References . . . . .	106
4.11	Supplementary Data . . . . .	106

## 5 Chapter 5

<i>Repin1</i> Deficiency in Adipose Tissue Improves Whole-body Insulin Sensitivity, and Lipid Metabolism	120
5.1 Abstract . . . . .	122
5.2 Introduction . . . . .	122
5.3 Materials and Methods . . . . .	124
5.3.1 Animal Care and Research diets . . . . .	124
5.3.2 Generation and Genotyping of iARep <sup>-/-</sup> Mice . . . . .	124
5.3.3 Phenotypic Characterization . . . . .	125
5.3.4 Analytical Procedures . . . . .	126
5.3.5 Adipocyte Isolation and Size Distribution . . . . .	126
5.3.6 RNA Isolation and Quantitative Real-Time PCR Analysis . . . . .	127
5.3.7 Western Blot Analysis . . . . .	127
5.3.8 Cell culture . . . . .	127
5.3.9 Statistical Analysis . . . . .	127
5.4 Results . . . . .	128
5.4.1 Generation of iARep <sup>-/-</sup> Mice . . . . .	128
5.4.2 Growth, Organ weights, Food Intake and Energy Expenditure of iARep <sup>-/-</sup> mice . . . . .	128
5.4.3 Repin1 deficiency in AT improves insulin sensitivity . . . . .	129

---

5.4.4	Deficiency of Repin1 in AT or knockdown in human <i>in vitro</i> differentiated adipocytes leads to altered Lipid Metabolism . . . . .	129
5.4.5	Target Genes of Repin1 . . . . .	130
5.5	Discussion . . . . .	138
5.6	Acknowledgements . . . . .	141
5.7	References . . . . .	142

**Appendix** **xxiv**

Curriculum vitae . . . . .	xxv
Selbstständigkeitserklärung . . . . .	xxix
Author contributions Chapter 2 . . . . .	xxx
Author contributions Chapter 3 . . . . .	xxxiii
Author contributions Chapter 4 . . . . .	xxxvi
Author contributions Chapter 5 . . . . .	xlii
Acknowledgement . . . . .	xlvi

## Summary

During recent decades obesity has developed into one of the world's greatest health public challenges, contributing to the development of secondary metabolic conditions such as cardiovascular diseases, type II diabetes mellitus, dyslipidemia and several types of cancer. Obesity is characterized as an excess of adipose tissue and arises from the combination of increased food intake and a lack of physical activity. Multiple factors can contribute and influence obesity development on an individual level, such as genetic background, environment, behavior and/or lifestyle. Twin, adoption and family studies have established that obesity is highly heritable. There are two genetic forms of obesity: monogenic and polygenic. Monogenic obesity in humans is very rare and has been characterized for only ten genes so far (e.g. leptin). In general, obesity is a result of the interaction of several genes acting on a specific obesogenic background. To understand factors that contribute to obesity, animal models have been a powerful tool. Mice have become the most popular model to address questions in understanding obesity mechanisms, due to several advantages such as their small body size, low cost, ease of maintenance and straightforwardness to breed in captivity. Also, a short gestation period of about 19 to 20 days contributed to their establishment as the animal model of choice. Early discoveries made in obesity research on animal models derived from spontaneous mutations such as those found in the *ob/ob* and *db/db* mice which possess a mutation in leptin or the leptin receptor gene, respectively. Mutagenic chemicals and or exposure of animals to radiation sped up the arbitrary nature of spontaneous mutational events. To overcome randomness of those created mutations, methodologies to create transgenic mice have been successively implemented. A widespread technique, not only in obesity research, is the *Cre/loxP* system with its ability to knockout genes either in a specific tissue and/or a time-specific manner. The system is based on recombination events after breeding a Cre recombinase mouse strain with another mouse strain expressing a target gene, flanked with Cre recombinase recognition (*loxP*) sites. Temporal control of the recombination event is afforded by Tamoxifen administration to mice, due to binding of Tamoxifen

to a specific estrogen receptor linked to a Cre recombinase. When identifying potential target genes involved in obesity mechanisms, quantitative trait locus (QTL) mapping is a preferred approach to determine areas in the genome which affect phenotype. QTLs are produced by breeding two different strains of a certain animal model, which differ in the trait of interest. Since, QTLs contain hundreds of possible target genes, parts of a certain genomic region will then be placed on the genome of a recipient strain to create congenic and subcongenic strains. This approach narrows down the number of potential target genes. One potential target gene, called replication initiator 1 (Repin1), has been identified using QTL technology followed by the production of congenic and subcongenic rat strains. Subcongenic rat strains BB.4S and BB.4W, where a segment on chromosome 4 from either SHR (Spontaneous Hypertensive Rat) or WOKW (Wistar Ottawa Karlsburg RT1<sup>u</sup>) rats was crossed on a BB/OK (BioBreeding/OttawaKarlsburg) background, developed obesity and dyslipidemia compared with their parental controls. Initially, Repin1 was discovered as a replication initiation region protein with a mass of 60 kDa involved in replication activation of the Chinese hamster dihydrofolate reductase (*dhfr*) gene. Later on it was identified as a polydactyl zinc finger protein of a Cys<sub>2</sub>-His<sub>2</sub> type. Preliminary studies could show an influence of a triplet repeat (TTT) size in the 3'UTR of the *Repin1* gene on body weight, serum triglyceride and cholesterol levels. Subsequent studies in Repin1 downregulated 3T3-L1 cells revealed influences on cell size, lipid and glucose transport compared to controls. These data indicate an important role for Repin1 in the regulation of adipose tissue function, glucose and lipid metabolism.

Therefore, the aims and hypothesis of the thesis presented here were to characterize the functional role of Repin1, specifically in adipose tissue. Based on preliminary findings, I hypothesized an influence of Repin1 depletion in liver and adipose tissue on body weight, lipid and glucose metabolism using specific knockout mice, as well as in double knockout animals of Repin1 and the leptin receptor. Previous studies could show an influence of estrogen levels on obesity related traits. Therefore, I additionally hypothesized an influence of Tamoxifen itself, as a selective estrogen receptor modula-

tor, on adipocyte biology in terms of energy expenditure, lipid and glucose metabolism.

In the first publication [**Chapter 2**], we tested the hypothesis that Tamoxifen administration causes changes in adipose tissue biology *in vivo*. Therefore, 1mg Tamoxifen (solved in 50  $\mu$ l Miglyol) was administered for 5 consecutive days to 12 weeks old male C57BL/6NTac mice, whereas control mice were treated with vehicle substance (50  $\mu$ l Miglyol). Both groups were characterized in terms of body composition, energy homeostasis, glucose and lipid metabolism up to an age of 18 weeks. In this study we could show that Tamoxifen treatment leads to an altered body composition of fat and lean mass, while body weight was maintained. More detailed investigations of adipose tissue revealed smaller adipocyte size in subcutaneous depots in Tamoxifen treated animals compared to controls, as a result of there being more beige/brite adipocytes (characterized by higher Ucp1 expression). Also, we were able to show that Tamoxifen treatment leads increased HbA<sub>1c</sub>, triglyceride and free fatty acid serum concentrations. Our data from this study clearly shows influences of Tamoxifen treatment on adipocyte biology *in vivo*, which need to be considered when using Tamoxifen as a tool to induce conditional transgenic mouse models. Also, Tamoxifen treatment and characterization of wildtype mice should always be done to control for tamoxifen administration effects.

In **Chapter 3**, we tested if whole body Repin1 deletion in diabetes prone *db/db* mice improves glucose metabolism. Double knockout mice (Repin1<sup>-/-</sup> x *db/db*) were compared to *db/db* controls and systematically characterized with state of the art methods. Repin1 deficient *db/db* mice gained significantly less body weight compared to controls, which was based on lower fat mass. Insulin sensitivity was improved in Repin1<sup>-/-</sup> x *db/db* mice, reflected by lower glucose infusion rate in clamp studies and HbA<sub>1c</sub> values. Further investigations on adipose tissue revealed a reduced adipose tissue inflammation area. Our study provides evidence that loss of Repin1 in *db/db* mice mitigates the pathogenesis of adipose tissue inflammation, insulin resistance and subsequent impairment of glucose homeostasis.

To elucidate the role of Repin1 in lipid metabolism *in vivo* [**Chapter 4**],



we generated a liver-specific Repin1 knockout mouse (LRep1<sup>-/-</sup>) and systematically characterized the consequences of Repin1 deficiency in the liver on body weight, glucose and lipid metabolism, liver lipid patterns, and protein/mRNA expression. Mice with hepatic deletion of Repin1 displayed significantly less body weight gain starting at week 28. These differences were based on lower fat mass and may have contributed to lower hepatic triglyceride content and improved whole body insulin sensitivity in LRep1<sup>-/-</sup> mice. Also, we could show altered gene/protein expression of genes/proteins involved in lipid and glucose metabolism, such as Cd36, Pparg, Glut2, Akt phosphorylation, lipocalin2, *Vamp4*, and *Snap23*. Our findings indicate that Repin1 plays a role in insulin sensitivity and lipid metabolism by regulating key genes of glucose and lipid metabolism.

Encouraged by the findings summarized above, in **Chapter 5** we inactivated the Repin1 gene in adipose tissue (iARep<sup>-/-</sup>) at an age of four weeks using Tamoxifen-inducible gene targeting strategies on the background of C57BL/6NTac mice. Adipose tissue specific Repin1 knockout led to a leaner phenotype with lower fat mass in both subcutaneous and epigonadal adipose tissue. Both fat depots were characterized by similar cell numbers, but smaller adipocytes. Interestingly, serum lipid parameters such as LDL-, HDL- and total cholesterol were significantly decreased in adipose tissue deficient mice compared to controls. Conditional Repin1 inactivation resulted in improved insulin sensitivity and glucose tolerance. Expression of potential Repin1 target genes *Cd36* and *Lcn2* was significantly reduced in mice lacking Repin1 in adipose tissue compared to control mice. Furthermore, we measured glycerol release in differentiated human primary adipocytes derived from subcutaneous adipose tissue *in vitro* and could show increased glycerol release in cells with *REPIN1* knockdown compared to control cells. In conclusion, we could show that deficiency of Repin1 in adipose tissue causes alterations in adipose tissue morphology and function, which may underlay lower body weight and improved parameters of insulin sensitivity, glucose and lipid metabolism.

In summary, the work presented here significant extends knowledge of the functional role of Repin1 in liver and adipose tissue. According to pre-

---

liminary *in vitro* studies of Repin1 in 3T3-L1 cell lines, the results presented in this thesis support the hypothesis that Repin1 is involved in lipid and glucose metabolism. In all the studies presented here, Repin1 deficiency was associated with reduced body weight gain, driven predominantly by lower fat mass. Also, all three presented models showed improved insulin sensitivity compared to their control groups. Potential target genes of Repin1 showed altered expression levels, in particular the long chain fatty acid transporter *Cd36*. Additionally, this thesis provides a better understanding of the temporal Cre/*loxP* knockout system using Tamoxifen as a trigger substance. In line with previous studies showing an effect of endogenous estrogen signaling, Tamoxifen acting as a selective estrogen receptor modulator influenced adipocyte biology *in vivo*. Therefore, data presented in this thesis suggests controlling for the effects of tamoxifen administration by treating control animals in a similar fashion.

## Zusammenfassung

Innerhalb der letzten Jahre hat sich Adipositas zu eines der größten Probleme im Gesundheitswesen entwickelt, welches zur Entwicklung sekundärer metabolischer Krankheiten, wie kardiovaskuläre Krankheiten, Typ II Diabetes, Dyslipidämie und verschiedene Typen von Krebs, beiträgt. Adipositas, charakterisiert durch einen Überschuss an Fettgewebe, entsteht durch eine Kombination aus erhöhter Nahrungsaufnahme und einem Mangel an physischer Aktivität. Mehrere Faktoren, wie der genetische Hintergrund, Umwelt, Verhalten und/oder Lebensstil, können zur Entwicklung von Adipositas beitragen und diese beeinflussen. Zwillings-, Adoptions- und Familienstudien zeigten eine hohe Vererbbarkeit von Adipositas auf. Adipositas wird in zwei genetische Formen unterteilt, in eine monogenetische und eine polygenetische. Die monogenetische Adipositas ist bei Menschen sehr selten und wurde bisher nur in zehn Genen beschrieben (zum Beispiel Leptin). Generell ist Adipositas das Resultat aus dem Zusammenspiel verschiedener Gene, die auf einen spezifischen zur Adipositas neigenden Hintergrund wirken. Um Adipositas beeinflussende Faktoren zu untersuchen, stellten sich Tiermodelle als ein leistungsfähiges Werkzeug heraus. Dabei haben sich Mäuse zu eines der beliebtesten Modelle, um die Mechanismen der Adipositas zu verstehen, auf Grund ihrer verschiedenen Vorteile, wie ihrer kleinen Körpergröße, der geringen Kosten, ihrer leichten Pflege und der unkomplizierten Zucht in Gefangenschaft, entwickelt. Eine kurze Tragzeit von 19 bis 20 Tagen trug ebenfalls zur Wahl als beliebtes Tiermodell bei. Die frühesten Entdeckungen im Gebiet der Adipositasforschung beruhen auf spontanen Mutationen, welche beispielsweise in *ob/ob* und *db/db* Mäusen gefunden wurden, die eine Mutation im Leptin Gen beziehungsweise im Leptinrezeptor Gen aufweisen. Der Einsatz mutagener Chemikalien oder die radioaktive Bestrahlung von Tieren haben den willkürlichen Prozess spontaner Mutationen beschleunigt. Um die Beliebigkeit der erzeugten Mutationen zu überwinden wurden Methoden zur Entwicklung transgener Mäuse entwickelt. Eine nicht nur in der Adipositasforschung beliebte Methode zur Erzeugung transgener Tiere, ist das *Cre/loxP* System mit der Möglichkeit

Gene nicht nur gewebsspezifisch sondern auch zeitspezifisch auszuschalten. Das System basiert auf der Verpaarung einer Cre-Rekombinase exprimierenden Mauslinie mit einer zweiten Mauslinie deren Zielgen mit einer Cre-Rekombinase Erkennungssequenz (*loxP*) flankiert ist. Die zeitliche Kontrolle der Rekombination erfolgt über eine Tamoxifen Injektion der Mäuse, wobei Tamoxifen spezifisch an einen Cre-Rekombinase gekoppelten Östrogenrezeptor bindet. Um potentielle Gene zu identifizieren, welche an Mechanismen der Adipositas beteiligt sind, ist die Kartierung sogenannter QTLs (Region eines quantitativen Merkmals – *quantitative trait locus*) eine bevorzugte Methode, um Bereiche im Genom zu finden, die einen bestimmten Phänotyp beeinflussen. QTLs werden durch Verpaarung eines bestimmten Tiermodells zweier unterschiedlicher Linien, die sich nur in einem spezifischen Merkmal unterscheiden, erzeugt. Weil QTLs immer noch hunderte verschiedene mögliche Kandidatengene enthalten, werden Teile der genomischen Sequenz auf ein anderes Genom einer Empfängerlinie platziert und kongene und subkongene Linien erzeugt. Mit Hilfe dieses Verfahrens wird die Anzahl möglicher Kandidatengene reduziert. Ein potentielles Kandidatengen namens *replication initiator 1* (*Repin1*) wurde mit Hilfe von QTL Kartierung und anschließender Erzeugung kongener und subkongener Rattenlinien identifiziert. Die subkongenen Rattenlinien BB.4S und BB.4W, bei denen ein Segment des Chromosoms 4 von entweder SHR (Spontaneous Hypertensive Rat) oder WOKW (Wistar Ottawa Karlsburg RT1<sup>u</sup>) auf BB/OK (BioBreeding/OttawaKarlsburg) Ratten gekreuzt wurde, entwickelten eine Adipositas und Dyslipidämie im Vergleich zu ihren elterlichen Kontrollen. Zunächst wurde *Repin1* als Replikationsinitiationsprotein mit einer Masse von 60 kDa, welches in die Aktivierung der Replikation des Dihydrofolatreduktasgens (*dhfr*) im Chinesischen Streifenhamster beteiligt ist, beschrieben. Später wurde es als polydaktyles Cys<sub>2</sub>-His<sub>2</sub> Zinkfingerprotein identifiziert. Vorausgehende Studien konnten einen Einfluss der Triplet-Wiederholung (TTT) Länge im 3'UTR des *Repin1* Gens auf Körpergewicht, Serum-Triglyceride und Cholesterin Level feststellen. Anschließende Studien mit *Repin1* herunterregulierten 3T3-L1 Zellen zeigten im Vergleich zu Kontrollen einen Einfluss auf Zellgröße, Fett- und Glucosestoffwechsel. Diese Daten implizieren

eine wichtige Rolle von Repin1 in der Regulation von Fettgewebefunktionen, Glucose- und Fettstoffwechsel.

Daher sind die Ziele und Hypothesen der hier präsentierten Promotionsarbeit die funktionale Rolle von Repin1 spezifisch im Fettgewebe zu charakterisieren. Auf vorhergehenden Studien basierend stellte ich die Hypothese auf, dass eine Deletion von Repin1 in der Leber und im Fettgewebe das Körpergewicht, den Fett- und Glucosestoffwechsel unter Verwendung spezifischer Knockout-Mäuse, als auch in Doppelknockout-Tieren von Repin1 und dem Leptinrezeptor, beeinflusst. Vorangegangene Studien konnten einen Einfluss des Östrogenspiegels auf Adipositas bezogene Eigenschaften zeigen. Deshalb stellte ich die Hypothese auf, dass Tamoxifen, als selektiven Östrogenrezeptor Modulator, die Adipozytenbiologie in Beziehung auf den Energiehaushalt, Fett- und Glucosestoffwechsel beeinflusst.

In der ersten Publikation [**Kapitel 2**] überprüften wir die Hypothese, ob die Tamoxifengabe Änderungen in der Adipozytenbiologie *in vivo* verursacht. Daher wurde 1 mg Tamoxifen (gelöst in 50  $\mu$ l Miglyol) für 5 aufeinanderfolgende Tage 12 Wochen alten männlichen C57BL/6NTac Mäusen verabreicht, während die Kontrolltiere nur die Trägersubstanz (50  $\mu$ l Miglyol) bekamen. Beide Gruppen wurden in Beziehung auf Energiehaushalt, Glucose- und Fettstoffwechsel bis zu ihrer 18. Lebenswoche charakterisiert. In dieser Studie konnten wir zeigen, dass die Tamoxifenbehandlung zu einer veränderten Körperzusammensetzung von Fett- und Magermasse führt, während das Körpergewicht unverändert blieb. Detailliertere Untersuchungen des Fettgewebes zeigten kleinere Adipozytengrößen in subkutanen Fettdepots in Tamoxifen behandelten Tieren im Vergleich zu Kontrolltieren resultierend aus brauneren Adipozyten (bestimmt durch höhere Ucp1 Expression). Des Weiteren konnten wir zeigen, dass die Tamoxifenbehandlung zu erhöhten HbA<sub>1c</sub>, Triglycerid und freien Fettsäure Konzentrationen im Serum führt. Unsere Daten dieser Studie zeigen eindeutig einen Einfluss einer Tamoxifenbehandlung auf die Adipozytenbiologie *in vivo*, was bei der Verwendung von Tamoxifen als Mittel zur Induktion konditioneller Knockout-Modelle berücksichtigt werden sollte. Des Weiteren sollte Tamoxifenbehandlung und die Charakterisierung wildtypischer Mäuse zur Kontrolle von Effekten auf die

Tamoxifengabe immer erfolgen.

In **Kapitel 3** untersuchten wir, ob eine Ganzkörperdeletion von Repin1 in der diabetesanfälligen ob/ob Maus den Glucosestoffwechsel verbessert. Die Doppelknockout Mäuse (Rep1<sup>-/-</sup> x db/db) wurden mit Hilfe aktueller Methoden charakterisiert und mit db/db Mäusen als Kontrolle verglichen. Repin1 defiziente db/db Mäuse erreichten, basierend auf geringerer Fettmasse, signifikant weniger Körpermasse im Vergleich zu den Kontrollen. Die Insulinsensitivität war in Rep1<sup>-/-</sup> x db/db Mäusen verbessert, was sich in einer geringeren Glucoseinfusionsrate in Clamp Studien und in HbA<sub>1c</sub> Konzentrationen widerspiegelte. Weitere Untersuchungen des Fettgewebes zeigten ein geringes Ausmaß an Fettgewebsinflammation. Unsere Studie liefert den Beweis, dass der Verlust von Repin1 in db/db Mäusen die Pathogenese der Fettgewebsinflammation, Insulinresistenz und nachfolgende Verschlechterung des Glucosehaushaltes lindert.

Um die Rolle von Repin1 im Fettstoffwechsel *in vivo* aufzuklären [**Kapitel 4**], generierten wir leberspezifische Repin1 Knockout-Mäuse (LRep1<sup>-/-</sup>) und charakterisierten systematisch die Konsequenzen des Repin1 Verlustes in der Leber auf das Körpergewicht, Glucose- und Fettstoffwechsel, Leberfettspiegel sowie Protein/mRNA Expression. Mäuse mit einer hepatischen Repin1 Deletion zeigten ab Woche 28 eine signifikant geringere Körpergewichtszunahme. Diese Unterschiede basieren auf einer geringeren Fettmasse und trugen wahrscheinlich zu dem geringeren hepatischen Triglyceridgehalt, der verbesserten Ganzkörperinsulinsensitivität in LRep1<sup>-/-</sup> Mäusen bei. Des Weiteren konnten wir veränderte Gen-/Proteinexpressionen von Genen/Protein, wie Cd36, Pparg, Glut2, Akt Phosphorylierung, lipocalin2, *Vamp4*, und *Snap23*, die am Fett- und Glucosestoffwechsel beteiligt sind, zeigen. Unsere Ergebnisse deuten auf einen Einfluss von Repin1 auf die Insulinsensitivität und den Fettstoffwechsel durch die Regulierung von Schlüsselgenen im Glucose- und Fettstoffwechsel hin.

Ermutigt durch die oben zusammengefassten Ergebnisse, inaktivierten wir in **Kapitel 5** das *Repin1* Gen im Fettgewebe (iARep<sup>-/-</sup>) ab einem Alter von vier Wochen unter Verwendung der tamoxifeninduzierten Gen-Knockout Strategien bei C57BL/6NTac Mäusen. Der fettgewebsspezifische Repin1

Knockout führte zu einem schlankeren Phänotyp mit geringeren Fettmassen im subkutanen und epigonadalen Fettgewebe. Beide Fettdepots waren durch gleiche Zellzahlen, aber kleinere Adipozyten, gekennzeichnet. Interessanterweise waren die Serum Lipide, wie LDL-, HDL- und Gesamtcholesterin, in Fettgewebeknockout Mäusen verglichen mit den Kontrollen signifikant verringert. Konditionelle Repin1-Inaktivierung führte zu einer verbesserten Insulinsensitivität und Glucosetoleranz. Die Expression möglicher Repin1 Zielgene, wie *Cd36* and *Lcn2*, war signifikant reduziert in Mäusen ohne Repin1 Expression im Fettgewebe im Vergleich zu Kontrollmäusen. Außerdem bestimmten wir die Glycerolabgabe *in vitro* in differenzierten humanen primären Adipozyten, welche aus subkutanem Fettgewebe stammten, und konnten eine erhöhte Glycerolabgabe der *REPIN1* herunterregulierten Zellen im Vergleich zu den Kontrollzellen zeigen. Schließlich konnten wir zeigen, dass ein Verlust von Repin1 im Fettgewebe zu Veränderungen, auf Grund von geringerem Körpergewicht und verbesserten Parametern der Insulinsensitivität, des Glucose- und Fettstoffwechsels, in der Fettgewebemorphologie und -funktion führt.

Zusammenfassend trägt die hier vorliegende Arbeit dazu bei das Wissen über die funktionelle Rolle von Repin1 in der Leber und im Fettgewebe zu erweitern. Gemäß vorangegangenen *in vitro* Studien von Repin1 an 3T3-L1 Zellen konnte in der hier vorliegenden Promotionsarbeit die Hypothese, dass Repin1 in den Fett- und Glucosestoffwechsel involviert ist, bestätigt werden. In allen hier aufgezeigten Studien, konnte ein Zusammenhang zwischen Repin1 Defizienz und geringerem Körpergewicht, vorwiegend durch geringere Fettmasse gesteuert, gezeigt werden. Des Weiteren, zeigten alle drei hier vorgestellten Modelle eine verbesserte Insulinsensitivität im Vergleich zu ihren Kontrollgruppen. Mögliche Repin1 Zielgene, besonders der Transporter langkettiger Fettsäuren *Cd36*, wiesen veränderte Expressionlevel auf. Zusätzlich liefert die Promotionsarbeit ein besseres Verständnis, des unter Verwendung von Tamoxifen gesteuerten, temporalen *Cre/loxP* Knockot-Systems. Im Einklang mit vorangegangenen Studien, welche Effekte von endogener Östrogen-signalisierung zeigen konnten, beeinflusste Tamoxifen, als selektiver Östrogenrezeptor Modulator, die Adipozytenbiologie

*in vivo*. Daher sprechen die hier präsentierten Daten für eine Kontrolle der Tamoxifeneffekte durch die Gleichbehandlung der Kontrolltiere.



# Chapter 1

## Introduction

### 1.1 Obesity

Obesity is defined as a nutritional disorder and metabolic disease, where patients massively increase body weight due to excess body fat to the extent that it may have pathological impact, such as cardiovascular diseases, type II diabetes mellitus, dyslipidemia and several types of cancer [1].

In 2014 the World Health Organization (WHO) reported that worldwide obesity had doubled since 1980 and that over 1.9 billion adults, aged 18 years and older, were overweight and that 600 million of those were obese. This corresponds to a value of 39% of people being overweight and 13% being obese. During this time period, obesity and its comorbidities killed more people than malnutrition and underweight [2]. A study published in 2012 estimated that overweight and obesity caused 3.4 million deaths globally in the year 2010 [3], [4] making it to one of the biggest challenges in worldwide health care systems. In another study data on body mass index (BMI) was collated from 200 countries from between 1975 to 2014 [5]. It was calculated that mean BMI had increased during that time period from 21.7 kg/m<sup>2</sup> to 24.2 kg/m<sup>2</sup> in men and from 22.2 kg/m<sup>2</sup> to 24.4 kg/m<sup>2</sup> in women [5]. It was also shown in a reanalysis of 1,698 population-based studies, if post 2000 trends continue, global obesity prevalence will reach 18% in men and surpass 21% in women by 2025 [5] stressing the importance of prevention and intervention of this disease.

The WHO classified obesity in three different categories according to BMI, which is defined as the body mass in kg divided by the square of the body height in m. Thus, a BMI of 30-34.9 kg/m<sup>2</sup> is class I obesity, 35-39.9 kg/m<sup>2</sup> class II obesity and above 40 kg/m<sup>2</sup> class III obesity [2].

Despite the prevalent usage of BMI, the risk of developing obesity-related diseases such as cardiovascular disease is more influenced by body fat distribution pattern. One simple and effective means of determining body fat

distribution is the measurement of waist circumference. Intraabdominal fat depots which cause the characteristic apple shape are strongly associated with the development of metabolic syndrome or type II diabetes mellitus. In contrast, the gluteo-femoral fat depot found in the legs which cause the characteristic pear shape, is related to lower health risks [6], [7].

The main causes for developing obesity is a combination of increased food intake and a lack of physical activity, which leads to an elevated energy balance [8]. Genetic factors, physiological and psychiatric illnesses have an impact and can cause obesity [9] but they do not adequately explain the worldwide massive increase in its incidence in recent decades. Sociocultural factors such as income inequality, fast food and advertising, influence eating behavior and appears to be the main cause. Overall, obesity emerges from a complex interaction between energy balance, genetics and environment [9].

## 1.2 Adipose Tissue

Adipose tissue is a loose connective tissue composed mainly of adipocytes. Additionally, it contains the stromal-vascular fraction (SVF), which includes preadipocytes, fibroblasts, vascular endothelial cells and immune cells such as adipose tissue macrophages [10]. Originally it was described as an inert tissue for storage of energy in form of lipids [11]. Over the last decades, several experimental data concerning the biology and biochemistry of adipose tissue showed that it is a metabolically dynamic and complex organ synthesizing various molecules, most notably leptin, that regulate metabolic homeostasis [12], [13], [14].

Two types of adipose tissues are known in mammals, white adipose tissue (WAT), which basically stores energy, and brown adipose tissue (BAT), which produces heat by non-shivering thermogenesis [15].

WAT consists of relatively large adipocytes (100  $\mu\text{m}$ ) and are characterized by a single large lipid droplet (univacular) and only a small number of mitochondria. There are several WAT depots that have been characterized, but main ones are subcutaneous (scAT) and visceral adipose tissue (visAT). While scAT is located beneath the skin and in gluteal-femoral regions, visAT

is located in the intra-peritoneum and is connected to the digestive system via the portal vein to the liver [16], [17], [18].

Brown adipocytes are generally smaller than adipocytes in WAT and have numerous cytoplasmic lipid droplets of different size (multilocular). They also have more mitochondria compared to WAT adipocytes that release heat by uncoupled respiration [19]. BAT was thought to be limited to infant humans and hibernating mammals [20]. Recent studies could show presence of BAT and its recruitment in adult humans following cold exposure in the chest and neck regions [21], [22], [23]. Several studies in animals and humans could further show that brown or so called beige or brite adipocytes arise in various WAT depots in response to cold [24]. Adipocytes of classical BAT derive from Myf5-positive stem cells whereas adipocytes of WAT derive from Myf5-negative stem cells [24], [25]. It remains controversial whether beige/brite adipocytes arise from transdifferentiation of white adipocytes or whether they have their own distinct lineage (e.g. Sma-positive stem cells) [24], [25].

In obesity research mice are the most commonly used model, but in adipose tissue distribution they have important differences compared to humans. To investigate visAT in mouse models, epigonadal adipose tissue (epiAT) is commonly used which humans lack, and mice have almost no omental fat depots which is prominent in humans [25]. Classical BAT is located in mice in the interscapular region, whereas in adult humans it is localized mainly in the supraclavicular region and more resembles beige or brite adipose tissue in terms of its gene expression profile [24].

### 1.3 Genetics of Obesity

Obesity is basically the result of a maladjusted energy balance, which is influenced by various non-genetic and genetic factors. Hence, it can be described as the outcome of an adverse obesogenic environment, working on a susceptibility genotype. However, there are specific features which effectively protect against obesity, possibly explaining why about one third of the population remains lean [26]. Even if the prevalence of obesity increased just over

the last 30 years, it is well believed that genetics has a major influence on obesity. Lifestyle and environment changed acting in an obesogenic manner against an evolutionary background, which could be maladaptive to this new behavior [27].

Family, twin and adoption studies have shown that obesity is highly heritable and the risk to develop an obese phenotype increases when one of the relatives is obese. The heritability of obesity ranges from 16 to 80% depending on the obesity determination parameter, like BMI, waist circumference or body fat [28]. Patterns of heritability show that it is more than twice as likely to get obesity when both parents are obese compared to lean parents [29]. Studies on monozygotic and dizygotic veteran twin pairs could show that there are high heritability values for BMI and fat mass [27], [30], [31]. Further, body corpulence and BMI of adopted children correlates more strongly with parameters of their biological compared to their adoptive parents [32]. Also, different prevalence rates in various ethnic populations could prove a genetic component for obesity, e.g. populations of Caucasian and Asian people show a prevalence of about 35% whereas the prevalence of obesity of populations among Pima Indians is about 50% [33]. However, the precise genetic influence on obesity remains elusive since population substructure, economic disadvantages or access to medical care have an impact on developing obesity as well, although it is still evident that genetic factors play a role on developing an obese phenotype. There are two forms of obesity, a monogenetic and a polygenetic [34]. Monogenetic forms of obesity in humans are rare and very severe, generally starting in early childhood [35]. They result from an alteration of a single gene and to date there are more than 200 single-gene mutations found in only ten genes [36], [37]. For example, mutations in human genes coding for leptin (LEP), leptin-receptor (LEPR), proopiomelanocortin (POMC) and melanocortin-4 receptor (MC4R) have been associated with early-onset obesity [38], [39], [40]. The monogenetic disorder in the leptin gene was first discovered in 1994 by extensive positional cloning experiments [12] in *ob/ob* mice which were spontaneously obese and developed hyperinsulinemic and hyperglycemic phenotype [41]. The leptin protein is mainly produced and secreted by white adipocytes and acts as part of the signaling

pathway controlling food intake and the sensation of hunger in the central nervous system [42]. Several other studies found that some obese patients show undetectable leptin serum concentrations caused by either a frameshift mutation which produces a truncated protein that is not secreted or a missense mutation which results in low level leptin serum concentrations [43], [44], [45]. Treatment of those patients with recombinant leptin leads to a normal phenotype [46]. In 1965 a second spontaneously occurring mutation causing obesity and a similar phenotype was found in mice at the Jackson Laboratories and named *db* for diabetes [47]. Subsequent studies identifying the product of this gene characterized it as a cytokine-receptor, binding leptin predominantly in the hypothalamic neurons regulating fat metabolism [48], [49]. A splice site mutation in the exon 16 leads to a truncated receptor lacking both the transmembrane and the intercellular domains [50]. Further studies revealed a monogenetic interaction of genes involved in the leptin-melanocortin pathway, such as *POMC* and *MC4R* with obesity [34]. The protein encoded by *MC4R* is a member of the melanocortin receptor family and interacts with MSH hormones and is mediated by G proteins [51]. It strongly contributes to food intake and energy expenditure regulation [52], [53]. Mutations in the *MC4R* gene leads to non-functional receptors causing severe early-onset obesity and represents the most common cause (1-6%) for the obese phenotype [40], [54], [55], [56].

Polygenic or common obesity is controlled by two or more genes at different loci on different chromosomes [37]. Those polygenic gene variants vary from one individual to the next and usually have small influence on body weight [57]. Obesity is a result of the interaction of several of these polygenic variants superimposed on an obesogenic environment to determine the phenotype [58]. Interindividual heterogeneity is most likely the reason why one specific set of polygenes leads to obesity in one individual while another individual stays lean. For this reason, the study of polygenic obesity is very complex. To study polygenic obesity genomic deoxyribonucleic acid (DNA) is analyzed in terms of variation, such as single-nucleotide polymorphism (SNPs) or microsatellites, within or near candidate genes. There are several technologies for analysis of polygenetic traits including linkage studies, can-

candidate gene association studies and the most commonly used genome wide association studies (GWAS). GWAS started in 2005 and up to date there have been six waves of discoveries for BMI [59], [60], [61], [62], [63]. The first gene identified by a GWAS which associated with obesity was the *FTO* gene [59]. A polymorphism was found in the first intron which strongly associated with BMI, with a difference of 3 kg between homozygous individuals of risk and protective alleles. These findings have been replicated and confirmed by several groups in different populations [64], [65], [66]. Until now five following GWAS have identified more than 50 genetic loci with at least one obesity related trait. But still GWAS could explain just 1-4% of variances of BMI compared to 40-70% of the estimated heritability. One main problems of GWAS is the failure to detect false negatives, loci that are associated with traits whose effect sizes are too small. Also, most GWAS were performed in samples of Caucasian adults, probably missing many variances and neglecting the true development of obesity. Despite being a relatively new field, epigenetic regulation of gene expression might have potential to explain individual differences in obesity risk [67], as it could affect gene function but not DNA sequence [68].

## 1.4 Animal Models in Obesity

To understand the factors that contribute to obesity and regulate energy expenditure, lipid and glucose metabolism, animal models have been a powerful tool. Several different models have been used, including rats, non-human primates, dogs and seasonal models, such as hamsters or voles, but mice remain one of the most popular models to address questions in understanding obesity mechanisms.

Mice were the obvious choice for genetic experimentation in the 1930s, because they were readily available from the fancy mouse collectors of the day [69]. Mice and humans share about 99% of their genes [70] and most physiological and pathological features, such as diabetes, cancer, anemia, osteoporosis, neurological disorders and obesity. Of course, other mammals also share these diseases, but mice are small, cheap, easy to maintain and

straightforward to breed in captivity. Also, mice have short gestation periods of about 19 to 20 days and only 20 generations of inbreeding is required to create genetically identical and homozygous mice at all loci [71], [72].

To study the physiological and genetic basis of obesity, different types of models have been employed. The first models possessed spontaneous single gene mutations, the most famous examples being *ob/ob* and *db/db* mice, mentioned already in the section genes of obesity. Also, the Zucker (*fa/fa*) obese rat is a classic case for spontaneous single gene mutation, with a mutation in the leptin receptor [73]. To speed up the arbitrary nature of spontaneous mutational events leading to a loss of function in critical genes, mutagenic chemicals or exposing animals to radiation was adopted. However, with this approach only the growth hormone receptor SMA-1 mutation producing animals of small body size but elevated adiposity, showed some relevance for obesity research [74]. Nevertheless, spontaneous single gene mutations or artificially induced mutations in animals are very random and genes with no or only minor effects are very unlikely to be discovered [75].

The ability to disrupt or over-express specific genes from the germline of animals has dramatically improved the study of gene function. Today there are hundreds of genes cited, that when mutated or expressed as transgenes in mice, result in phenotypes affecting body weight and obesity. These genetically modified animal models led to a significant expansion in our understanding of molecular mechanisms of obesity. In addition, advanced techniques to knockout select genes only in specific tissues and at specific time-points have further contributed to this understanding [76]. For example, to elucidate the insulin signaling pathway, the insulin receptor was disrupted specifically in different tissues, like muscle, liver or fat [77], [78], [79]. Thus, the fat-specific insulin receptor knockout mouse, the FIRKO mouse, revealed that insulin signaling in adipocytes is critical for the development of obesity [79].

### 1.4.1 Cre loxP System

Conventional knockout strategies manipulated either embryonic stem cells or fertilized mice eggs using homologous recombination to alter genes in their



original location. A major problem associated with the conventional knockout system is that the knockout may lead to premature embryonic death preventing the study of its effects in adults. Also, compensatory changes during the period of development could be problematic to examine the function of a certain gene. For example, neuropeptide Y (NPY) is one of the most potent stimulators of feeding behavior [80], but when NPY was knocked out, mice showed no abnormal phenotype [81],[82].

The Cre/*loxP* system is a tool to knockout genes either in a specific tissue and/or at a specific time-point, which allows to investigate gene functions in adolescents. This system requires two different transgenic mouse lines, one expressing a Cre recombinase and another which has Cre recombinase recognition (*loxP*) sites flanking the gene of interest [83], [84]. This system is part of the bacteriophage P1 viral life cycle, which plays a crucial role for the phage genome replication in bacterial host chromosomes by mediating site-specific recombination [85]. The Cre recombinase catalyzes recombination between the two *loxP* sites, which consist of two palindromic 13 bp separated by an 8 bp spacer region [86], that results in excision of DNA placed between the two *loxP* sites [87].

Because Cre recombinase is not naturally expressed it has to be driven by a particular promotor, either tissue-specific or time-dependent, allowing spatial and temporal control of recombination.

To generate temporal control of recombination, a mutated ligand binding domain (LBD) of the human estrogen receptor (ER) is linked to the Cre recombinase [88], [89]. This Cre-ER recombinase requires binding of a ligand to be activated. The mutation of the LBD abolishes binding of naturally present estrogen to the ER, while retaining affinity towards 4-hydroxytamoxifen, one of the main metabolites of Tamoxifen [90]. Hence, intraperitoneal injection of Tamoxifen is a standard procedure to trigger the recombination event in mouse lines expressing Cre-ER recombinases.

### 1.4.2 Tamoxifen

Tamoxifen is a nonsteroidal antiestrogen compound discovered in 1962 [91], [92]. It is a selective estrogen receptor modulator (SERM), activating the estrogen receptor in some tissues by acting as an agonist, while inhibiting the receptor in other tissues by acting as an antagonist. Today, Tamoxifen has two important applications. On one side, it is a widely used drug for chemotherapy to treat patients with metastatic ER-positive tumors. On the other side, it serves as a triggering compound in genetic engineering to activate the Cre-loxP system [93], [94], [95]. Tamoxifen is a prodrug with relatively little affinity to the target protein, the estrogen receptor, therefore it needs to be activated by liver cytochrome P450 enzymes, undergoing extensive oxidation. Endoxifen and 4-hydroxytamoxifen are the most potent metabolites, which have a 100-fold higher affinity with the ER than Tamoxifen itself [93], [96].

### 1.4.3 Estrogen pathway

Adipose Tissue is a source of estrogen and contributes to the circulating pool of this hormone [97]. Also, the estrogen receptor (ER) occurs in adipocytes, thus completing the estrogen signaling pathway in white adipose tissue [98], [99]. It has been widely proven that estrogen has an influence on energy metabolism, adipose tissue distribution, inflammation and glucose homeostasis [100]. Further studies could show that a lack of estrogens is associated with obesity pointing out the influence of estrogens on adipocyte biology [101]. This explains why female mice are less likely to develop obesity on a high fat diet than males [102].

Today, two different forms of ER are known, the estrogen receptor  $\alpha$  (ER $\alpha$ ), encoded by the gene ESR1 located on chromosome 6 and the estrogen receptor  $\beta$  (ER $\beta$ ), encoded by the gene ESR2 on chromosome 14 [103], [104]. They are ligand-activated transcription factors, which form homodimers ( $\alpha\alpha$ ,  $\beta\beta$ ) or heterodimers ( $\alpha\beta$ ), to mediate gene expression. While ER $\alpha$  has a partial agonist/antagonist action, ER $\beta$  is an inhibitor with a pure antagonist action [105], [106]. This different behavior was shown for both

the natural 17- $\beta$  estradiol and Tamoxifen [106].

17- $\beta$  estradiol is the strongest sex steroid hormone and it is mainly biosynthesized in the ovaries from cholesterol, but also adipose tissue contributes to its production with conversion of testosterone to estradiol [97].

There are two different signal transduction pathways known so far, a genomic and a non-genomic mechanism, each involving different components. The genomic mechanism involves estrogen receptors located in either the cytoplasm or directly in the nucleus. Because estrogen is a lipophilic molecule, it is able to diffuse through the cell membrane of the target cells and interact with cytosolic estrogen receptors [107]. Ligand receptor interaction breaks binding with associated heat shock proteins which allows translocation in the nucleus [108]. Translocation of the hormone receptor complex is followed by homo- and heterodimerization between the receptors to bind specific sequences of DNA [109]. Finally, this complex will either activate or inhibit transcription of several genes. The non-genomic mechanism involves membrane associated ER and G-protein coupled ER, which induces intracellular signaling pathways like calcium mobilization, kinase activation (PKA, PKC, MAPK) and nitric oxide production [110], [104], [111].

## 1.5 Identification of target genes protecting against obesity using QTL mapping

To identify target genes protecting against obesity several methodologies are possible as discussed in the section genetics of obesity. For monogenetic traits, positional cloning is an adequate method, as done for the identification of the leptin gene in *ob/ob* mice [12]. However, obesity is usually caused by many genes (polygenic), thus quantitative trait locus (QTL) mapping is a preferred approach to determine areas in the genome which affect phenotypes like obesity and diabetes. QTL mapping is a method for mapping genes underlying complex quantitative traits by using genetic linkage maps in a cross between two mouse strains [112]. The obtained locus contains hundreds of genes, where one or more influence the target trait. To produce a QTL,

one crosses two inbred strains, which differ in the trait of interest, followed by either intercross of the first filial generation (F1) or backcross to one of the parental strains to create the second filial generation (F2) with different genotypes: totaling three after intercrossing and two after backcrossing. Markers, such as SNPs or microsatellites, all over the genome are used for genotyping to identify which of the parental strains contribute the allele. Finally, regression analysis of phenotype-genotype is performed to map the QTL on the genome [113], [114].

Using the QTL mapping approach, many naturally occurring alleles have been shown to influence obesity in mice, such as a cross of glucose intolerant and insulin resistant KK mice to BALB/c mice which identified two loci contributing to impaired glucose metabolism and three loci to triglyceride levels [115]. Further, in BSB mice QTLs for other obesity related traits such as adiposity, body weight, plasma cholesterol and hepatic lipase activity have been identified [116], [117]. Also, backcrosses using wild mice, like *Mus musculus castaneus* captured from the Philippines, to inbred C57BL/6JJcl could reveal new QTLs correlating with obesity. The identified QTL was associated with increased body weight and length, despite the fact that wild mice have smaller body size [118], [119]. Another QTL obtained in those mice was linked to decreased abdominal white fat weight and prevents obesity under standard and high fat diet [119], [120].

One of the problems associated with using QTL mapping approach however, is that it is not easy to pinpoint causative genes underlying QTLs, especially QTLs with small phenotypic effects on traits as most of the QTLs have small effects [121].

Following QTL mapping, congenic and subcongenic strains are made to isolate and fine map the identified loci. They are produced by breeding two different strains so that a certain genomic region from the donor strain is placed on the genome of a recipient strain. To subdivide the congenic region, subcongenic strains can be made until the gene of interest is located within a region containing very few genes. For example, congenic and subcongenic rat strains revealed new genes in a QTL on chromosome 10 which are linked to body fat mass, preadipocyte number and adipocyte size [122].

## 1.6 Repin1

To identify discrete genetic factors contributing to complex quantitative traits, such as body weight, diabetes or lipid metabolism, the inbred strains Spontaneously Hypertensive (SHR) and Wistar Ottawa Karlsburg RT1<sup>u</sup> (WOKW) rats, who develop a polygenic and complete metabolic syndrome with obesity, hyperinsulinemia, dyslipidemia, impaired glucose tolerance and hypertension, were crossed and backcrossed onto diabetes-prone BioBreeding/Ottawa Karlsburg (BB/OK) rats and finally phenotyped and genotyped [123], [124]. Both mentioned studies could produce congenic rats in which either SHR or WOKW rats served as donors for a chromosome 4 segment, which was associated with cholesterol and phospholipid phenotypes, and crossed on BB/OK background. Those newly produced congenic rat strains, termed BB.4S and BB.4W, developed obesity and dyslipidemia compared with their parental strain BB/OK. Also, BB/OK strains developed type I diabetes with a frequency of 86%, whereas the congenic strains BB.4S and BB.4W did not [125], [126]. Further analysis of genes located on this chromosome 4 locus, revealed one potential candidate gene, replication initiator 1 (*Repin1*), which might be responsible for observed phenotypes. Gene expression profiling of 92 genes located on either chromosome 4 or genes involved in obesity, insulin resistance and other facets of metabolic syndrome could show only significantly different expression of Repin1 in epigonadal and subcutaneous adipose tissue [127].

Repin1 was initially discovered as replication initiation region protein (RIP60) with a mass of 60 kDa in a study investigating DNA binding proteins involved in replication activation of the Chinese hamster dihydrofolate reductase gene (*dhfr*) [128]. The protein of Repin1 binds to two ATT-rich sites in *oriβ*, a short region 3' to the *dhfr* gene, acting as an enhancer of DNA bending during initiation of DNA synthesis [129]. Further characterization of DNA binding and bending properties revealed first structural insight into Repin1/RIP60 and classified it as polydactyl zinc finger protein of a Cys<sub>2</sub>-His<sub>2</sub> type [130].

Initial studies establishing and characterizing Repin1 as candidate gene

for obesity and metabolic syndrome involved investigations on gene structure and *in vitro* experiments on 3T3-L1 cells [131], [132]. Genetic variation in the Repin1 gene, in particular a coding region SNP (C/T 449) and a triplet repeat (TTT) in the 3'UTR is associated with facets of the metabolic syndrome, including body weight, serum insulin, leptin, triglyceride and cholesterol levels in rats [131]. Further, it could be shown *in vitro* in 3T3-L1 cells that Repin1 regulates adipocyte size and glucose transport. Small interfering RNA (siRNA) mediated knockdown of Repin1 led to altered *Cd36* expression, reduced palmitate uptake and changes in gene expression involved in lipid droplet formation such as *Vamp4* and *Snap23* [132]. Also, it could be shown that Repin1 is ubiquitously expressed, but is enriched in liver and adipose tissue indicating a role in glucose and lipid metabolism [132].

Preliminary studies on human gene expression of REPIN1 indicate associations with body fat and adipocyte size in visceral and subcutaneous adipose tissue [132]. Also, sequencing of human REPIN1 gene revealed a 12 bp deletion within the coding region (rs3832490) and found associations with decreased body fat mass, fasting plasma glucose, and lower maximum adipocyte size in patients homozygous for the deletion compared to non-carriers [unpublished].

These data indicate an important role for Repin1 in the regulation of adipose tissue function, insulin sensitivity, lipid- and glucose metabolism pointing it out as potential and interesting candidate gene for obesity research.

### 1.6.1 Zinc finger proteins

Zinc finger proteins are the largest transcription factor family in mammals serving a wide variety of biological functions, such as DNA recognition, RNA packaging, transcription activation, regulation of apoptosis, protein folding and assembly and lipid binding [133], [134]. They all share the requirement for at least one zinc ion to stabilize their secondary structure. The zinc ion is bound to two conserved Cys and His residues, which form the zinc finger motif, consisting of an  $\alpha$ -helix and an antiparallel  $\beta$ -sheet forming a hairpin structure, the so called finger. One zinc finger protein contains one or more

zinc finger motif(s), which bind to the major groove of DNA [135], [136].

The first recognized zinc finger protein was the transcriptional factor IIIA (TFIIIA) in *Xenopus laevis* in immature oocytes, which activated transcription of 5SRNA by binding of its DNA control region [137], [138].

Past investigations discovered that zinc finger motif proteins play a regulatory role in adipogenesis in particular in adipocyte determination. For example Zfp423 promotes adipocyte commitment as well as Zfp467, while suppressing osteoblast differentiation [139], [140]. Another study could show that ZNF395 promotes adipogenesis via coordination with PPAR $\gamma$ . Ablation of ZNF395 leads to reduced adipocyte number, whereas co-transfection with PPAR $\gamma$  increased adipocyte size [141]. They also play a role in regulation of brown adipogenesis without affecting white adipogenesis, such as PRDM16 [142], [143], [144].

## 1.6.2 Lipid metabolism and insulin action on adipose tissue

Adipose tissue plays a central role in regulating lipid metabolism, glucose homeostasis and whole body energy expenditure and therefore exerts an impact on whole body metabolism. It is no longer considered to be an inert tissue that stores energy in the form of triglycerides [145]. Today adipose tissue is well known as an endocrine organ that produces and secretes numerous hormones, which modulate a range of metabolic pathways, such as leptin which controls nutritional intake or TNF- $\alpha$  which controls insulin sensitivity and inflammatory processes [12], [146], [147], [148].

The ability to accumulate and provide energy when necessary makes adipose tissue an important buffering system for lipid energy balance, in particular fatty acids, which are a very efficient energy fuel. The highly reduced hydrocarbon tail can be readily oxidized to produce large quantities of adenosine triphosphate (ATP) [149]. Fat accumulation is determined by the balance between fat synthesis (lipogenesis) and fat breakdown (lipolysis).

Lipogenesis is the synthesis of fatty acids and happens predominantly in adipose tissue, but it also happens in the liver and muscle. Fatty acids

serve as energy reserves stored in adipocytes as triglycerides. This process is stimulated by a high carbohydrate diet and it is inhibited by polyunsaturated fatty acids and fasting. Stimulation of lipogenesis leads to elevated plasma triglyceride levels, whereas inhibition is related with a decrease in plasma glucose and an increase in plasma free fatty acids (FFA) [150]. Moreover, hormones like angiotensin contribute to stimulation and adipokines like leptin to inhibition. This process encompasses *de novo* fatty acid synthesis from acetyl-coenzyme A (acetyl-CoA) and triglyceride biosynthesis. Glucose catabolism generates acetyl-CoA and stimulates pancreatic insulin release. As a result, insulin stimulates glucose uptake in adipocytes and activates glycolytic and lipogenic enzymes, such as sterol regulatory element-binding protein 1 (SREBP1) that controls the expression of genes for lipogenesis [151], [152]. However, *de novo* lipogenesis is very low under normal conditions in WAT compared to liver and BAT [153], [154]. Under normal conditions, triglycerides are transported in blood vessels with the help of lipoproteins, chylomicrons and very low-density lipoprotein (VLDL), to target organs such as liver and adipose tissue. Lipoprotein lipase (LPL) hydrolyzes one fatty acid from circulating triglycerides and facilitates the entry of one fatty acid into the adipocyte [155], [156], [157]. Finally, diacylglycerol acyltransferase (DGAT) catalyzes triglyceride synthesis from uptaken free fatty acids and glycerol, provided from glucose [158], [159]. Insulin, as a predominant stimulus, promotes fatty acid uptake through multiple mechanisms including activation of LPL, induction of translocation of fatty acid transport protein and upregulation of related gene expression in adipocytes [160], [161], [162]. The capacity of how much lipid can be stored in adipose tissue is a main factor of insulin resistance and ectopic lipid infiltration into other tissues, like liver and muscle [157].

Lipolysis describes the breakdown of triglycerides, which are destined for hydrolysis to FFAs and glycerol in adipose tissue [163], [164] [165]. Released fatty acids bind to albumin and are carried to other tissues, such as liver and muscle for  $\beta$ -oxidation and glycerol is shuttled back to liver for oxidation or gluconeogenesis [166]. This process is stimulated by metabolic stress, like fasting or prolonged exercise, when the body needs more energy [167]. Glucagon



and epinephrine contributes to stimulation of lipolysis [150], whereas insulin inhibits lipolysis [149]. As already mentioned, lipolysis is the breakdown of tri-, di- and monoacylglycerides into individual fatty acids. During fasting periods, decreased levels of insulin result in suppression of lipogenesis and activation of lipolysis. Moreover, elevated glucagon levels activate the protein kinase A (PKA) pathway, which also stimulates lipolysis. Activation is also achieved via binding of catecholamine to  $\beta$ -adrenoreceptor [164]. PKA polyphosphorylates lipid droplet-associated proteins, such as perilipin and translocate hormone-sensitive lipase (HSL) to lipid droplets [168], [169], [170]. Adipocyte triglyceride lipase (ATGL) and HSL are responsible for conversion of triglycerides to diglycerides and hydrolysis of diglycerides to monoglycerides [171], [172]. The role of lipolytic enzymes ATGL and HSL in obesity was shown in several studies, where global deficiency of ATGL leads to impaired lipolysis, severe defects in BAT thermogenesis and mild obesity [173]. Adipose tissue specific knockout of ATGL showing decreased lipolysis and fat mass, but improved hepatic insulin sensitivity, confirmed these findings [174]. Deficiency of HSL leads to decreased lipolysis, but no other strong effects, suggesting a compensatory mechanism [175]. Obesity-induced fatty acid secretion of adipocytes and transport to other organs is a main cause of insulin resistance. Hence, it has been considered to inhibit lipolysis to improve insulin sensitivity [176]. On the other hand, inhibition of lipogenesis protects from diet-induced obesity and insulin resistance [177], suggesting that a balance between lipogenesis and lipolysis is important for maintaining systemic energy homeostasis and insulin sensitivity [178].

Insulin resistance is a condition where the effects of insulin on glucose uptake, metabolism and storage are compromised. In obesity insulin resistance is manifested by decreased insulin-stimulated glucose transport and metabolism in adipocytes and skeletal muscle and impaired suppression of hepatic glucose output [179]. Sensitivity of insulin can be stimulated by several adipokines, like leptin [180] and adiponectin [181], whereas insulin resistance can be induced by resistin [182] and TNF- $\alpha$ . Insulin is a regulator of many aspects of adipocyte biology, which includes control of metabolism of lipids, carbohydrates and proteins. Its role on metabolism is analogous

to that explained for lipid metabolism, promoting anabolism and inhibiting catabolism. In lipid metabolism, insulin upregulates LPL for fatty acid uptake and stimulates gene expression of lipogenic enzymes, such as acetyl-CoA carboxylase (ACC) and fatty acid synthase (FAS). Insulin also stimulates PDE5 which catalyzes the breakdown of cyclic nucleotides. In this way, LPL activity and thus lipolysis is reduced [183].

## 1.7 Aims and Hypothesis

The work presented in this thesis aims to characterize the functional role of Repin1 [Chapter 3 and 4], specifically in adipose tissue [Chapter 5]. Repin1 was identified as the most potential candidate gene for obesity, mapping to a QTL of congenic and subcongenic rat strains influencing body weight, serum lipid and insulin levels. Preliminary *in vitro* studies on 3T3-L1 cells confirmed a correlation of Repin1 expression and a changed lipid and glucose metabolism. Therefore, I hypothesized in this thesis an influence of Repin1 depletion on body weight, lipid and glucose homeostasis in liver [Chapter 4] and adipose tissue [Chapter 5] specific knockout mice, as well as in double knockout animals of Repin1 and leptin receptor [Chapter 3]. Hence, loss of Repin1 expression should lead to leaner phenotype, to improved glucose homeostasis and lipid metabolism.

Additionally, this work was devoted to analyze the influence of Tamoxifen on adipocyte biology *in vivo* [Chapter 2]. Tamoxifen is used to trigger the activity of Cre-recombinase to create gene knockouts in adolescent animals. Because, Tamoxifen is a selective modulator of the estrogen receptor and previous studies showed an influence of estrogen levels influencing obesity related traits, I hypothesized an influence of Tamoxifen itself to adipocyte biology in terms of energy expenditure, lipid metabolism and glucose homeostasis.

## 1.8 References

### Bibliography

- [1] WHO. <http://www.who.int/topics/obesity/en/>. 2017.
- [2] WHO. <http://www.who.int/mediacentre/factsheets/fs311/en/>. 2017.
- [3] Y. Wang and H. Lim. The global childhood obesity epidemic and the association between socio-economic status and childhood obesity. *Int Rev Psychiatry*, 24(3):176–188, Jun 2012.
- [4] M. Ng, et. al., and E. Gakidou. Global, regional, and national prevalence of overweight and obesity in children and adults during 1980–2013: a systematic analysis for the Global Burden of Disease Study 2013. *Lancet*, 384(9945):766–781, Aug 2014.
- [5] Y. Wang and H. Lim. Trends in adult body-mass index in 200 countries from 1975 to 2014: a pooled analysis of 1698 population-based measurement studies with 19.2 million participants. *Int Rev Psychiatry*, 24(3):176–188, Jun 2012.
- [6] M. Bluher. Adipose tissue dysfunction contributes to obesity related metabolic diseases. *Best Pract. Res. Clin. Endocrinol. Metab.*, 27(2):163–177, Apr 2013.
- [7] M. B. Snijder, M. Visser, J. M. Dekker, B. H. Goodpaster, T. B. Harris, S. B. Kritchevsky, N. De Rekeneire, A. M. Kanaya, A. B. Newman, F. A. Tylavsky, and J. C. Seidell. Low subcutaneous thigh fat is a risk factor for unfavourable glucose and lipid levels, independently of high abdominal fat. The Health ABC Study. *Diabetologia*, 48(2):301–308, Feb 2005.
- [8] G. A. Bray. Medical consequences of obesity. *J. Clin. Endocrinol. Metab.*, 89(6):2583–2589, Jun 2004.
- [9] P. G. Kopelman. Obesity as a medical problem. *Nature*, 404(6778):635–643, Apr 2000.

- 
- [10] E. Ottaviani, D. Malagoli, and C. Franceschi. The evolution of the adipose tissue: a neglected enigma. *Gen. Comp. Endocrinol.*, 174(1):1–4, Oct 2011.
- [11] J. K. Sethi and A. J. Vidal-Puig. Thematic review series: adipocyte biology. Adipose tissue function and plasticity orchestrate nutritional adaptation. *J. Lipid Res.*, 48(6):1253–1262, Jun 2007.
- [12] Y. Zhang, R. Proenca, M. Maffei, M. Barone, L. Leopold, and J. M. Friedman. Positional cloning of the mouse obese gene and its human homologue. *Nature*, 372(6505):425–432, Dec 1994.
- [13] R. S. Ahima and J. S. Flier. Adipose tissue as an endocrine organ. *Trends Endocrinol. Metab.*, 11(8):327–332, Oct 2000.
- [14] M. H. Fonseca-Alaniz, J. Takada, M. I. Alonso-Vale, and F. B. Lima. Adipose tissue as an endocrine organ: from theory to practice. *J Pediatr (Rio J)*, 83(5 Suppl):192–203, Nov 2007.
- [15] M. Giralt and F. Villarroya. White, brown, beige/brite: different adipose cells for different functions? *Endocrinology*, 154(9):2992–3000, Sep 2013.
- [16] B. Markman and F. E. Barton. Anatomy of the subcutaneous tissue of the trunk and lower extremity. *Plast. Reconstr. Surg.*, 80(2):248–254, Aug 1987.
- [17] S. R. Smith, J. C. Lovejoy, F. Greenway, D. Ryan, L. deJonge, J. de la Bretonne, J. Volafova, and G. A. Bray. Contributions of total body fat, abdominal subcutaneous adipose tissue compartments, and visceral adipose tissue to the metabolic complications of obesity. *Metab. Clin. Exp.*, 50(4):425–435, Apr 2001.
- [18] T. Tchkonina, T. Thomou, Y. Zhu, I. Karagiannides, C. Pothoulakis, M. D. Jensen, and J. L. Kirkland. Mechanisms and metabolic implications of regional differences among fat depots. *Cell Metab.*, 17(5):644–656, May 2013.

- 
- [19] I. G. Shabalina, N. Petrovic, J. M. de Jong, A. V. Kalinovich, B. Cannon, and J. Nedergaard. UCP1 in brite/beige adipose tissue mitochondria is functionally thermogenic. *Cell Rep*, 5(5):1196–1203, Dec 2013.
- [20] B. Cannon and J. Nedergaard. Brown adipose tissue: function and physiological significance. *Physiol. Rev.*, 84(1):277–359, Jan 2004.
- [21] J. Nedergaard, T. Bengtsson, and B. Cannon. Unexpected evidence for active brown adipose tissue in adult humans. *Am. J. Physiol. Endocrinol. Metab.*, 293(2):E444–452, Aug 2007.
- [22] K. A. Virtanen, M. E. Lidell, J. Orava, M. Heglind, R. Westergren, T. Niemi, M. Taittonen, J. Laine, N. J. Savisto, S. Enerback, and P. Nuutila. Functional brown adipose tissue in healthy adults. *N. Engl. J. Med.*, 360(15):1518–1525, Apr 2009.
- [23] A. M. Cypess, S. Lehman, G. Williams, I. Tal, D. Rodman, A. B. Goldfine, F. C. Kuo, E. L. Palmer, Y. H. Tseng, A. Doria, G. M. Kolodny, and C. R. Kahn. Identification and importance of brown adipose tissue in adult humans. *N. Engl. J. Med.*, 360(15):1509–1517, Apr 2009.
- [24] L. Sidossis and S. Kajimura. Brown and beige fat in humans: thermogenic adipocytes that control energy and glucose homeostasis. *J. Clin. Invest.*, 125(2):478–486, Feb 2015.
- [25] E. D. Rosen and B. M. Spiegelman. What we talk about when we talk about fat. *Cell*, 156(1-2):20–44, Jan 2014.
- [26] S. O’Rahilly and I. S. Farooqi. Human obesity: a heritable neurobehavioral disorder that is highly sensitive to environmental conditions. *Diabetes*, 57(11):2905–2910, Nov 2008.
- [27] Q. Xia and S. F. Grant. The genetics of human obesity. *Ann. N. Y. Acad. Sci.*, 1281:178–190, Apr 2013.
- [28] W. Yang, T. Kelly, and J. He. Genetic epidemiology of obesity. *Epidemiol Rev*, 29:49–61, 2007.

- 
- [29] R. C. Whitaker, J. A. Wright, M. S. Pepe, K. D. Seidel, and W. H. Dietz. Predicting obesity in young adulthood from childhood and parental obesity. *N. Engl. J. Med.*, 337(13):869–873, Sep 1997.
- [30] M. Feinleib, R. J. Garrison, R. Fabsitz, J. C. Christian, Z. Hrubec, N. O. Borhani, W. B. Kannel, R. Rosenman, J. T. Schwartz, and J. O. Wagner. The NHLBI twin study of cardiovascular disease risk factors: methodology and summary of results. *Am. J. Epidemiol.*, 106(4):284–285, Oct 1977.
- [31] A. J. Stunkard, T. T. Foch, and Z. Hrubec. A twin study of human obesity. *JAMA*, 256(1):51–54, Jul 1986.
- [32] A. J. Stunkard, T. I. Sørensen, C. Hanis, T. W. Teasdale, R. Chakraborty, W. J. Schull, and F. Schulsinger. An adoption study of human obesity. *N. Engl. J. Med.*, 314(4):193–198, Jan 1986.
- [33] R. G. Nelson, M. Shlossman, L. M. Budding, D. J. Pettitt, M. F. Saad, R. J. Genco, and W. C. Knowler. Periodontal disease and NIDDM in Pima Indians. *Diabetes Care*, 13(8):836–840, Aug 1990.
- [34] D. Albuquerque, E. Stice, R. Rodriguez-Lopez, L. Manco, and C. Nobrega. Current review of genetics of human obesity: from molecular mechanisms to an evolutionary perspective. *Mol. Genet. Genomics*, 290(4):1191–1221, Aug 2015.
- [35] E. Gonzalez-Jimenez, M. J. Aguilar Cordero, C. A. Padilla Lopez, and I. Garcia Garcia. [Monogenic human obesity: role of the leptin-melanocortin system in the regulation of food intake and body weight in humans]. *An Sist Sanit Navar*, 35(2):285–293, 2012.
- [36] D. M. Mutch and K. Clement. Unraveling the genetics of human obesity. *PLoS Genet.*, 2(12):e188, Dec 2006.
- [37] T. Rankinen, A. Zuberi, Y. C. Chagnon, S. J. Weisnagel, G. Argyropoulos, B. Walts, L. Perusse, and C. Bouchard. The human obesity

- gene map: the 2005 update. *Obesity (Silver Spring)*, 14(4):529–644, Apr 2006.
- [38] C. T. Montague, I. S. Farooqi, J. P. Whitehead, M. A. Soos, H. Rau, N. J. Wareham, C. P. Sewter, J. E. Digby, S. N. Mohammed, J. A. Hurst, C. H. Cheetham, A. R. Earley, A. H. Barnett, J. B. Prins, and S. O’Rahilly. Congenital leptin deficiency is associated with severe early-onset obesity in humans. *Nature*, 387(6636):903–908, Jun 1997.
- [39] H. Krude, H. Biebermann, W. Luck, R. Horn, G. Brabant, and A. Gruters. Severe early-onset obesity, adrenal insufficiency and red hair pigmentation caused by POMC mutations in humans. *Nat. Genet.*, 19(2):155–157, Jun 1998.
- [40] C. Vaisse, K. Clement, B. Guy-Grand, and P. Froguel. A frameshift mutation in human MC4R is associated with a dominant form of obesity. *Nat. Genet.*, 20(2):113–114, Oct 1998.
- [41] A. M. INGALLS, M. M. DICKIE, and G. D. SNELL. Obese, a new mutation in the house mouse. *J. Hered.*, 41(12):317–318, Dec 1950.
- [42] M. D. Klok, S. Jakobsdottir, and M. L. Drent. The role of leptin and ghrelin in the regulation of food intake and body weight in humans: a review. *Obes Rev*, 8(1):21–34, Jan 2007.
- [43] C. T. Montague, I. S. Farooqi, J. P. Whitehead, M. A. Soos, H. Rau, N. J. Wareham, C. P. Sewter, J. E. Digby, S. N. Mohammed, J. A. Hurst, C. H. Cheetham, A. R. Earley, A. H. Barnett, J. B. Prins, and S. O’Rahilly. Congenital leptin deficiency is associated with severe early-onset obesity in humans. *Nature*, 387(6636):903–908, Jun 1997.
- [44] H. Rau, B. J. Reaves, S. O’Rahilly, and J. P. Whitehead. Truncated human leptin (delta133) associated with extreme obesity undergoes proteasomal degradation after defective intracellular transport. *Endocrinology*, 140(4):1718–1723, Apr 1999.

- [45] A. Strobel, T. Issad, L. Camoin, M. Ozata, and A. D. Strosberg. A leptin missense mutation associated with hypogonadism and morbid obesity. *Nat. Genet.*, 18(3):213–215, Mar 1998.
- [46] I. S. Farooqi, S. A. Jebb, G. Langmack, E. Lawrence, C. H. Cheetham, A. M. Prentice, I. A. Hughes, M. A. McCamish, and S. O’Rahilly. Effects of recombinant leptin therapy in a child with congenital leptin deficiency. *N. Engl. J. Med.*, 341(12):879–884, Sep 1999.
- [47] K. P. Hummel, M. M. Dickie, and D. L. Coleman. Diabetes, a new mutation in the mouse. *Science*, 153(3740):1127–1128, Sep 1966.
- [48] L. A. Tartaglia, M. Dembski, X. Weng, N. Deng, J. Culpepper, R. Devos, G. J. Richards, L. A. Campfield, F. T. Clark, J. Deeds, C. Muir, S. Sanker, A. Moriarty, K. J. Moore, J. S. Smutko, G. G. Mays, E. A. Wool, C. A. Monroe, and R. I. Tepper. Identification and expression cloning of a leptin receptor, OB-R. *Cell*, 83(7):1263–1271, Dec 1995.
- [49] S. H. Bates and M. G. Myers. The role of leptin receptor signaling in feeding and neuroendocrine function. *Trends Endocrinol. Metab.*, 14(10):447–452, Dec 2003.
- [50] K. Clement, C. Vaisse, N. Lahlou, S. Cabrol, V. Pelloux, D. Cassuto, M. Gourmelen, C. Dina, J. Chambaz, J. M. Lacorte, A. Basdevant, P. Bougneres, Y. Lebouc, P. Froguel, and B. Guy-Grand. A mutation in the human leptin receptor gene causes obesity and pituitary dysfunction. *Nature*, 392(6674):398–401, Mar 1998.
- [51] A. Hinney, A. L. Volckmar, and N. Knoll. Melanocortin-4 receptor in energy homeostasis and obesity pathogenesis. *Prog Mol Biol Transl Sci*, 114:147–191, 2013.
- [52] I. Gantz, H. Miwa, Y. Konda, Y. Shimoto, T. Tashiro, S. J. Watson, J. DelValle, and T. Yamada. Molecular cloning, expression, and gene localization of a fourth melanocortin receptor. *J. Biol. Chem.*, 268(20):15174–15179, Jul 1993.



- 
- [53] K. G. Mountjoy, M. T. Mortrud, M. J. Low, R. B. Simerly, and R. D. Cone. Localization of the melanocortin-4 receptor (MC4-R) in neuroendocrine and autonomic control circuits in the brain. *Mol. Endocrinol.*, 8(10):1298–1308, Oct 1994.
- [54] G. S. Yeo, I. S. Farooqi, S. Aminian, D. J. Halsall, R. G. Stanhope, and S. O’Rahilly. A frameshift mutation in MC4R associated with dominantly inherited human obesity. *Nat. Genet.*, 20(2):111–112, Oct 1998.
- [55] I. S. Farooqi, J. M. Keogh, G. S. Yeo, E. J. Lank, T. Cheetham, and S. O’Rahilly. Clinical spectrum of obesity and mutations in the melanocortin 4 receptor gene. *N. Engl. J. Med.*, 348(12):1085–1095, Mar 2003.
- [56] S. Beckers, I. Mertens, A. Peeters, L. Van Gaal, and W. Van Hul. Screening for melanocortin-4 receptor mutations in a cohort of Belgian morbidly obese adults and children. *Int J Obes (Lond)*, 30(2):221–225, Feb 2006.
- [57] A. Hinney, C. I. Vogel, and J. Hebebrand. From monogenic to polygenic obesity: recent advances. *Eur Child Adolesc Psychiatry*, 19(3):297–310, Mar 2010.
- [58] C. Razquin, A. Marti, and J. A. Martinez. Evidences on three relevant obesogenes: MC4R, FTO and PPAR $\gamma$ . Approaches for personalized nutrition. *Mol Nutr Food Res*, 55(1):136–149, Jan 2011.
- [59] T. M. Frayling and et. al. Timpson. A common variant in the FTO gene is associated with body mass index and predisposes to childhood and adult obesity. *Science*, 316(5826):889–894, May 2007.
- [60] C. J. Willer, Speliotes, et. al., and J. N. Hirschhorn. Six new loci associated with body mass index highlight a neuronal influence on body weight regulation. *Nat. Genet.*, 41(1):25–34, Jan 2009.

- 
- [61] E. K. Speliotes, C. J. Willer, et. al., and R. J. Loos. Association analyses of 249,796 individuals reveal 18 new loci associated with body mass index. *Nat. Genet.*, 42(11):937–948, Nov 2010.
- [62] S. I. Berndt, et. al., and S. L. Slager. Genome-wide association study identifies multiple risk loci for chronic lymphocytic leukemia. *Nat. Genet.*, 45(8):868–876, Aug 2013.
- [63] A. E. Locke and et al. Genetic studies of body mass index yield new insights for obesity biology. *Nature*, 518(7538):197–206, Feb 2015.
- [64] D. Albuquerque, C. Nobrega, and L. Manco. Association of FTO polymorphisms with obesity and obesity-related outcomes in Portuguese children. *PLoS ONE*, 8(1):e54370, 2013.
- [65] Y. C. Chang, P. H. Liu, W. J. Lee, T. J. Chang, Y. D. Jiang, H. Y. Li, S. S. Kuo, K. C. Lee, and L. M. Chuang. Common variation in the fat mass and obesity-associated (FTO) gene confers risk of obesity and modulates BMI in the Chinese population. *Diabetes*, 57(8):2245–2252, Aug 2008.
- [66] S. F. Grant, M. Li, J. P. Bradfield, C. E. Kim, K. Annaiah, E. Santa, J. T. Glessner, T. Casalunovo, E. C. Frackelton, F. G. Otieno, J. L. Shaner, R. M. Smith, M. Imielinski, A. W. Eckert, R. M. Chiavacci, R. I. Berkowitz, and H. Hakonarson. Association analysis of the FTO gene with obesity in children of Caucasian and African ancestry reveals a common tagging SNP. *PLoS ONE*, 3(3):e1746, Mar 2008.
- [67] J. Champion, F. I. Milagro, and J. A. Martinez. Individuality and epigenetics in obesity. *Obes Rev*, 10(4):383–392, Jul 2009.
- [68] A. Bird. DNA methylation patterns and epigenetic memory. *Genes Dev.*, 16(1):6–21, Jan 2002.
- [69] K. Paigen. One hundred years of mouse genetics: an intellectual history. I. The classical period (1902-1980). *Genetics*, 163(1):1–7, Jan 2003.

- [70] R. H. Waterston, et. al., and E. S. Lander. Initial sequencing and comparative analysis of the mouse genome. *Nature*, 420(6915):520–562, Dec 2002.
- [71] N. Rosenthal and S. Brown. The mouse ascending: perspectives for human-disease models. *Nat. Cell Biol.*, 9(9):993–999, Sep 2007.
- [72] L. L. Peters, R. F. Robledo, C. J. Bult, G. A. Churchill, B. J. Paigen, and K. L. Svenson. The mouse as a model for human biology: a resource guide for complex trait analysis. *Nat. Rev. Genet.*, 8(1):58–69, Jan 2007.
- [73] L. M. Zucker and T. F. Zucker. Fatty, a new mutation in the rat. *Journal of Heredity*, 52(6):275, Nov 1961.
- [74] C. W. Meyer, D. Korthaus, W. Jagla, E. Cornali, J. Grosse, H. Fuchs, M. Klingenspor, S. Roemheld, M. Tschop, G. Heldmaier, M. H. De Angelis, and M. Nehls. A novel missense mutation in the mouse growth hormone gene causes semidominant dwarfism, hyperghrelinemia, and obesity. *Endocrinology*, 145(5):2531–2541, May 2004.
- [75] J. N. Crawley. Behavioral phenotyping of rodents. *Comp. Med.*, 53(2):140–146, Apr 2003.
- [76] R. A. Davey and H. E. MacLean. Current and future approaches using genetically modified mice in endocrine research. *Am. J. Physiol. Endocrinol. Metab.*, 291(3):E429–438, Sep 2006.
- [77] J. C. Bruning, M. D. Michael, J. N. Winnay, T. Hayashi, D. Horsch, D. Accili, L. J. Goodyear, and C. R. Kahn. A muscle-specific insulin receptor knockout exhibits features of the metabolic syndrome of NIDDM without altering glucose tolerance. *Mol. Cell*, 2(5):559–569, Nov 1998.
- [78] M. D. Michael, R. N. Kulkarni, C. Postic, S. F. Previs, G. I. Shulman, M. A. Magnuson, and C. R. Kahn. Loss of insulin signaling in hepatocytes leads to severe insulin resistance and progressive hepatic dysfunction. *Mol. Cell*, 6(1):87–97, Jul 2000.

- [79] M. Bluher, M. D. Michael, O. D. Peroni, K. Ueki, N. Carter, B. B. Kahn, and C. R. Kahn. Adipose tissue selective insulin receptor knock-out protects against obesity and obesity-related glucose intolerance. *Dev. Cell*, 3(1):25–38, Jul 2002.
- [80] S. Lin, D. Boey, and H. Herzog. NPY and Y receptors: lessons from transgenic and knockout models. *Neuropeptides*, 38(4):189–200, Aug 2004.
- [81] J. C. Erickson, K. E. Clegg, and R. D. Palmiter. Sensitivity to leptin and susceptibility to seizures of mice lacking neuropeptide Y. *Nature*, 381(6581):415–421, May 1996.
- [82] J. C. Erickson, G. Hollopeter, and R. D. Palmiter. Attenuation of the obesity syndrome of ob/ob mice by the loss of neuropeptide Y. *Science*, 274(5293):1704–1707, Dec 1996.
- [83] R. Kuhn and R. M. Torres. Cre/loxP recombination system and gene targeting. *Methods Mol. Biol.*, 180:175–204, 2002.
- [84] C. H. Kos. Cre/loxP system for generating tissue-specific knockout mouse models. *Nutr. Rev.*, 62(6 Pt 1):243–246, Jun 2004.
- [85] S. Austin, M. Ziese, and N. Sternberg. A novel role for site-specific recombination in maintenance of bacterial replicons. *Cell*, 25(3):729–736, Sep 1981.
- [86] R. H. Hoess, M. Ziese, and N. Sternberg. P1 site-specific recombination: nucleotide sequence of the recombining sites. *Proc. Natl. Acad. Sci. U.S.A.*, 79(11):3398–3402, Jun 1982.
- [87] B. Sauer. Inducible gene targeting in mice using the Cre/lox system. *Methods*, 14(4):381–392, Apr 1998.
- [88] R. Feil, J. Brocard, B. Mascrez, M. LeMeur, D. Metzger, and P. Chambon. Ligand-activated site-specific recombination in mice. *Proc. Natl. Acad. Sci. U.S.A.*, 93(20):10887–10890, Oct 1996.

- 
- [89] D. Metzger, J. Clifford, H. Chiba, and P. Chambon. Conditional site-specific recombination in mammalian cells using a ligand-dependent chimeric Cre recombinase. *Proc. Natl. Acad. Sci. U.S.A.*, 92(15):6991–6995, Jul 1995.
- [90] W. P. Bocchinfuso and K. S. Korach. Estrogen receptor residues required for stereospecific ligand recognition and activation. *Mol. Endocrinol.*, 11(5):587–594, May 1997.
- [91] V. C. Jordan. Tamoxifen (ICI46,474) as a targeted therapy to treat and prevent breast cancer. *Br. J. Pharmacol.*, 147 Suppl 1:S269–276, Jan 2006.
- [92] V. C. Jordan. Long-term tamoxifen therapy to control or to prevent breast cancer: laboratory concept to clinical trials. *Prog. Clin. Biol. Res.*, 262:105–123, 1988.
- [93] Z. Desta, B. A. Ward, N. V. Soukhova, and D. A. Flockhart. Comprehensive evaluation of tamoxifen sequential biotransformation by the human cytochrome P450 system in vitro: prominent roles for CYP3A and CYP2D6. *J. Pharmacol. Exp. Ther.*, 310(3):1062–1075, Sep 2004.
- [94] C. K. Osborne. Tamoxifen in the treatment of breast cancer. *N. Engl. J. Med.*, 339(22):1609–1618, Nov 1998.
- [95] S. Hayashi and A. P. McMahon. Efficient recombination in diverse tissues by a tamoxifen-inducible form of Cre: a tool for temporally regulated gene activation/inactivation in the mouse. *Dev. Biol.*, 244(2):305–318, Apr 2002.
- [96] A. Ahmad, S. Shahabuddin, S. Sheikh, P. Kale, M. Krishnappa, R. C. Rane, and I. Ahmad. Endoxifen, a new cornerstone of breast cancer therapy: demonstration of safety, tolerability, and systemic bioavailability in healthy human subjects. *Clin. Pharmacol. Ther.*, 88(6):814–817, Dec 2010.

- 
- [97] L. R. Nelson and S. E. Bulun. Estrogen production and action. *J. Am. Acad. Dermatol.*, 45(3 Suppl):S116–124, Sep 2001.
- [98] S. B. Pedersen, P. S. Hansen, S. Lund, P. H. Andersen, A. Odgaard, and B. Richelsen. Identification of oestrogen receptors and oestrogen receptor mRNA in human adipose tissue. *Eur. J. Clin. Invest.*, 26(4):262–269, Apr 1996.
- [99] J. F. Louet, C. LeMay, and F. Mauvais-Jarvis. Antidiabetic actions of estrogen: insight from human and genetic mouse models. *Curr Atheroscler Rep*, 6(3):180–185, May 2004.
- [100] K. E. Davis, M. D Neinast, K. Sun, W. M Skiles, J. D Bills, J. A Zehr, D. Zeve, L. D Hahner, D. W Cox, L. M Gent, Y. Xu, Z. V Wang, S. A Khan, and D. J. Clegg. The sexually dimorphic role of adipose and adipocyte estrogen receptors in modulating adipose tissue expansion, inflammation, and fibrosis. *Mol Metab*, 2(3):227–242, 2013.
- [101] C. Ohlsson, N. Hellberg, P. Parini, O. Vidal, M. Bohlooly-Y, M. Bohlooly, M. Rudling, M. K. Lindberg, M. Warner, B. Angelin, and J. A. Gustafsson. Obesity and disturbed lipoprotein profile in estrogen receptor-alpha-deficient male mice. *Biochem. Biophys. Res. Commun.*, 278(3):640–645, Nov 2000.
- [102] R. E. Stubbins, K. Najjar, V. B. Holcomb, J. Hong, and N. P. Nunez. Oestrogen alters adipocyte biology and protects female mice from adipocyte inflammation and insulin resistance. *Diabetes Obes Metab*, 14(1):58–66, Jan 2012.
- [103] J. R. Gosden, P. G. Middleton, and D. Rout. Localization of the human oestrogen receptor gene to chromosome 6q24—q27 by in situ hybridization. *Cytogenet. Cell Genet.*, 43(3-4):218–220, 1986.
- [104] M. H. Faulds, C. Zhao, K. Dahlman-Wright, and J. A. Gustafsson. The diversity of sex steroid action: regulation of metabolism by estrogen signaling. *J. Endocrinol.*, 212(1):3–12, Jan 2012.

- 
- [105] J. Matthews and J. A. Gustafsson. Estrogen signaling: a subtle balance between ER alpha and ER beta. *Mol. Interv.*, 3(5):281–292, Aug 2003.
- [106] T. Barkhem, B. Carlsson, Y. Nilsson, E. Enmark, J. Gustafsson, and S. Nilsson. Differential response of estrogen receptor alpha and estrogen receptor beta to partial estrogen agonists/antagonists. *Mol. Pharmacol.*, 54(1):105–112, Jul 1998.
- [107] C. Helsen, S. Kerkhofs, L. Clinckemalie, L. Spans, M. Laurent, S. Boonen, D. Vanderschueren, and F. Claessens. Structural basis for nuclear hormone receptor DNA binding. *Mol. Cell. Endocrinol.*, 348(2):411–417, Jan 2012.
- [108] M. Marino, P. Galluzzo, and P. Ascenzi. Estrogen signaling multiple pathways to impact gene transcription. *Curr. Genomics*, 7(8):497–508, 2006.
- [109] R. M. Evans. The steroid and thyroid hormone receptor superfamily. *Science*, 240(4854):889–895, May 1988.
- [110] T. M. D’Eon, S. C. Souza, M. Aronovitz, M. S. Obin, S. K. Fried, and A. S. Greenberg. Estrogen regulation of adiposity and fuel partitioning. Evidence of genomic and non-genomic regulation of lipogenic and oxidative pathways. *J. Biol. Chem.*, 280(43):35983–35991, Oct 2005.
- [111] S. Kato, H. Endoh, Y. Masuhiro, T. Kitamoto, S. Uchiyama, H. Sasaki, S. Masushige, Y. Gotoh, E. Nishida, H. Kawashima, D. Metzger, and P. Chambon. Activation of the estrogen receptor through phosphorylation by mitogen-activated protein kinase. *Science*, 270(5241):1491–1494, Dec 1995.
- [112] E. S. Lander and D. Botstein. Mapping mendelian factors underlying quantitative traits using RFLP linkage maps. *Genetics*, 121(1):185–199, Jan 1989.

- 
- [113] J. S. Fisler and C. H. Warden. Mapping of mouse obesity genes: A generic approach to a complex trait. *J. Nutr.*, 127(9):1909S–1916S, Sep 1997.
- [114] A. Ishikawa and S. Okuno. Fine mapping and candidate gene search of quantitative trait loci for growth and obesity using mouse intersub-specific subcongenic intercrosses and exome sequencing. *PLoS ONE*, 9(11):e113233, 2014.
- [115] T. Shike, S. Hirose, M. Kobayashi, K. Funabiki, T. Shirai, and Y. Tomino. Susceptibility and negative epistatic loci contributing to type 2 diabetes and related phenotypes in a KK/Ta mouse model. *Diabetes*, 50(8):1943–1948, Aug 2001.
- [116] C. H. Warden, J. S. Fisler, M. J. Pace, K. L. Svenson, and A. J. Lusis. Coincidence of genetic loci for plasma cholesterol levels and obesity in a multifactorial mouse model. *J. Clin. Invest.*, 92(2):773–779, Aug 1993.
- [117] N. Yi, S. Chiu, D. B. Allison, J. S. Fisler, and C. H. Warden. Epistatic interaction between two nonstructural loci on chromosomes 7 and 3 influences hepatic lipase activity in BSB mice. *J. Lipid Res.*, 45(11):2063–2070, Nov 2004.
- [118] M. B. Mollah and A. Ishikawa. Intersubspecific subcongenic mouse strain analysis reveals closely linked QTLs with opposite effects on body weight. *Mamm. Genome*, 22(5-6):282–289, Jun 2011.
- [119] A. Ishikawa, E. H. Kim, H. Bolor, M. B. Mollah, and T. Namikawa. A growth QTL (Pbwg1) region of mouse chromosome 2 contains closely linked loci affecting growth and body composition. *Mamm. Genome*, 18(4):229–239, Apr 2007.
- [120] M. B. Mollah and A. Ishikawa. A wild derived quantitative trait locus on mouse chromosome 2 prevents obesity. *BMC Genet.*, 11:84, Sep 2010.



- [121] J. Flint and T. F. Mackay. Genetic architecture of quantitative traits in mice, flies, and humans. *Genome Res.*, 19(5):723–733, May 2009.
- [122] A. Weingarten, L. Turchetti, K. Krohn, I. Kloting, M. Kern, P. Kovacs, M. Stumvoll, M. Bluher, and N. Kloting. Novel genes on rat chromosome 10 are linked to body fat mass, preadipocyte number and adipocyte size. *Int J Obes (Lond)*, 40(12):1832–1840, Dec 2016.
- [123] P. Kovacs, J. van den Brandt, A. C. Bonne, L. F. van Zutphen, H. A. van Lith, and I. Kloting. Congenic BB.SHR rat provides evidence for effects of a chromosome 4 segment (D4Mit6-Npy approximately 1 cm) on total serum and lipoprotein lipid concentration and composition after feeding a high-fat, high-cholesterol diet. *Metab. Clin. Exp.*, 50(4):458–462, Apr 2001.
- [124] N. Kloting, B. Wilke, and I. Kloting. Phenotypic and genetic analyses of subcongenic BB.SHR rat lines shorten the region on chromosome 4 bearing gene(s) for underlying facets of metabolic syndrome. *Physiol. Genomics*, 18(3):325–330, Aug 2004.
- [125] I. Kloting, P. Kovacs, and B. Kuttler. Phenotypic consequences after restoration of lymphopenia in the diabetes-prone BB/OK rat. *Biochem. Biophys. Res. Commun.*, 239(1):106–110, Oct 1997.
- [126] N. Kloting, B. Wilke, and I. Kloting. Alleles on rat chromosome 4 (D4Got41-Fabp1/Tacr1) regulate subphenotypes of obesity. *Obes. Res.*, 13(3):589–595, Mar 2005.
- [127] J. Bahr, N. Kloting, I. Kloting, and N. Follak. Gene expression profiling supports the role of Repin1 in the pathophysiology of metabolic syndrome. *Endocrine*, 40(2):310–314, Oct 2011.
- [128] L. Dailey, M. S. Caddle, N. Heintz, and N. H. Heintz. Purification of RIP60 and RIP100, mammalian proteins with origin-specific DNA-binding and ATP-dependent DNA helicase activities. *Mol. Cell. Biol.*, 10(12):6225–6235, Dec 1990.

- [129] M. S. Caddle, L. Dailey, and N. H. Heintz. RIP60, a mammalian origin-binding protein, enhances DNA bending near the dihydrofolate reductase origin of replication. *Mol. Cell. Biol.*, 10(12):6236–6243, Dec 1990.
- [130] C. R. Houchens, W. Montigny, L. Zeltser, L. Dailey, J. M. Gilbert, and N. H. Heintz. The dhfr oribeta-binding protein RIP60 contains 15 zinc fingers: DNA binding and looping by the central three fingers and an associated proline-rich region. *Nucleic Acids Res.*, 28(2):570–581, Jan 2000.
- [131] N. Kloting, B. Wilke, and I. Kloting. Triplet repeat in the Repin1 3'-untranslated region on rat chromosome 4 correlates with facets of the metabolic syndrome. *Diabetes Metab. Res. Rev.*, 23(5):406–410, Jul 2007.
- [132] K. Ruschke, M. Illes, M. Kern, I. Kloting, M. Fasshauer, M. R. Schon, J. Kosacka, G. Fitzl, P. Kovacs, M. Stumvoll, M. Bluher, and N. Kloting. Repin1 maybe involved in the regulation of cell size and glucose transport in adipocytes. *Biochem. Biophys. Res. Commun.*, 400(2):246–251, Sep 2010.
- [133] B. Ganss and A. Jheon. Zinc finger transcription factors in skeletal development. *Crit. Rev. Oral Biol. Med.*, 15(5):282–297, Sep 2004.
- [134] J. H. Laity, B. M. Lee, and P. E. Wright. Zinc finger proteins: new insights into structural and functional diversity. *Curr. Opin. Struct. Biol.*, 11(1):39–46, Feb 2001.
- [135] N. P. Pavletich and C. O. Pabo. Zinc finger-DNA recognition: crystal structure of a Zif268-DNA complex at 2.1 Å. *Science*, 252(5007):809–817, May 1991.
- [136] M. Elrod-Erickson, M. A. Rould, L. Nekludova, and C. O. Pabo. Zif268 protein-DNA complex refined at 1.6 Å: a model system for understanding zinc finger-DNA interactions. *Structure*, 4(10):1171–1180, Oct 1996.

- [137] J. S. Hanas, D. F. Bogenhagen, and C. W. Wu. Cooperative model for the binding of *Xenopus* transcription factor A to the 5S RNA gene. *Proc. Natl. Acad. Sci. U.S.A.*, 80(8):2142–2145, Apr 1983.
- [138] J. Miller, A. D. McLachlan, and A. Klug. Repetitive zinc-binding domains in the protein transcription factor IIIA from *Xenopus* oocytes. *EMBO J.*, 4(6):1609–1614, Jun 1985.
- [139] R. K. Gupta, Z. Arany, P. Seale, R. J. Mepani, L. Ye, H. M. Conroe, Y. A. Roby, H. Kulaga, R. R. Reed, and B. M. Spiegelman. Transcriptional control of preadipocyte determination by Zfp423. *Nature*, 464(7288):619–623, Mar 2010.
- [140] J. M. Quach, E. C. Walker, E. Allan, M. Solano, A. Yokoyama, S. Kato, N. A. Sims, M. T. Gillespie, and T. J. Martin. Zinc finger protein 467 is a novel regulator of osteoblast and adipocyte commitment. *J. Biol. Chem.*, 286(6):4186–4198, Feb 2011.
- [141] R. Hasegawa, Y. Tomaru, M. de Hoon, H. Suzuki, Y. Hayashizaki, and J. W. Shin. Identification of ZNF395 as a novel modulator of adipogenesis. *Exp. Cell Res.*, 319(3):68–76, Feb 2013.
- [142] S. Kajimura, P. Seale, K. Kubota, E. Lunsford, J. V. Frangioni, S. P. Gygi, and B. M. Spiegelman. Initiation of myoblast to brown fat switch by a PRDM16-C/EBP-beta transcriptional complex. *Nature*, 460(7259):1154–1158, Aug 2009.
- [143] S. Kajimura, P. Seale, T. Tomaru, H. Erdjument-Bromage, M. P. Cooper, J. L. Ruas, S. Chin, P. Tempst, M. A. Lazar, and B. M. Spiegelman. Regulation of the brown and white fat gene programs through a PRDM16/CtBP transcriptional complex. *Genes Dev.*, 22(10):1397–1409, May 2008.
- [144] P. Seale, B. Bjork, W. Yang, S. Kajimura, S. Chin, S. Kuang, A. Scime, S. Devarakonda, H. M. Conroe, H. Erdjument-Bromage, P. Tempst, M. A. Rudnicki, D. R. Beier, and B. M. Spiegelman. PRDM16 controls

- a brown fat/skeletal muscle switch. *Nature*, 454(7207):961–967, Aug 2008.
- [145] E. Ottaviani, D. Malagoli, and C. Franceschi. The evolution of the adipose tissue: a neglected enigma. *Gen. Comp. Endocrinol.*, 174(1):1–4, Oct 2011.
- [146] J. M. Friedman and J. L. Halaas. Leptin and the regulation of body weight in mammals. *Nature*, 395(6704):763–770, Oct 1998.
- [147] L. J. Old. Tumor necrosis factor (TNF). *Science*, 230(4726):630–632, Nov 1985.
- [148] G. S. Hotamisligil, N. S. Shargill, and B. M. Spiegelman. Adipose expression of tumor necrosis factor- $\alpha$ : direct role in obesity-linked insulin resistance. *Science*, 259(5091):87–91, Jan 1993.
- [149] W. Kiess, S. Petzold, M. Topfer, A. Garten, S. Bluher, T. Kapellen, A. Korner, and J. Kratzsch. Adipocytes and adipose tissue. *Best Pract. Res. Clin. Endocrinol. Metab.*, 22(1):135–153, Feb 2008.
- [150] S. Kersten. Mechanisms of nutritional and hormonal regulation of lipogenesis. *EMBO Rep.*, 2(4):282–286, Apr 2001.
- [151] F. Assimacopoulos-Jeannet, S. Brichard, F. Rencurel, I. Cusin, and B. Jeanrenaud. In vivo effects of hyperinsulinemia on lipogenic enzymes and glucose transporter expression in rat liver and adipose tissues. *Metab. Clin. Exp.*, 44(2):228–233, Feb 1995.
- [152] P. Ferre and F. Foufelle. SREBP-1c transcription factor and lipid homeostasis: clinical perspective. *Horm. Res.*, 68(2):72–82, 2007.
- [153] J. Swierczynski, E. Goyke, L. Wach, A. Pankiewicz, Z. Kochan, W. Adamonis, Z. Sledzinski, and Z. Aleksandrowicz. Comparative study of the lipogenic potential of human and rat adipose tissue. *Metab. Clin. Exp.*, 49(5):594–599, May 2000.

- [154] D. Letexier, C. Pinteur, V. Large, V. Frering, and M. Beylot. Comparison of the expression and activity of the lipogenic pathway in human and rat adipose tissue. *J. Lipid Res.*, 44(11):2127–2134, Nov 2003.
- [155] S. Kersten. Physiological regulation of lipoprotein lipase. *Biochim. Biophys. Acta*, 1841(7):919–933, Jul 2014.
- [156] B. A. Fielding and K. N. Frayn. Lipoprotein lipase and the disposition of dietary fatty acids. *Br. J. Nutr.*, 80(6):495–502, Dec 1998.
- [157] K. N. Frayn. Adipose tissue as a buffer for daily lipid flux. *Diabetologia*, 45(9):1201–1210, Sep 2002.
- [158] S. J. Smith, S. Cases, D. R. Jensen, H. C. Chen, E. Sande, B. Tow, D. A. Sanan, J. Raber, R. H. Eckel, and R. V. Farese. Obesity resistance and multiple mechanisms of triglyceride synthesis in mice lacking Dgat. *Nat. Genet.*, 25(1):87–90, May 2000.
- [159] C. A. Harris, J. T. Haas, R. S. Streeper, S. J. Stone, M. Kumari, K. Yang, X. Han, N. Brownell, R. W. Gross, R. Zechner, and R. V. Farese. DGAT enzymes are required for triacylglycerol synthesis and lipid droplets in adipocytes. *J. Lipid Res.*, 52(4):657–667, Apr 2011.
- [160] M. S. RABEN and C. H. HOLLENBERG. Effect of glucose and insulin on the esterification of fatty acids by isolated adipose tissue. *J. Clin. Invest.*, 39:435–439, Feb 1960.
- [161] F. Picard, N. Naimi, D. Richard, and Y. Deshaies. Response of adipose tissue lipoprotein lipase to the cephalic phase of insulin secretion. *Diabetes*, 48(3):452–459, Mar 1999.
- [162] G. Dimitriadis, P. Mitrou, V. Lambadiari, E. Maratou, and S. A. Raptis. Insulin effects in muscle and adipose tissue. *Diabetes Res. Clin. Pract.*, 93 Suppl 1:S52–59, Aug 2011.
- [163] R. Zechner, J. G. Strauss, G. Haemmerle, A. Lass, and R. Zimmermann. Lipolysis: pathway under construction. *Curr. Opin. Lipidol.*, 16(3):333–340, Jun 2005.

- 
- [164] G. Y. Carmen and S. M. Victor. Signalling mechanisms regulating lipolysis. *Cell. Signal.*, 18(4):401–408, Apr 2006.
- [165] D. Langin. Adipose tissue lipolysis as a metabolic pathway to define pharmacological strategies against obesity and the metabolic syndrome. *Pharmacol. Res.*, 53(6):482–491, Jun 2006.
- [166] M. Laclaustra, D. Corella, and J. M. Ordovas. Metabolic syndrome pathophysiology: the role of adipose tissue. *Nutr Metab Cardiovasc Dis*, 17(2):125–139, Feb 2007.
- [167] H. Kuriyama, I. Shimomura, K. Kishida, H. Kondo, N. Furuyama, H. Nishizawa, N. Maeda, M. Matsuda, H. Nagaretani, S. Kihara, T. Nakamura, Y. Tochino, T. Funahashi, and Y. Matsuzawa. Coordinated regulation of fat-specific and liver-specific glycerol channels, aquaporin adipose and aquaporin 9. *Diabetes*, 51(10):2915–2921, Oct 2002.
- [168] A. Marcinkiewicz, D. Gauthier, A. Garcia, and D. L. Brasaemle. The phosphorylation of serine 492 of perilipin a directs lipid droplet fragmentation and dispersion. *J. Biol. Chem.*, 281(17):11901–11909, Apr 2006.
- [169] D. L. Brasaemle. Thematic review series: adipocyte biology. The perilipin family of structural lipid droplet proteins: stabilization of lipid droplets and control of lipolysis. *J. Lipid Res.*, 48(12):2547–2559, Dec 2007.
- [170] M. Lafontan and D. Langin. Lipolysis and lipid mobilization in human adipose tissue. *Prog. Lipid Res.*, 48(5):275–297, Sep 2009.
- [171] G. Haemmerle, R. Zimmermann, M. Hayn, C. Theussl, G. Waeg, E. Wagner, W. Sattler, T. M. Magin, E. F. Wagner, and R. Zechner. Hormone-sensitive lipase deficiency in mice causes diglyceride accumulation in adipose tissue, muscle, and testis. *J. Biol. Chem.*, 277(7):4806–4815, Feb 2002.

- [172] R. Zimmermann, J. G. Strauss, G. Haemmerle, G. Schoiswohl, R. Birner-Gruenberger, M. Riederer, A. Lass, G. Neuberger, F. Eisenhaber, A. Hermetter, and R. Zechner. Fat mobilization in adipose tissue is promoted by adipose triglyceride lipase. *Science*, 306(5700):1383–1386, Nov 2004.
- [173] G. Haemmerle, A. Lass, R. Zimmermann, G. Gorkiewicz, C. Meyer, J. Rozman, G. Heldmaier, R. Maier, C. Theussl, S. Eder, D. Kratky, E. F. Wagner, M. Klingenspor, G. Hoefler, and R. Zechner. Defective lipolysis and altered energy metabolism in mice lacking adipose triglyceride lipase. *Science*, 312(5774):734–737, May 2006.
- [174] M. Ahmadian, M. J. Abbott, T. Tang, C. S. Hudak, Y. Kim, M. Bruss, M. K. Hellerstein, H. Y. Lee, V. T. Samuel, G. I. Shulman, Y. Wang, R. E. Duncan, C. Kang, and H. S. Sul. Desnutrin/ATGL is regulated by AMPK and is required for a brown adipose phenotype. *Cell Metab.*, 13(6):739–748, Jun 2011.
- [175] J. Osuga, S. Ishibashi, T. Oka, H. Yagyu, R. Tozawa, A. Fujimoto, F. Shionoiri, N. Yahagi, F. B. Kraemer, O. Tsutsumi, and N. Yamada. Targeted disruption of hormone-sensitive lipase results in male sterility and adipocyte hypertrophy, but not in obesity. *Proc. Natl. Acad. Sci. U.S.A.*, 97(2):787–792, Jan 2000.
- [176] A. Guilherme, J. V. Virbasius, V. Puri, and M. P. Czech. Adipocyte dysfunctions linking obesity to insulin resistance and type 2 diabetes. *Nat. Rev. Mol. Cell Biol.*, 9(5):367–377, May 2008.
- [177] I. J. Lodhi, L. Yin, A. P. Jensen-Urstad, K. Funai, T. Coleman, J. H. Baird, M. K. El Ramahi, B. Razani, H. Song, F. Fu-Hsu, J. Turk, and C. F. Semenkovich. Inhibiting adipose tissue lipogenesis reprograms thermogenesis and PPAR $\alpha$  activation to decreased diet-induced obesity. *Cell Metab.*, 16(2) : 189 – –201, Aug2012.
- [178] L. Luo and M. Liu. Adipose tissue in control of metabolism. *J. Endocrinol.*, 231(3):R77–R99, Dec 2016.

- [179] N. Maeda, I. Shimomura, K. Kishida, H. Nishizawa, M. Matsuda, H. Nagaretani, N. Furuyama, H. Kondo, M. Takahashi, Y. Arita, R. Komuro, N. Ouchi, S. Kihara, Y. Tochino, K. Okutomi, M. Horie, S. Takeda, T. Aoyama, T. Funahashi, and Y. Matsuzawa. Diet-induced insulin resistance in mice lacking adiponectin/ACRP30. *Nat. Med.*, 8(7):731–737, Jul 2002.
- [180] F. M. van Dielen, C. van't Veer, A. M. Schols, P. B. Soeters, W. A. Burman, and J. W. Greve. Increased leptin concentrations correlate with increased concentrations of inflammatory markers in morbidly obese individuals. *Int. J. Obes. Relat. Metab. Disord.*, 25(12):1759–1766, Dec 2001.
- [181] Y. Yamamoto, H. Hirose, I. Saito, M. Tomita, M. Taniyama, K. Matsumura, Y. Okazaki, T. Ishii, K. Nishikai, and T. Saruta. Correlation of the adipocyte-derived protein adiponectin with insulin resistance index and serum high-density lipoprotein-cholesterol, independent of body mass index, in the Japanese population. *Clin. Sci.*, 103(2):137–142, Aug 2002.
- [182] L. K. Heilbronn, J. Rood, L. Janderova, J. B. Albu, D. E. Kelley, E. Ravussin, and S. R. Smith. Relationship between serum resistin concentrations and insulin resistance in nonobese, obese, and obese diabetic subjects. *J. Clin. Endocrinol. Metab.*, 89(4):1844–1848, Apr 2004.
- [183] A. Armani, V. Marzolla, G. M. Rosano, A. Fabbri, and M. Caprio. Phosphodiesterase type 5 (PDE5) in the adipocyte: a novel player in fat metabolism? *Trends Endocrinol. Metab.*, 22(10):404–411, Oct 2011.



## Chapter 2

Tamoxifen affects glucose and lipid metabolism parameters, causes browning of subcutaneous adipose tissue and transient body composition changes in C57BL/6NTac mice

Nico Hesselbarth<sup>a</sup>, Chiara Pettinelli<sup>a</sup>, Martin Gericke<sup>b</sup>, Claudia Berger<sup>c</sup>,  
Anne Kunath<sup>d</sup>, Michael Stumvoll<sup>a</sup>, Matthias Blüher<sup>a</sup>, Nora Klötting<sup>c,\*</sup>

<sup>a</sup>Department of Medicine, University of Leipzig, D-04103 Leipzig, Germany

<sup>b</sup>Institute of Anatomy, University of Leipzig, D-04103 Leipzig, Germany

<sup>c</sup>IFB Adiposity Disease, Core Unit Animal Models, University of Leipzig,  
D-04103 Leipzig, Germany

<sup>d</sup>German Center for Diabetes Research (DZD), Leipzig, Germany

*Biochemical and Biophysical Research Communications*

(2015) 464(3):724–729

## 2.1 Abstract

Tamoxifen is a selective estrogen receptor (ER) modulator which is widely used to generate inducible conditional transgenic mouse models. Activation of ER signaling plays an important role in the regulation of adipose tissue (AT) metabolism. We therefore tested the hypothesis that tamoxifen administration causes changes in AT biology in vivo. 12 weeks old male C57BL/6NTac mice were treated with either tamoxifen (n = 18) or vehicle (n = 18) for 5 consecutive days. Tamoxifen treatment effects on body composition, energy homeostasis, parameters of AT biology, glucose and lipid metabolism were investigated up to an age of 18 weeks.

We found that tamoxifen treatment causes: I) significantly increased HbA<sub>1c</sub>, triglyceride and free fatty acid serum concentrations (p < 0.01), II) browning of subcutaneous AT and increased UCP-1 expression, III) increased AT proliferation marker *Ki67* mRNA expression, IV) changes in adipocyte size distribution, and V) transient body composition changes.

Tamoxifen may induce changes in body composition, whole body glucose and lipid metabolism and has significant effects on AT biology, which need to be considered when using Tamoxifen as a tool to induce conditional transgenic mouse models. Our data further suggest that tamoxifen-treated wildtype mice should be characterized in parallel to experimental transgenic models to control for tamoxifen administration effects.

## 2.2 Introduction

Conditional transgenic mouse models provide a powerful tool for functional analyses of genes expressed preferentially in a particular tissue. Efficient silencing of a specific gene can be achieved by the CreER-*loxP* recombination technology, which allows for a temporally and tissue-specifically (promoter dependent) regulated recombination induced by tamoxifen administration [1]. Tamoxifen is a selective estrogen receptor (ER) modulator, which may affect whole body metabolism, but also adipose tissue (AT) biology. In ovariectomized rats, tamoxifen mimicked the effects of estradiol and caused signifi-

cant changes in food intake, body weight and composition [2].

Although expression of the CreER tamoxifen-induced system (CreER(T)<sup>2</sup>) in adipocytes does not seem to affect AT biology itself [3], [4], tamoxifen may contribute to the regulation of various AT processes. Therefore, we tested the hypothesis that tamoxifen administration causes changes in parameters of AT biology, whole body glucose and lipid metabolism in male C57BL/6NTac mice.

## 2.3 Material and methods

### 2.3.1 Animals

Animal experiments followed the ‘Principles of laboratory animal care’ (NIH publication no. 85–23, revised 1985) as well as specific national laws approved by the local authorities of the state of Saxony, Germany as recommended by the responsible local animal ethics review board (Regierungspräsidium Leipzig, TVV21.23/12, Germany). Twenty 11 weeks old C57BL/6NTac male mice were obtained from Taconic Laboratories (Taconic Europe, Denmark) and randomly assigned to either tamoxifen (n = 18) or vehicle (Miglyol, n = 18) administration groups. Tamoxifen (SigmaAldrich; #T5648-1G, St. Louis, MO, USA) was dissolved in Miglyol (Fagron, #700282-0001, Rotterdam, NL) at a concentration of 20 mg/ml. At an age of 12 weeks, 1 mg tamoxifen or 50  $\mu$ l Miglyol was administered intraperitoneally for five consecutive days, changing the injection site daily. All mice were housed in pathogen-free facilities in groups of three to five at  $22 \pm 2$  °C on a 12-h light/dark cycle. All animals had free access to water and were fed with standard chow (Sniff GmbH, Soest, Germany).

### 2.3.2 Phenotypic characterization

Mice were studied from 10 up to an age of 18 weeks. Body weight and food intake were recorded daily; naso-anal length and rectal body temperature (TH-5, Thermalert Monitoring Thermometer, Clifton, NJ, USA) were

measured at the end at 18 weeks of age ( $n = 10$  per experimental group). Intraperitoneal insulin tolerance tests (ITTs) were performed at the age of 11 and 16 weeks as described previously [5]. Whole body composition (fat mass, lean mass, water) was determined in awake mice by using NMR technology with EchoMRI700<sup>TM</sup> instrument (Houston, TX, USA) at 11, 13, 15 and 17 weeks of age. Indirect calorimetry was assessed by a Calorimetry Module (TSE Systems, Bad Homburg, Germany) at an age of 16 weeks as previously described [5].

Mice were sacrificed at the age of 18 weeks by an overdose of isofluran (Baxter, Unterschleißheim, Germany). Liver, brown (BAT), subcutaneous (SC) and epigonadal (EPI) adipose tissue were immediately removed and weighed.

### 2.3.3 Analytical procedures

Blood glucose values were determined from whole venous blood samples using a glucose monitor (FreeStyle, Abbott GmbH, Ludwigshafen, Germany). Insulin, leptin and adiponectin serum concentrations were measured by ELISA (mInsulin/Leptin ELISA; CrystalChem Inc, Downers Grove, IL., Adiponectin ELISA; AdipoGen Inc, Incheon, Korea). Serum lipid profile and HbA<sub>1c</sub> level were measured by an automated analyzer (COBAS8000, Roche, Basel, Switzerland).

### 2.3.4 Adipocyte size and AT histology

Adipocytes were isolated from (EPI) and (SC) fat pads by 1 mg/ml collagenase digestion and adipocyte size distribution was determined in 200 ml suspension in a Coulter Counter (Multisizer III; Beckman Coulter, Krefeld, Germany) as described [5]. Biopsies of SC and EPI AT were fixed in 10% buffered formalin and imbedded in paraffin. Multiple sections were obtained from EPI and SC fat pads and analyzed systematically with respect to adipocyte size and number. The sections were stained with hematoxylin/eosin and UCP-1 (1:200, Abcam, ab10983, Cambridge, UK) immunohistochemistry was performed as previously described [5].

### 2.3.5 mRNA expression

Total RNA was isolated from SC and EPI AT and cDNA was subsequently amplified as described [5]. Customized primers (Biomers, Ulm, Germany) were used for the detection of *Esr1*, *Ucp1*, *Ki67*, *18Sr* and *L19r* mRNA (Table 1). mRNA expression was measured in a fluorescence temperature cyclers (ABI PRISM7500, Applied Biosystems, Darmstadt, Germany) and calculated relative to *18S* or *L19* rRNA.

### 2.3.6 Western blot analyses

SC and EPI AT was removed and homogenized with tissue-mill homogenizer (MM400Retsch GmbH, Haan, Germany) in sucrose buffer as previously described [5] with antibodies raised against Estrogen Receptor alpha (ER $\alpha$ , 1:500, Abcam, ab32063, Cambridge, UK) and Uncoupling protein 1 (UCP1, 1:200, ab10983, Cambridge, UK). D-glyceraldehyde-3-phosphate dehydrogenase antibody (GAPDH, 1:3.000; Research Diagnostics, Flanders, Netherlands) served as loading control.

### 2.3.7 Statistical analyses

Data are given as means  $\pm$  SEM. Data sets were analyzed for statistical significance using a two-tailed unpaired t test or ANOVA. P values less than  $< 0.05$  were considered significant.

## 2.4 Results

### 2.4.1 Tamoxifen administration transiently affects body composition

During the entire study course, tamoxifen administration did not affect body weight dynamics, food intake, energy expenditure (mean oxygen consumption), spontaneous activity (Fig.1A-D), CO<sub>2</sub> production, respiratory quotient, water intake (data not shown). However, tamoxifen led to an acute

decrease in body fat mass 1 week after initiation of the treatment, which converted into a significantly higher relative body fat mass 5 weeks after the treatment (Fig. 1E) with reciprocal effects on lean body mass (Fig. 1F). In contrast, there were no significant body composition changes in vehicle treated controls (Fig. 1E and F). At 18 weeks, there was only a trend for higher relative organ weights of both subcutaneous (SC) and epigonadal AT of mice treated with tamoxifen (Fig. 2A and B).

### 2.4.2 Tamoxifen administration induces browning and adipocyte proliferation in subcutaneous AT

In an automated adipocyte size analysis, we found that tamoxifen administration led to a bimodal adipocyte distribution curve (Fig. 2C). Analysis of histological AT slides confirmed a significant reduction of mean adipocyte size in SC AT (Table 2) and the appearance of multilocular and mitochondria-rich adipocytes. The two adipocyte size peaks may therefore represent distinct subclasses of adipocytes. We then tested the hypothesis that tamoxifen may induce browning of SC AT. Indeed, positive UCP-1 immunostaining in AT (SC > epigonadal) of tamoxifen treated mice, but not in controls suggests a change of a subgroup of adipocytes into a more brown-like phenotype (Fig. 2D). At the mRNA level, tamoxifen treated mice displayed significantly higher (in SC AT) *Ucp-1* expression 6 weeks after tamoxifen administration (Fig. 2E), which could be confirmed at least as a tendency for UCP-1 protein (Fig. 2E).

Moreover, as a marker for increased proliferation, we found significantly higher *Ki67* expression in SC AT of mice treated with tamoxifen as compared to controls (Fig. 2F).

Tamoxifen effects on AT biology may be caused by alterations in ER expression. Supporting this hypothesis, we found higher Estrogen Receptor- $\alpha$  protein expression in tamoxifen treated compared to control mice (Fig. 2G).

### **2.4.3 Tamoxifen administration induces changes in glucose and lipid metabolism**

6 weeks after tamoxifen administration, we found a significantly higher HbA<sub>1c</sub> in tamoxifen compared to vehicle treated mice (Fig. 2H). This significant difference could not be explained by group differences in insulin sensitivity as determined by ITTs at 16 weeks (data not shown), adiponectin or insulin serum concentrations at 18 weeks (Table 2). In addition, tamoxifen administration causes significantly higher serum triglyceride and free fatty acid concentrations (Fig. 2I and J) at 18 weeks. In contrast, total cholesterol, HDL- and LDL-cholesterol were not different between tamoxifen and vehicle treated mice (Table 2).



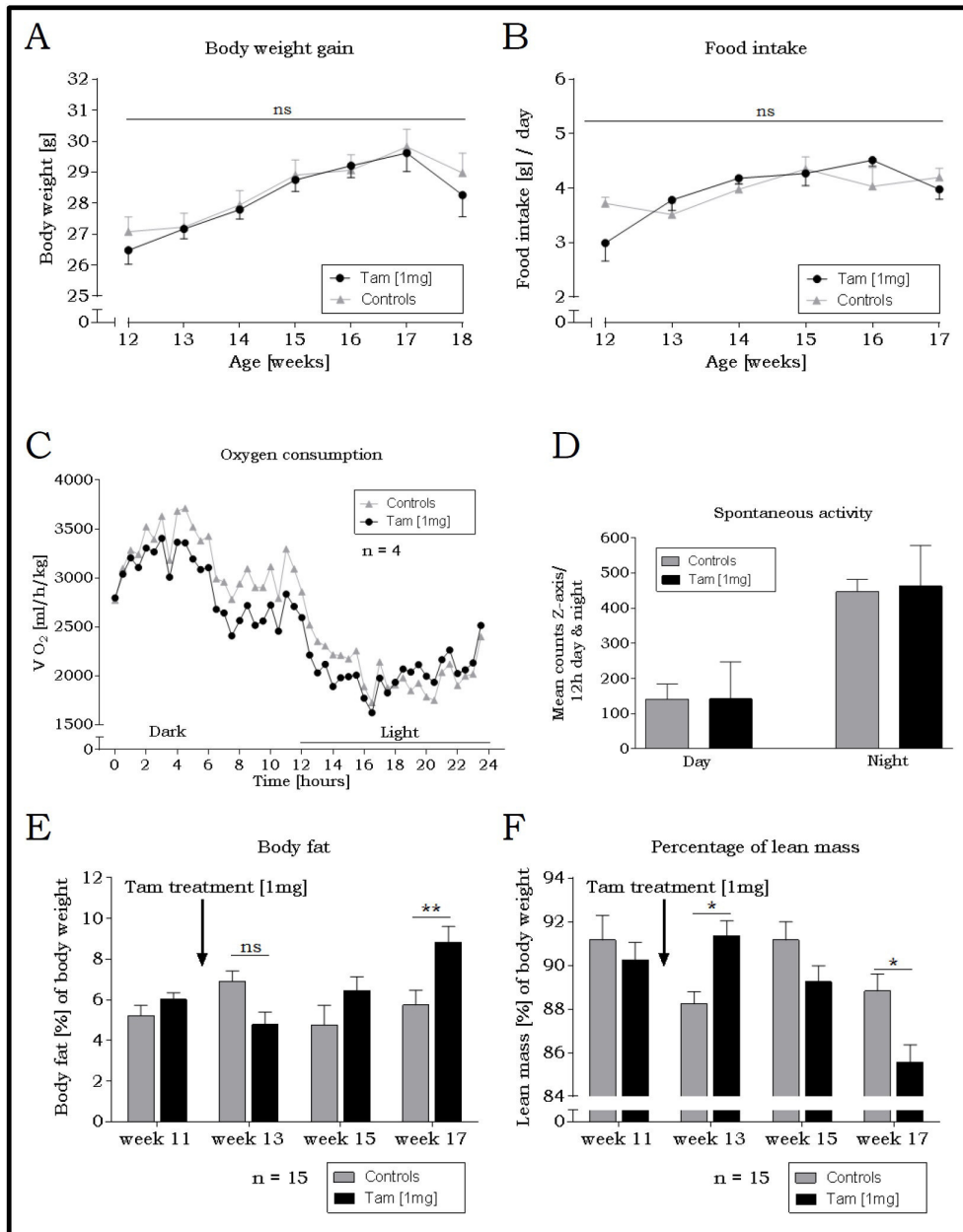


Figure 2.1: Effects of tamoxifen on body composition and energy expenditure. (A) Body weight change and (B) food intake were indistinguishable between Tamoxifen (Tam) treated mice ( $N = 10$ ) and controls (Con) ( $N = 10$ ) over the entire study period. (C) Mean oxygen consumption ( $VO_2$ ) in tamoxifen (Tam) treated ( $N = 4$ ) and control mice ( $N = 4$ ) at an age of 17 weeks. (D) Spontaneous activity was estimated as sit up of the mice on the z-axis and depicted as means over an observation period of overall 72 h. Whole body fat mass (E) and lean mass (F) was determined in awake mice by using NMR technology (EchoMRI700, Medical Systems, Houston, TX, USA) in control ( $N = 15$ ) and tamoxifen-treated mice ( $N = 15$ ) at 11, 13, 15 and 17 weeks of age. Data are given as means  $\pm$  SEM. \*,  $p < 0.05$ ; \*\*,  $p < 0.01$ .

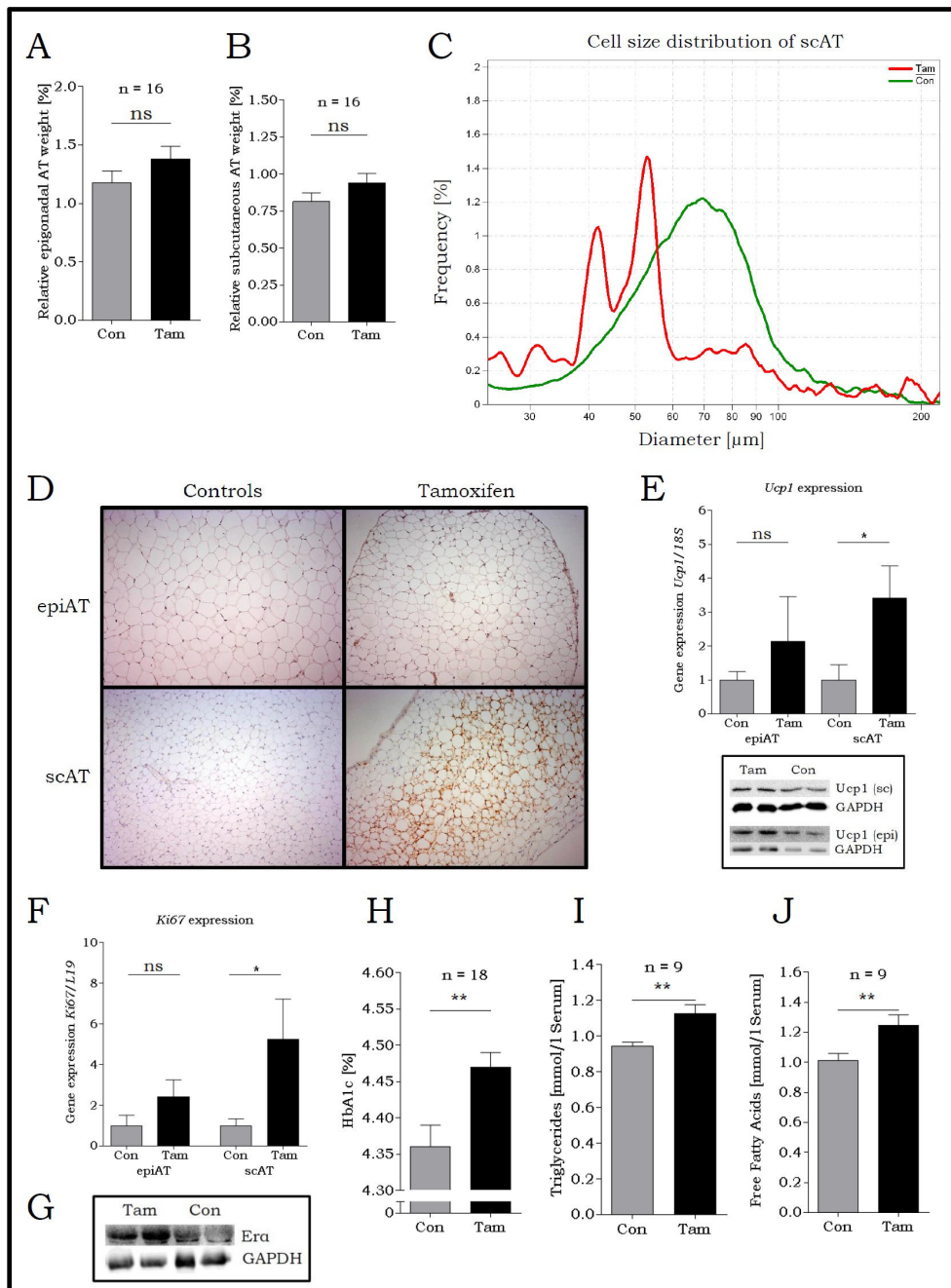


Figure 2.2: Effects of tamoxifen on adipose tissue biology and parameters of glucose and lipid metabolism. Relative weight of epigonadal (A) and subcutaneous (B) adipose tissue (AT) are presented relative to total body weight from control (Con; N = 16) and tamoxifen treated (Tam; N = 16) mice. (C) Subcutaneous cell size (scAT) distribution of adipocytes measured in a Coulter Counter (Multisizer III; Beckman Coulter, Krefeld, Germany). 6 weeks after initiation of tamoxifen administration (red), adipocyte size distribution changes towards a bimodal curve and smaller mean adipocyte diameters as compared to controls (green). The two peaks of the adipocyte size distribution curve in tamoxifen treated mice may represent distinct cell types (beige/brite versus white adipocytes).

Figure 2.2: (Previous page.) (D) Representative images (original magnification x200) of UCP-1 immunohistochemistry (positive staining of the UCP-1 protein with DAB as chromogen in brown) of epigonadal (epiAT) and subcutaneous (scAT) adipose tissue 5 mm paraffin sections of control mice (left panels) and tamoxifen treated mice (right panels) at an age of 18 weeks. SC adipose tissue of tamoxifen treated mice displays strongly positive UCP-1 staining (supporting a browning effect of tamoxifen), whereas control mice in both fat depots and epigonadal tissue of tamoxifen treated mice were UCP-1 negative. (E) *Ucp-1* mRNA analyses revealed a significantly higher expression in scAT of tamoxifen treated mice compared to controls, whereas in epiAT there was only a non-significant trend for higher *Ucp-1* expression in tamoxifen treated mice compared to controls (n = 6 per treatment group). Representative Western blots for UCP-1 (compared to GAPDH) of subcutaneous (sc) and epigonadal (epi) adipose tissue of control (Con) and tamoxifen treated (Tam) mice. (F) Expression of proliferation marker *Ki67* was significantly higher in scAT of tamoxifen treated (Tam; N = 6) mice compared to controls (Con; N = 6), whereas in epiAT no significant differences could be observed. (G) Representative Western blots for ER $\alpha$  compared to GAPDH of epigonadal adipose tissue of control (Con) and tamoxifen treated (Tam) mice. Tamoxifen administration caused significantly higher (H) HbA<sub>1c</sub>, (I) triglyceride, and (J) free fatty acids serum concentrations at 18 weeks compared to controls (n = 18). Data are given as means  $\pm$  SEM. (\*, p < 0.05; ns, non-significant). (For interpretation of the references to colour in this figure legend, the reader is referred to the web version of this article.)

Table 2.1: Primer sequences used for mRNA detection.

Gene	Forward	Backward	Acc. no
<i>Ki67</i>	TGAAGTCAAAGAGCAAGAGGTATGA	TTCAAGTCCCCAAAGCCTGG	AC_000029
<i>Ucp1</i>	ACTGCCACACCTCCAGTCATT	TTGTCATCTACGGGCACAAAG	AC_000030.1
<i>Esr1</i>	TCTCTGGGCGACATTCCTCT	GCTTTGGTGTGAAGGGTCAT	AC_000032.1
<i>L19</i>	GGAAAAAGAAGGTCTGGTTGGA	TGCTGCTGTTCCCTGTTTTTC	NC_000077.6

Table 2.2: Characterization of treatment groups. Circulating parameters of lipid and glucose metabolism as well as parameters of adipose tissue biology at an age of 18 weeks (N = 18). FFA, free fatty acids, epiAT, epigonadal adipose tissue, scAT, subcutaneous adipose tissue. Data are given as means  $\pm$  SEM. Data sets were analyzed for statistical significance using a two-tailed unpaired t test (\*p-value < 0.05; \*\*p-value < 0.001)

Parameter	Controls	Tamoxifen	p-value
Triglycerides [mmol/l]	0.94 $\pm$ 0.02	1.13 $\pm$ 0.05	**
Total cholesterol [mmol/l]	2.42 $\pm$ 0.10	2.35 $\pm$ 0.20	ns
HDL-cholesterol [mmol/l]	2.20 $\pm$ 0.10	2.06 $\pm$ 0.18	ns
LDL-cholesterol [mmol/l]	0.27 $\pm$ 0.02	0.30 $\pm$ 0.04	ns
FFA [mmol/l]	1.01 $\pm$ 0.05	1.25 $\pm$ 0.07	*
Leptin [ng/ml]	42.9 $\pm$ 8.28	36.5 $\pm$ 5.73	ns
Adiponectin [mg/ml]	68.5 $\pm$ 3.67	64.9 $\pm$ 4.22	ns
Insulin [mg/l]	1.03 $\pm$ 0.16	1.10 $\pm$ 0.11	ns
HbA <sub>1c</sub> [%]	4.36 $\pm$ 0.03	4.47 $\pm$ 0.02	**
Relative liver weight [%]	4.85 $\pm$ 0.19	4.65 $\pm$ 0.16	ns
Relative BAT weight [%]	0.37 $\pm$ 0.03	0.33 $\pm$ 0.06	ns
Mean cell size scAT [ $\mu$ m]	71.3 $\pm$ 1.89	62.9 $\pm$ 2.82	*
Mean cell size epiAT [ $\mu$ m]	84.8 $\pm$ 4.62	88.9 $\pm$ 4.11	ns
Adipocytes/mg scAT (n)	341 $\pm$ 37	357 $\pm$ 50	ns
Adipocytes/mg epiAT (n)	337 $\pm$ 21	445 $\pm$ 56	ns

## 2.5 Discussion

Tamoxifen has been widely used to activate Cre-recombinase that spatiotemporally controls target gene expression in animal models. Recently, it has been demonstrated that tamoxifen itself may affect adipose tissue accumulation and function by inducing reactive oxygen species production, apoptosis and autophagy [6]. We confirm the observed reduction in fat mass [6], which was transient and followed by an over-compensation resulting in increased fat mass. The higher percentage of fat mass in Tam treated animals compared to controls is consistent with previous research works, which suggest a negative impact of Tamoxifen on body composition, translating into increased fat content in women who undergo this treatment [7], [8].

In addition, we identified previously unrecognized effects of tamoxifen on browning of subcutaneous AT, adipocyte proliferation, but also tamoxifen-associated changes in glucose and lipid metabolism. Together with the notion, that tamoxifen may induce apoptosis in AT followed by a recovery phase [6], additional changes in AT biology have to be considered which may affect whole body glucose and lipid homeostasis even after normalization of AT function. To check if cell proliferation is influenced we performed gene expression analysis of proliferation marker *Ki67* [9]. Expression levels of *Ki67* were significantly increased in subcutaneous AT of Tam treated animals compared to controls. This finding suggests that Tamoxifen injection promotes cellular division in subcutaneous AT, which could be another evidence of brown adipocyte proliferation.

We could confirm that Tamoxifen induced up-regulation of *ER $\alpha$*  which was obtained by previous studies on the reproductive system: Tam treatment was associated with up-regulation of *ER $\alpha$*  in seminal vesicles of neonatal male rats [10] and in the uterus and vagina of neonatal and ovariectomized adult mice [11]. These results suggest that Tamoxifen up-regulates *ER $\alpha$*  expression by increasing promoter activity of the *ER $\alpha$*  gene (*Ers1*) at the transcriptional level [12].

Furthermore, Tam treated animals showed increased serum levels of triglycerides and free fatty acids compared to control animals. Serum HDL, LDL

and total cholesterol levels were comparable between the two groups, in spite of what was shown by previous investigations [13], [14]. Higher levels of serum triglycerides and free fatty acids might be a direct consequence of the conversion from white to beige adipocytes, because as known from literature lipid droplets of brown and beige adipocytes are smaller and scattered throughout. An important limitation of our study is that data presented herein only reflect the time up to 6 weeks after tamoxifen administration and long-term effects have not been evaluated.

Taken together, the observed effects of tamoxifen on AT biology and circulating parameters of glucose and lipid metabolism may confound the functional study of target genes in adipose tissue. Therefore, we propose that experiments using the CreER tamoxifen-induced system to generate transgenic mice should include appropriate tamoxifen-treated wildtype controls.

## **2.6 Contribution statement**

All authors made substantial contribution to the concept and design of this study, acquisition of data or analyses and interpretation of data and to drafting of the article. All authors gave final approval of the version to be published. NH and NK are the guarantors of this work, had full access to all data and take fully responsibility for integrity of data and the accuracy of data analysis.

## **2.7 Duality of interest**

The authors declare that there is no duality interest associated with the manuscript.

## **2.8 Acknowledgments**

We would like to thank Eva Böge, Viola Döbel and Daniela Kern of University of Leipzig for technical assistance. This work was supported by GV-SOLAS

(ADI-014 to NK), Deutsche Forschungsgemeinschaft (SFB B01 to MB, B04 to NK), and supported by the Federal Ministry of Education and Research (BMBF), Germany, FKZ: 01EO1501 (N. Klötting) and FKZ: 82DZD00601 (M. Stumvoll).

## 2.9 Transparency document

Transparency document related to this article can be found online at <http://dx.doi.org/10.1016/j.bbrc.2015.07.015>.

## 2.10 References

- [1] V. Vasioukhin, L. Degenstein, B. Wise, and E. Fuchs. The magical touch: genome targeting in epidermal stem cells induced by tamoxifen application to mouse skin. *Proc. Natl. Acad. Sci. U.S.A.*, 96(15):8551–8556, Jul 1999.
- [2] G. N. Wade and H. W. Heller. Tamoxifen mimics the effects of estradiol on food intake, body weight, and body composition in rats. *Am. J. Physiol.*, 264(6 Pt 2):R1219–1223, Jun 1993.
- [3] K. Y. Lee, S. J. Russell, S. Ussar, J. Boucher, C. Vernochet, M. A. Mori, G. Smyth, M. Rourk, C. Cederquist, E. D. Rosen, B. B. Kahn, and C. R. Kahn. Lessons on conditional gene targeting in mouse adipose tissue. *Diabetes*, 62(3):864–874, Mar 2013.
- [4] A. Sassmann, S. Offermanns, and N. Wettschureck. Tamoxifen-inducible Cre-mediated recombination in adipocytes. *Genesis*, 48(10):618–625, Oct 2010.
- [5] M. Kern, J. Kosacka, N. Hesselbarth, J. Bruckner, J. T. Heiker, G. Flehmig, I. Klötting, P. Kovacs, M. Matz-Soja, R. Gebhardt, K. Krohn, S. Sales, K. Abshagen, A. Shevchenko, M. Stumvoll, M. Bluher, and N. Klötting. Liver-restricted Repin1 deficiency improves

- whole-body insulin sensitivity, alters lipid metabolism, and causes secondary changes in adipose tissue in mice. *Diabetes*, 63(10):3295–3309, Oct 2014.
- [6] L. Liu, P. Zou, L. Zheng, L. E. Linarelli, S. Amarell, A. Passaro, D. Liu, and Z. Cheng. Tamoxifen reduces fat mass by boosting reactive oxygen species. *Cell Death Dis*, 6:e1586, Jan 2015.
- [7] P. A. Ali, F. H. al Ghorabie, C. J. Evans, A. M. el Sharkawi, and D. A. Hancock. Body composition measurements using DXA and other techniques in tamoxifen-treated patients. *Appl Radiat Isot*, 49(5-6):643–645, 1998.
- [8] P. M. Sheean, K. Hoskins, and M. Stolley. Body composition changes in females treated for breast cancer: a review of the evidence. *Breast Cancer Res. Treat.*, 135(3):663–680, Oct 2012.
- [9] T. Scholzen and J. Gerdes. The Ki-67 protein: from the known and the unknown. *J. Cell. Physiol.*, 182(3):311–322, Mar 2000.
- [10] K. Williams, J. S. Fisher, K. J. Turner, C. McKinnell, P. T. Saunders, and R. M. Sharpe. Relationship between expression of sex steroid receptors and structure of the seminal vesicles after neonatal treatment of rats with potent or weak estrogens. *Environ. Health Perspect.*, 109(12):1227–1235, Dec 2001.
- [11] T. Sato, Y. Ohta, H. Okamura, S. Hayashi, and T. Iguchi. Estrogen receptor (ER) and its messenger ribonucleic acid expression in the genital tract of female mice exposed neonatally to tamoxifen and diethylstilbestrol. *Anat. Rec.*, 244(3):374–385, Mar 1996.
- [12] Y. Miyoshi, K. Murase, M. Saito, M. Imamura, and K. Oh. Mechanisms of estrogen receptor- $\alpha$  upregulation in breast cancers. *Med Mol Morphol*, 43(4):193–196, Dec 2010.
- [13] A. M. Dnistrian, M. K. Schwartz, E. J. Greenberg, C. A. Smith, and D. C. Schwartz. Effect of tamoxifen on serum cholesterol and lipopro-



teins during chemohormonal therapy. *Clin. Chim. Acta*, 223(1-2):43–52, Dec 1993.

- [14] A. L. Holleran, B. Lindenthal, T. A. Aldaghlis, and J. K. Kelleher. Effect of tamoxifen on cholesterol synthesis in HepG2 cells and cultured rat hepatocytes. *Metab. Clin. Exp.*, 47(12):1504–1513, Dec 1998.

# Chapter 3

Repin1 deficiency improves insulin sensitivity and  
glucose metabolism in *db/db* mice by reducing adipose  
tissue mass and inflammation

Anne Kunath<sup>a,1</sup>, Nico Hesselbarth<sup>b,1</sup>, Martin Gericke<sup>c</sup>, Matthias Kern<sup>a</sup>,  
Sebastian Dommel<sup>d</sup>, Peter Kovacs<sup>d</sup>, Michael Stumvoll<sup>a,b,d</sup>, Matthias  
Blüher<sup>a,b,d</sup>, Nora Klötting<sup>d,\*</sup>

<sup>a</sup>German Diabetes Center Leipzig, University of Leipzig, 04103, Leipzig,  
Germany

<sup>b</sup>Department of Medicine, University of Leipzig, 04103, Leipzig, Germany

<sup>c</sup>Institute of Anatomy, University of Leipzig, 04103, Leipzig, Germany

<sup>d</sup>IFB AdiposityDiseases, University of Leipzig, 04103, Leipzig, Germany

<sup>1</sup>Equal contribution

*Biochemical and Biophysical Research Communications*

(2016) 478(1):398–402

### 3.1 Abstract

Replication initiator 1 (Repin1) is a zinc finger protein playing a role in insulin sensitivity, body fat mass and lipid metabolism by regulating the expression key genes of glucose and lipid metabolism. Here, we tested the hypothesis that introgression of a Repin1 deletion into *db/db* mice improves glucose metabolism *in vivo*. We generated a whole body Repin1 deficient *db/db* double knockout mouse (Rep1<sup>-/-</sup>x *db/db*) and systematically characterized the consequences of Repin1 deficiency on insulin sensitivity, glucose and lipid metabolism parameters and fat mass. Hyperinsulinemic-euglycemic clamp studies revealed significantly improved insulin sensitivity in Rep1<sup>-/-</sup>x *db/db* mice, which are also characterized by lower HbA<sub>1c</sub>, lower body fat mass and reduced adipose tissue (AT) inflammation area. Our study provides evidence that loss of Repin1 in *db/db* mice improves insulin sensitivity and reduces chronic hyperglycemia most likely by reducing fat mass and AT inflammation.

### 3.2 Introduction

Replication initiator 1 (Repin1) is a polydactyl zinc finger protein organized in three clusters with a mass of 60 kDa [1], [2], [3]. The gene is located in humans on chromosome 7, in mice on chromosome 6 and on chromosome 4 in rats [4]. Repin1 was first described as an origin specific DNA binding protein, which acts as an enhancer of DNA bending of the Chinese hamster dihydrofolate (*dhfr*) gene due to replication. It binds to two ATT-rich sites in *oriβ*, a short region 3' to the *dhfr* gene [1], [2]. As the case for many other zinc finger proteins, the cellular localization and function of Repin1 remains elusive.

Recently, we demonstrated that replication initiator 1 (Repin1) plays a role in the modulation of insulin sensitivity, fat accumulation, glucose and lipid metabolism by regulating the expression of key molecules involved in these processes [5], [6], [7]. Moreover, *REPIN1* mRNA expression in human adipose tissue is significantly associated with adipocyte size and parameters

of glucose metabolism [7]. To further investigate the role of Repin1 in glucose homeostasis, we generated a Repin1 deficient *db/db* knockout mouse model  $\text{Repin1}^{-/-} \times \text{db/db}$  and systematically characterized the consequences of Repin1 deficiency on insulin sensitivity, glucose and lipid metabolism parameters and fat mass.

### 3.3 Material and methods

#### 3.3.1 Animals

All animal studies were approved by the local authorities of the state of Saxony, Germany as recommended by the responsible local animal ethics review board (Landesregierung Leipzig, TVV21/14, T01/13, Germany). All mice were housed in pathogen-free facilities in groups of three to five at  $22 \pm 2$  °C on a 12-h light/dark cycle in our animal facility at the University of Leipzig. Animals were fed a standard chow diet and had *ad libitum* access to water at all times and food was only withdrawn if required for an experiment.

#### 3.3.2 Generation of whole body Repin1 ( $\text{Repin1}^{-/-}$ ) deficiency in *db/db* knockout mice

The *Repin1* gene was inactivated using conditional gene targeting strategies as previously described [5]. Mice with *loxP*-flanked Rep1 allele ( $\text{Repin1}^{flox/flox}$ ) were crossed with mice expressing a Cre-recombinase gene under the transcriptional control of a human cytomegalovirus (CMV) minimal promoter (B6.C-Tg(CMVcre)1Cgn/J; stock#006054 from Jackson Laboratory).  $\text{Repin1}^{-/-}$  mice were crossed with *db/+* mice (BKS.Cg-m+/+Lepr db/Bom/Tac; #0709F3, Taconic) to generate double knockout mice ( $\text{Repin1}^{-/-} \times \text{db/db}$ ). Genotyping was performed by PCR using genomic DNA isolated from the tail tip. Genotyping PCR was performed as previously described [5]. Knockdown efficiency was determined as by RT-PCR and Western Blot as previously described [5].

### 3.3.3 Phenotypic characterization

Eight male and female mice of each genotype ( $Rep1^{-/-}$   $db/db$  and control  $db/db$  littermates) were studied from the age of 6 up to 20 weeks. Body weight was recorded weekly; whole body composition (Echo Medical Systems, Houston, TX, USA) was measured once at the end of 20 weeks. At an age of 20 weeks organs (liver, epigonadal, subcutaneous AT) were weighed and relative organ mass was calculated, blood was taken for measuring HbA<sub>1c</sub> levels, and serum was collected for measurements of free fatty acids (FFA), total cholesterol, triglycerides, HDL-cholesterol, insulin, c-peptide, leptin, adiponectin and monocyte chemotactic protein (Mcp1) as previously described [5].

### 3.3.4 Hyperinsulinemic-euglycemic clamp studies

In a subgroup of 6 animals per genotype, hyperinsulinemic-euglycemic clamps were performed as described previously at an age of 20 weeks [8], [9]. Briefly, catheters were implanted in the left jugular vein and clamps started after an overnight fast. A 120 min hyperinsulinemic-euglycemic clamp was conducted with a continuous infusion of human insulin at a rate of 60 mU/kg/min. Insulin is infused at a constant rate resulting in a drop in blood glucose. To maintain blood glucose at a constant level, exogenous glucose (D20%) is infused into the circulation. Variable glucose infusion rate (GIR) is determined by measuring blood glucose at brief intervals throughout the experiment and adjusting the GIR accordingly. GIR was calculated as mg/kg/min.

### 3.3.5 Histology and immunohistochemistry

For evaluation of AT inflammation subcutaneous AT and visceral AT were fixed, paraffin embedded, sectioned and HE stained as described before [10]. Immunohistochemical staining of F4/80 was performed. Antigen retrieval in citrate buffer (pH 6.0) was applied using a microwave and sections were incubated with anti-F4/80 (1:200; Abcam; ab6640) overnight. Next day, after buffer rinses, appropriate biotin-coupled secondary antibody (1:200; Vector- Laboratories, Wertheim-Bettingen, Germany) was applied for 2 h

at RT. Binding of the primary antibody was visualized using an avidinebiotin (ABC) kit (Vector-Laboratories) with DAB as chromogen according to the manufacturer's instructions. For analysis of crown-like structure (CLS) density, five images of visceral AT were taken from each mouse at a 200-fold magnification. Number of CLS and number of adipocytes were counted blinded to the investigator. CLS density is presented as the ratio of CLS per 100 adipocytes. In addition, the area of inflammatory infiltrates identified in HE stained sections was measured and related to entire tissue area using ImageJ software v. 1.47 [11].

### 3.3.6 Statistical analysis

Data are given as means  $\pm$  SD. Data sets were analyzed for statistical significance using a students t-test. P values  $< 0.05$  were considered significant.

## 3.4 Results

### 3.4.1 Generation of whole body deletion of Repin1 in *db/db* mice (Rep1<sup>-/-</sup> × *db/db*)

In order to generate whole body deletion of Repin1 in *db/db* mice, *db/+* mice homozygous for the loxP-flanked Rep1 allele (Rep1<sup>lox/lox</sup>) were crossed with mice expressing a Cre-recombinase gene under the transcriptional control of a human cytomegalovirus (CMV) minimal promoter. Efficiency and specificity of the Repin1 knockout were examined in tissue from *db/db* and Rep1<sup>-/-</sup> × *db/db* by qPCR and Western blot analyses (Fig. 1a-b). Western blot and qPCR analysis confirmed a reduced Repin1 expression by  $\sim 70-80\%$  (Fig. 1a).

### 3.4.2 Growth, fat mass and tissue mass of double knock-outs ( $Rep1^{-/-}$ x $db/db$ )

Compared with  $db/db$ ,  $Rep1$  deficient  $db/db$  mice gained significantly less body weight starting at 8 weeks of age up to an age of 20 weeks (Fig. 1c-d). At an age of 20 weeks,  $Rep1^{-/-}$  x  $db/db$  mice have a  $\sim 10\%$  lower ( $p < 0.05$ ) body fat mass compared to  $db/db$  mice (Fig. 1e). *Repin1* deficiency did not have a significant influence on body length, relative liver weight (data not shown) and daily food intake (Fig. 1f).

### 3.4.3 *Repin1* deficiency improves insulin sensitivity

Hyperinsulinemic-euglycemic clamp studies revealed significantly higher whole body insulin sensitivity in  $Rep1^{-/-}$  x  $db/db$  compared to  $db/db$  mice (Fig. 1h). At the steady state, glucose infusion rate was  $\sim 20\%$  higher in  $Rep1$  deficient  $db/db$  mice (Fig. 1h). Moreover C-peptide and blood glucose levels were significantly reduced in  $Rep1^{-/-}$  x  $db/db$  compared to  $db/db$  (Table 1). Compared to  $db/db$  mice,  $Rep1^{-/-}$  x  $db/db$  have significantly lower HbA<sub>1c</sub> levels (Fig. 1g). Noteworthy, circulating parameters of lipid metabolism as well as leptin and adiponectin serum concentrations were not affected by the reduction of *Repin1* expression in  $db/db$  mice (Table 1).

### 3.4.4 *Repin1* deficiency causes reduced inflammatory infiltrates in AT

We detected inflammatory infiltrates, mainly consisting of polymorphonuclear neutrophils, in AT of all  $db/db$  mice, whereas inflammatory infiltrates were almost absent in  $Rep1^{-/-}$  x  $db/db$  mice (Fig. 1k-l). However, density of crown like structures, mainly consisting of macrophages, was similar in  $Rep1^{-/-}$  x  $db/db$  compared to control mice (Fig. 1i-j). Interestingly, circulating *Mcp1* levels were significantly reduced in  $Rep1^{-/-}$  x  $db/db$  compared to  $db/db$  mice (Table 1).



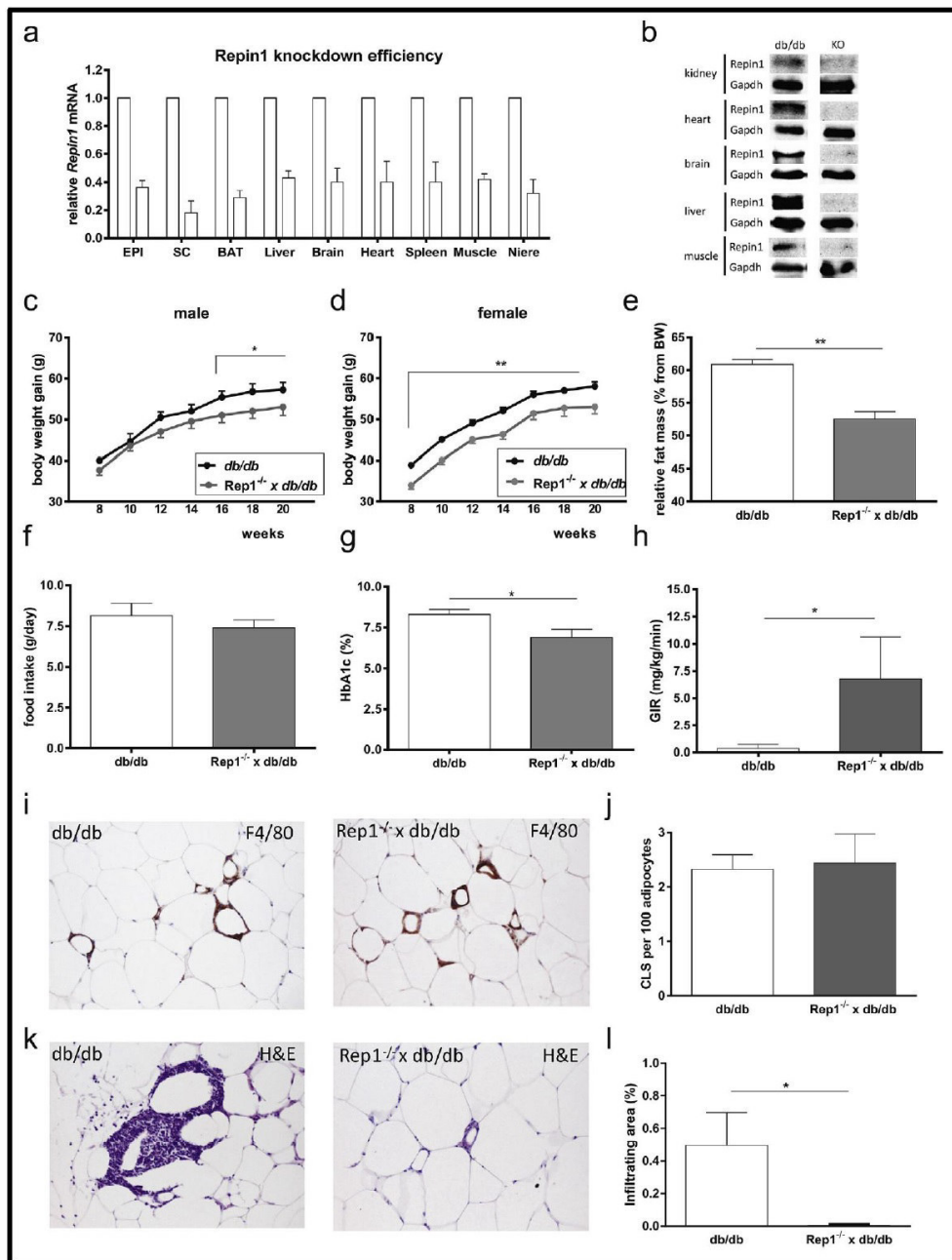


Figure 3.1: Phenotype of *Repin1* deficient *db/db* mice. (a) Knockdown efficiency on *Repin1* mRNA level in different tissues of *Rep1*<sup>-/-</sup> × *db/db* mice (N = 8) and *db/db* controls (N = 8). (b) Representative *Repin1* protein level (c, d) Growth phenotype of *Rep1*<sup>-/-</sup> × *db/db* mice (N = 8) and *db/db* littermate controls (N = 8) up to an age of 20 weeks was determined. *Rep1*<sup>-/-</sup> × *db/db* mice are significant lighter at an age of 16 weeks (a, male) and 8 weeks (b, female) up to an age of 20 weeks.

Figure 3.1: (Previous page.) (e) Whole body fat mass was determined in awake male mice by using nuclear magnetic resonance technology with EchoMRI700 instrument (Echo Medical Systems, Houston, TX, USA) in control *db/db* and *Rep1<sup>-/-</sup>x db/db* mice at 20 weeks of age. Data are presented as percentage of total body fat from body weight. Results are expressed as means  $\pm$  SE from at least 4 animals per genotype and time point. (f) Food intake was not affected at an age of 16 weeks. The daily food intake was calculated as the average intake of chow over a period of one week. Results are expressed as means  $\pm$  SE from at least 4 male animals per genotype. (g) Significant lower HbA<sub>1c</sub> (%) levels in male *Rep1<sup>-/-</sup>x db/db* mice (N = 8) compared to controls (N = 8) at an age of 20 weeks. Results are expressed as means  $\pm$  SE. (h) Glucose infusion rate (GIR) during a hyperinsulinemic-euglycemic clamp was increased in male *Rep1<sup>-/-</sup>x db/db* mice (N = 6) and *db/db* littermate controls (N = 6) at an age of 20 weeks. GIR was calculated as mg/kg/min. Results are expressed as means  $\pm$  SE. (i,j) Histological images of representative epigonadal AT slights and quantification (k,l) of crown like structures (CLS) areas and macrophages (F4-80antibody) from male *db/db* and *Rep1<sup>-/-</sup>x db/db* mice at an age of 20 weeks. For analysis of CLS density, five images of visceral AT were taken from each mouse at a 200-fold magnification. Number of CLS and number of adipocytes were counted blinded to the investigator. CLS density is presented as the ratio of CLS per 100 adipocytes. Area of inflammatory infiltrates identified in HE stained sections was measured and related to entire tissue area. The different degrees of significance was indicated as follows in the graphs- \*P < 0.05; \*\*P < 0.01; \*\*\*P < 0.001. All results are expressed as means  $\pm$  SE.

Table 3.1: Phenotype of *Repin1* deficient *db/db* male mice at an age of 20 weeks. Significant different at  $p < 0.05$  level, results indicate mean  $\pm$  SD.

	<b>db/db</b> N = 8	<b>Rep1<sup>-/-</sup>x db/db</b> N = 8
Triglyceride [mmol/l]	2.8 $\pm$ 1.0	1.9 $\pm$ 1.1
Total cholesterol [mmol/l]	4.7 $\pm$ 1.3	5.7 $\pm$ 1.1
HDL-cholesterol [mmol/l]	3.7 $\pm$ 0.9	3.8 $\pm$ 1.4
FFA [mmol/l]	2.8 $\pm$ 0.7	2.4 $\pm$ 0.8
Blood glucose [mmol/l]	20.1 $\pm$ 4.2	13.1 $\pm$ 8.0*
Fasting blood glucose [mmol/l]	15.2 $\pm$ 4.8	9.4 $\pm$ 4.9*
Adiponectin [ng/ml]	36 $\pm$ 13	33 $\pm$ 6
Insulin [ $\mu$ g/l]	4.9 $\pm$ 2.6	4.8 $\pm$ 2.7
C-peptid [nM]	5.5 $\pm$ 0.2	4.8 $\pm$ 0.6*
Leptin [ng/ml]	68 $\pm$ 24	75 $\pm$ 25
Mcp1 [pg/ml]	416 $\pm$ 92	274 $\pm$ 85*

### 3.5 Discussion

We demonstrate that Repin1 deletion significantly improves insulin sensitivity and chronic hyperglycemia in *db/db* mice. These beneficial effects of reduced Repin1 are most likely mediated by reduced fat mass and significantly lower inflammatory infiltrates areas in AT of *Rep1<sup>-/-</sup> × db/db* compared to *db/db* mice. Chronic inflammation of AT as well as chronic circulating inflammation [12] has been shown to play a crucial role in the development of obesity-associated insulin resistance [13]. Neutrophils secrete several proteases, one of which is neutrophil elastase, which can promote inflammatory responses in several disease models [14]. Furthermore reduced circulating levels of *Mcp1* may contribute to beneficial effects. One possibility is that absence of Repin1 generates signals that restricts against AT inflammation. Taken together, our findings indicate that alterations in Repin1 expression may contribute the pathogenesis of AT inflammation, insulin resistance and subsequent impairment of glucose homeostasis.

### 3.6 Funding

This work was supported by Deutsche Forschungsgemeinschaft (SFB1052; B04 to NK) and supported by the Federal Ministry of Education and Research (BMBF), Germany, FKZ: 01EO1501 (NK), DZD:82DZD00601 (AK, MS, NK).

### 3.7 Conflict of interest

The authors declare that there is no duality of interest associated with this manuscript.

### 3.8 Contribution statement

All authors made substantial contribution to the concept and design of this study, acquisition of data or analyses and interpretation of data and to draft-

ing of the article. All authors gave final approval of the version to be published. NH, AK and NK are the guarantors of this work, had full access to all data and take fully responsibility for integrity of data and the accuracy of data analysis.

### 3.9 Duality of interest

The authors declare that there is no duality interest associated with the manuscript.

### 3.10 Acknowledgements

We would like to thank Eva Böge, Viola Döbel, Susan Berthold and Daniela Kern of University of Leipzig for technical assistance.

### 3.11 Transparency document

Transparency document related to this article can be found online at <http://dx.doi.org/10.1016/j.bbrc.2016.07.038>

### 3.12 References

- [1] M. S. Caddle, L. Dailey, and N. H. Heintz. RIP60, a mammalian origin-binding protein, enhances DNA bending near the dihydrofolate reductase origin of replication. *Mol. Cell. Biol.*, 10(12):6236–6243, Dec 1990.
- [2] L. Dailey, M. S. Caddle, N. Heintz, and N. H. Heintz. Purification of RIP60 and RIP100, mammalian proteins with origin-specific DNA-binding and ATP-dependent DNA helicase activities. *Mol. Cell. Biol.*, 10(12):6225–6235, Dec 1990.
- [3] C. R. Houchens, W. Montigny, L. Zeltser, L. Dailey, J. M. Gilbert, and N. H. Heintz. The dhfr oribeta-binding protein RIP60 contains 15 zinc

- fingers: DNA binding and looping by the central three fingers and an associated proline-rich region. *Nucleic Acids Res.*, 28(2):570–581, Jan 2000.
- [4] N. Kloting, B. Wilke, and I. Kloting. Triplet repeat in the Repin1 3'-untranslated region on rat chromosome 4 correlates with facets of the metabolic syndrome. *Diabetes Metab. Res. Rev.*, 23(5):406–410, Jul 2007.
- [5] M. Kern, J. Kosacka, N. Hesselbarth, J. Bruckner, J. T. Heiker, G. Flehmig, I. Kloting, P. Kovacs, M. Matz-Soja, R. Gebhardt, K. Krohn, S. Sales, K. Abshagen, A. Shevchenko, M. Stumvoll, M. Bluher, and N. Kloting. Liver-restricted Repin1 deficiency improves whole-body insulin sensitivity, alters lipid metabolism, and causes secondary changes in adipose tissue in mice. *Diabetes*, 63(10):3295–3309, Oct 2014.
- [6] J. T. Heiker and N. Kloting. Replication initiator 1 in adipose tissue function and human obesity. *Vitam. Horm.*, 91:97–105, 2013.
- [7] K. Ruschke, M. Illes, M. Kern, I. Kloting, M. Fasshauer, M. R. Schon, J. Kosacka, G. Fitzl, P. Kovacs, M. Stumvoll, M. Bluher, and N. Kloting. Repin1 maybe involved in the regulation of cell size and glucose transport in adipocytes. *Biochem. Biophys. Res. Commun.*, 400(2):246–251, Sep 2010.
- [8] M. Kern, N. Kloting, H. G. Niessen, L. Thomas, D. Stiller, M. Mark, T. Klein, and M. Bluher. Linagliptin improves insulin sensitivity and hepatic steatosis in diet-induced obesity. *PLoS ONE*, 7(6):e38744, 2012.
- [9] S. J. Fisher and C. R. Kahn. Insulin signaling is required for insulin's direct and indirect action on hepatic glucose production. *J. Clin. Invest.*, 111(4):463–468, Feb 2003.
- [10] R. Berry, C. D. Church, M. T. Gericke, E. Jeffery, L. Colman, and M. S. Rodeheffer. Imaging of adipose tissue. *Meth. Enzymol.*, 537:47–73, 2014.

- 
- [11] C. A. Schneider, W. S. Rasband, and K. W. Eliceiri. NIH Image to ImageJ: 25 years of image analysis. *Nat. Methods*, 9(7):671–675, Jul 2012.
- [12] J. M. Fernandez-Real and W. Ricart. Insulin resistance and chronic cardiovascular inflammatory syndrome. *Endocr. Rev.*, 24(3):278–301, Jun 2003.
- [13] Haiyan Xu, Glenn T Barnes, Qing Yang, Guo Tan, Daseng Yang, Chieh J Chou, Jason Sole, Andrew Nichols, Jeffrey S Ross, Louis A Tartaglia, et al. Chronic inflammation in fat plays a crucial role in the development of obesity-related insulin resistance. *The Journal of clinical investigation*, 112(12):1821–1830, 2003.
- [14] S. Talukdar, D. Y. Oh, G. Bandyopadhyay, D. Li, J. Xu, J. McNelis, M. Lu, P. Li, Q. Yan, Y. Zhu, J. Ofrecio, M. Lin, M. B. Brenner, and J. M. Olefsky. Neutrophils mediate insulin resistance in mice fed a high-fat diet through secreted elastase. *Nat. Med.*, 18(9):1407–1412, Sep 2012.

# Chapter 4

Liver-Restricted Repin1 Deficiency Improves  
Whole-Body Insulin Sensitivity, Alters Lipid  
Metabolism, and Causes Secondary Changes in Adipose  
Tissue in Mice

Matthias Kern<sup>1</sup>, Joanna Kosacka<sup>1</sup>, Nico Hesselbarth<sup>1</sup>, Julia Brückner<sup>1</sup>,  
John T. Heiker<sup>1</sup>, Gesine Flehmig<sup>2</sup>, Ingrid Klöting<sup>3</sup>, Peter Kovacs<sup>2</sup>, Madlen  
Matz-Soja<sup>4</sup>, Rolf Gebhardt<sup>4</sup>, Knut Krohn<sup>5</sup>, Susanne Sales<sup>6</sup>, Kerstin  
Abshagen<sup>7</sup>, Andrej Shevchenko<sup>6</sup>, Michael Stumvoll<sup>1,2</sup>, Matthias Blüher<sup>1,2</sup>,  
Nora Klöting<sup>1,2</sup>

<sup>1</sup>Department of Medicine, University of Leipzig, Leipzig, Germany

<sup>2</sup>IFB AdiposityDiseases, University of Leipzig, Leipzig, Germany

<sup>3</sup>Department of Laboratory Animal Science, University of Greifswald,  
Karlsburg, Germany

<sup>4</sup>Institute of Biochemistry, Medical Faculty, University of Leipzig, Leipzig,  
Germany

<sup>5</sup>Interdisciplinary Center for Clinical Research, Core Unit DNA  
Technologies, University of Leipzig, Leipzig, Germany

<sup>6</sup>Max Planck Institute of Molecular Cell Biology and Genetics, Dresden,  
Germany

<sup>7</sup>Institute for Experimental Surgery, Rostock University Medical School,  
Rostock, Germany



## 4.1 Abstract

Replication initiator 1 (Repin1) is a zinc finger protein highly expressed in liver and adipose tissue and maps within a quantitative trait locus (QTL) for body weight and triglyceride (TG) levels in the rat. The QTL has further been supported as a susceptibility locus for dyslipidemia and related metabolic disorders in congenic and subcongenic rat strains. Here, we elucidated the role of Repin1 in lipid metabolism *in vivo*. We generated a liver-specific Repin1 knockout mouse (LRep1<sup>-/-</sup>) and systematically characterized the consequences of Repin1 deficiency in the liver on body weight, glucose and lipid metabolism, liver lipid patterns, and protein/mRNA expression. Hyperinsulinemic-euglycemic clamp studies revealed significantly improved wholebody insulin sensitivity in LRep1<sup>-/-</sup> mice, which may be due to significantly lower TG content in the liver. Repin1 deficiency causes significant changes in potential downstream target molecules including Cd36, Ppar $\gamma$ , Glut2 protein, Akt phosphorylation, and *lipocalin2*, *Vamp4*, and *Snap23* mRNA expression. Mice with hepatic deletion of Repin1 display secondary changes in adipose tissue function, which may be mediated by altered hepatic expression of lipocalin2 or chemerin. Our findings indicate that Repin1 plays a role in insulin sensitivity and lipid metabolism by regulating key genes of glucose and lipid metabolism.

## 4.2 Introduction

Previously, we identified a quantitative trait locus (QTL) for body weight, serum fasting insulin, and triglycerides (TGs) on rat chromosome 4 [1], [2], [3]. Replication initiator 1 (Repin1) emerged as a potential positional candidate gene within the QTL region considering associations of metabolic alterations in rats with a single nucleotide polymorphism (449C/T) in the Repin1 coding region and with the size of a triplet repeat in the 3'-untranslated region of the *Repin1* gene [4]. Repin1 was initially discovered as replication initiation region protein 60 kDa (RIP60) in a study investigating DNA binding proteins involved in replication activation of the Chinese hamster dihydrofo-

late reductase gene (*dhfr*) [5]. Repin1 binds to two ATT-rich sites in *oriB*, a short region 39 to the *dhfr* gene, acting as an enhancer of DNA bending during initiation of DNA synthesis [6], [7]. Plasmid replication assays demonstrated only weak replication enhancing activity, and thus Repin1 may act as an accessory factor in origin recognition prior to the assembly of preinitiation complexes [8]. After it was first cloned in 2000, characterization of DNA binding and bending properties revealed the first structural insight into Repin1/RIP60 function as a polydactyl zinc finger protein of the Cys<sub>2</sub>-His<sub>2</sub> type [8].

Repin1 is ubiquitously expressed with the highest expression levels in adipose tissue and the liver [4]. Moreover, hepatic expression levels of *Repin1* are significantly associated with genotype and serum lipid profiles of different rat strains [4]. Recently, we showed that Repin1 plays a role in the regulation of lipid accumulation in 3T3-L1 adipocytes as knockdown of Repin1 by small interfering RNA (siRNA) resulted in reduced palmitate uptake and altered mRNA expression of fatty acid transporter *Cd36* and genes involved in lipid droplet formation (*Vamp4* and *Snap23*), adipogenesis, and glucose transport [9]. A balance between storage and release of lipids by adipose tissue is essential for maintenance of normal energy homeostasis and prevention of ectopic lipid accumulation in peripheral tissues, such as liver, pancreas, or skeletal muscle [10].

Based on our previous findings, we hypothesize that Repin1 is involved in glucose homeostasis and hepatic lipid storage and may contribute to alterations in glucose homeostasis and lipid metabolism associated with obesity. We therefore tested the *in vivo* consequences of *Repin1* gene disruption in mice with a liver-restricted, Cre-*loxP* -mediated Repin1 deletion (LRep1<sup>-/-</sup>).

## 4.3 Research Design and Methods

### 4.3.1 Animal Studies

All animal studies were approved by the local authorities of the state of Saxony, Germany, and of Mecklenburg-West Pomerania, Germany, as rec-

ommended by the responsible local animal ethics review board (Regierungspräsidium Leipzig, TVV20/08, T02/13, TVV15/14, and Rostock LALLF M-V/TSD /7221.3-1.1-099/12, Germany). All mice were housed in pathogen-free facilities in groups of three to five at  $22 \pm 2$  °C on a 12-h light/dark cycle. Animals were bred and kept in the animal laboratories at the University of Leipzig and were fed a standard chow diet (Altromin GmbH, Lage, Germany). A subgroup of eight LRep1<sup>-/-</sup> and eight wild-type (WT) mice were kept on a high-fat diet (HFD) containing 55.2% of calories from fat (C1057; Altromin). Animals had *ad libitum* access to water at all times, and food was only withdrawn if required for an experiment.

### 4.3.2 Generation of LRep1<sup>-/-</sup> Mice

The *Repin1* gene in the liver was inactivated using conditional gene-targeting strategies. Floxed LRep1<sup>-/-</sup> mice were generated by Artemis Pharmaceuticals (Köln, Germany). Exon 2 was flanked by *loxP* sites, and two positive selection markers were used in order to increase corecombination frequency of both *loxP* sites (Fig. 1A). The selection markers are flanked by *frt* (Neo) or F3 sites (Puro). The conditional knockout (KO) occurs after *in vivo* Flp-mediated removal of selection markers and constitutive KO by Cre-mediated deletion of exon 2. The deletion of exon 2 resulted in loss of function by removing the complete open reading frame.

### 4.3.3 Vector Construction ET (SIS17)

Mouse genomic fragments were ET subcloned using RP23 BAC library and recloned into the basic targeting vector harboring the indicated features. Mice homozygous for the loxP-flanked Rep1 allele (Rep1<sup>lox/lox</sup>) were crossed with mice expressing a Cre recombinase under control of the albumin (Alb) promoter (C57BL/6-TgN(AlbCre) 21Mgn, stock 003574; The Jackson Laboratory). In the liver, Cre recombinase mediates the deletion of all floxed alleles. LRep1 mice were on C57BL/6N background.

### 4.3.4 Molecular Characterization and Genotyping of LRep1<sup>AlbCre</sup> Mice

Genotyping was performed by PCR using genomic DNA isolated from the tail tip. Genomic DNA was prepared by using the DNeasy Kit (Qiagen, Hilden, Germany). The following two primer pairs were used to genotype LRep1 *loxP* sites: 5'-CCCAACACTGATTACAGATCC-3' (forward) and 5'-GTGGGATCAGATAGAACTTAGC-3' (reverse) as well as the AlbCre recombinase 5'-GCGGTCTGGCAGTAAAACTATC-3' (forward) and 5'-GTGAAACAGCATTGCTGTCACTT-3' (reverse). PCR was performed for 35 cycles of 95 °C (*loxP* sites) or 94 °C (AlbCre), 60 °C (30 s, *loxP* sites), or 51 °C (60 s, AlbCre) and 72 °C (60 s each) using the Fermentas DreamTaq Polymerase (Fermentas GmbH, St. Leon-Rot, Germany) and a Peltier Thermal Cycler PTC-200 (Bio-Rad, Hercules, CA). DNA from WT mice produced a 292-bp band, and a 484-bp band was detected in LRep1<sup>AlbCre</sup> *lox* mice.

### 4.3.5 Phenotypic Characterization

Twelve male mice of each genotype (LRep1<sup>-/-</sup> and control littermates [Rep1<sup>fl<sub>ox</sub>/fl<sub>ox</sub></sup>, Rep1<sup>fl<sub>ox</sub>/+</sup>, and WT]) were studied from the age of 6 weeks up to 40 weeks. Body weight was recorded weekly, and body length (naso-anal length) was measured once at an age of 32 weeks (n = 10 per genotype).

Intraperitoneal glucose tolerance tests (GTTs) and insulin tolerance tests (ITTs) were performed in males at the age of 12, 24, and 40 weeks as described previously [11]. In brief, GTT was performed after an overnight fast of 14 h by injecting 2 g glucose per kg body weight into LRep1<sup>-/-</sup> and littermate controls. Blood samples for glucose measurements were taken at different time points after 0, 15, 30, 60, and 120 min as described previously [11].

ITT was performed in random-fed animals by injecting 0.75 units/kg body weight human regular insulin (40 units Insuman Rapid; Sanofi, Frankfurt/Main, Germany). Glucose levels were determined in blood collected

from tail tip immediately before and 15, 30, and 60 min after the intraperitoneal injection.

Indirect calorimetry was assessed by a calorimetry module (CaloSys V2.1; TSE Systems, Bad Homburg, Germany) at an age of 30 weeks. After 2 h of acclimatization, mean oxygen consumption ( $\text{VO}_2$ ) as well as spontaneous activity (XYZ cage movement) and ability to run on a treadmill were recorded for 72 h. At an age of 16 weeks, a subgroup of 20 ( $n = 10$  per genotype) mice underwent a food intake measurement over a time period of 1 week. The daily food intake was calculated as the average intake of chow within the time stated. Rectal body temperature was measured at an age of 32 weeks. Wholebody composition (fat mass, lean mass, and total body water) was determined in awake mice by using nuclear magnetic resonance technology with EchoMRI-700 instrument (Echo Medical Systems, Houston, TX) in control and LRep1<sup>-/-</sup> mice at 3, 8, 16, 24, and 80 weeks of age. At least four animals per genotype and time point were measured. Data were analyzed by the manufacturer's software.

Mice were killed at the age of 32 weeks by an overdose of anesthetic (isoflurane; Baxter, Unterschleißheim, Germany). Liver, heart, brain, lung, spleen, pancreas, kidney, muscle, and subcutaneous (SC) and epigonadal adipose tissue (Epi) were immediately removed. The organs (liver, brown adipose tissue [BAT], and Epi) were weighed, and organ mass was related to whole-body mass to obtain relative organ weights.

### 4.3.6 Analytical Procedures

Blood glucose values were determined from wholeâ€œvenous blood samples using an automated glucose monitor (FreeStyle Mini; Abbott GmbH, Ludwigshafen, Germany). Insulin, leptin, and adiponectin serum concentrations were measured by ELISA using mouse standards according to the manufacturer's guidelines (Mouse/Rat Insulin ELISA and Mouse Leptin ELISA; Crystal Chem Inc., Downers Grove, IL; and Mouse Adiponectin ELISA; Adipogen International, Incheon, Korea). Serum concentrations of alanine aminotransferase (ALT), aspartate aminotransferase (AST), Alb, free fatty

acids (FFAs), TGs, LDL cholesterol, and HDL cholesterol were analyzed by an automatic chemical analyzer in our Institute of Laboratory Medicine and Clinical Chemistry. Serum glycerol concentration was measured using Adipolysis Assay Kit (Merck Millipore, Billerica, MA) in male LRep1<sup>-/-</sup> and controls at an age of 30 weeks.

### 4.3.7 Hyperinsulinemic-Euglycemic Clamp Studies

Catheters were implanted in the left jugular vein and hyperinsulinemic-euglycemic clamps of six males of each genotype were performed at the age of 20 weeks. Clamp was performed as described previously [12], [13], [14].

### 4.3.8 Liver Lipidomics

Lipids were extracted from mouse hepatocytes using the Folch *et al.* [15] protocol with minor modification [16]. Molecular lipid species were identified and quantified using LipidXplorer software [17] developed by MPI CBG (Dresden, Germany). Species were quantified by comparing the intensities of their peaks to peaks of spiked internal standards; lipid quantities determined in individual samples were normalized by the total protein content determined by Bradford assay. Cholesterol was quantified as previously described [18].

### 4.3.9 RNA Isolation and Quantitative Real-Time PCR Analysis

RNA isolation and quantitative real-time PCR were performed as previously described [11]. mRNA expression of genes listed in Supplementary Table 3 was determined. Specific mRNA expression was calculated relative to *18s* RNA, which was used as an internal control due to its resistance to glucose-dependent regulation [19].

#### 4.3.10 *In Vivo* Lipogenesis in Liver, *In Vivo* VLDL TG Production, and Fat Load Test

*In vivo* lipogenesis was performed as previously described in detail [20], [21]. To measure hepatic TG production rate, mice were intraperitoneally injected with Poloxamer 407 (p407; Sigma-Aldrich) in saline  $\sim$ 4 h into the light cycle, and plasma TG was measured over a 4 h period as described elsewhere [22]. At an age of 16 weeks, after an overnight fast, 200 mL olive oil was administered by intragastric gavage feeding tube. Blood samples were taken by submandibular bleeding at 0, 1, 2, 3, and 4 h after fat load for TG measurements. Eight male mice per genotype were studied.

#### 4.3.11 *Ex Vivo* Glucose Transport, *Ex Vivo* Lipolysis, and Palmitate Uptake Into Adipocytes

The determination of glucose transport, lipolysis, palmitate uptake, and adipocyte size distribution was performed as previously described [9], [23].

#### 4.3.12 Western Blot Analysis

For Western blot analysis, tissues were removed and homogenized in homogenization buffer with tissue-mill homogenizer (MM 400; Retsch GmbH, Haan, Germany), proteins were isolated using standard techniques, and Western blot analysis was performed with antibodies raised against Repin1 (N-20, 1:1,000; Santa Cruz Biotechnology, Santa Cruz, CA), Ppar $\gamma$  (1:100, #351540; Antikörper Online), Irs1 and pIrs1 (1:1,000; Cell Signaling Technology), Akt and pAkt (1:1,000; Cell Signaling Technology), Glut2 (1:200, ab85715, Abcam, Cambridge, U.K.), Ppar $\gamma$  (1:1,000; Cell Signaling Technology), ACC (1:1,000; Cell Signaling Technology), lipocalin2 (Lcn2) (1:1,000; Abcam), Cd36 (1:500; Antibodies Online), and GAPDH antibody (1:3,000; Research Diagnostics, Flanders, Netherlands) as loading control. For Cd36 protein detection, supernatant was centrifuged at 100,000g for 45 min at 4 °C. To get the membrane and cytosol fractions, the pellet was suspended in ice-cold sucrose buffer and taken to Cd36 analysis in Western blot.

### 4.3.13 Insulin Signaling

Mice were anesthetized by intraperitoneal injection, and adequacy of the anesthesia was ensured by loss of pedal reflexes. The abdominal cavity of the mice was opened, and 125  $\mu$ L samples containing 5 units regular human insulin diluted in 0.9% saline were injected into the vena cava inferior. Sham injections were performed with 125  $\mu$ L of 0.9% saline. Samples of liver tissue were harvested 10 min after injection, respectively, and proteins (Akt, pAkt, Irs1, and pIrs1) were extracted from tissues for Western blot analysis.

### 4.3.14 Liver Affymetrix GeneChip Analysis

RNA from liver samples of three male WT and three male LRep1<sup>-/-</sup> mice was used for microarray RNA analysis. Analysis of RNA integrity and RNA concentration as well as probe synthesis, hybridization, and scanning was performed as previously described [24].

### 4.3.15 Histology and Immunohistochemistry

Histology and immunohistochemistry were performed as previously described [23], [25].

### 4.3.16 Statistical Analysis

Data are given as means  $\pm$  SE. Data sets were analyzed for statistical significance using a two-tailed unpaired Student *t* test or Mann-Whitney *U* test. *P* values < 0.05 were considered significant.

## 4.4 Results

### 4.4.1 Generation of LRep1<sup>-/-</sup> Mice

In order to generate LRep1<sup>-/-</sup> mice, mice homozygous for the *loxP*-flanked Rep1 allele (Rep1<sup>*fllox/fllox*</sup>) were crossed with mice expressing the Cre recombinase under control of the liver-specific Alb promoter. The targeting



strategy is shown in Fig. 1A. LRep1<sup>-/-</sup> mice obtained with the expected Mendelian frequency were fertile. Efficiency and specificity of the Repin1 KO were examined in tissue lysates from control and LRep1 mice by Western blot analyses (Fig. 1B and C). Western blot analysis of liver lysates from LRep1<sup>-/-</sup> mice confirmed reduced Repin expression by ~85% in livers (Fig. 1C). Since the Cre recombinase is only active in hepatocytes, and since hepatocytes make up ~85% of the total number of cells in the liver, it is likely that the minimal Repin1 protein in LRep1<sup>-/-</sup> mice is derived from vascular endothelial cells, Kupffer cells, and other nonparenchymal cells. Immunohistochemistry of Repin1 in the liver was performed to test whether nonparenchymal cells are responsible for the remaining Repin1 expression in LRep1<sup>-/-</sup> mice. The immunohistochemical images of the liver of LRep1<sup>-/-</sup> mice demonstrate the absence of Repin1 in hepatocytes but positive Repin1 staining for endothelial cells, Kupffer cells, and hepatic stellate cells (Fig. 1D). In contrast, hepatocellular cytoplasm of WT mice showed positive staining for Repin1 (Fig. 1D). Repin1 expression in all other tissues was indistinguishable between LRep1<sup>-/-</sup> and control littermates (Fig. 1B).

#### 4.4.2 Growth, Tissue Mass, and Energy Expenditure of LRep1<sup>-/-</sup> Mice

LRep1<sup>-/-</sup> mice had normal body weight compared with control littermates (Rep1<sup>lox/lox</sup>, LRep1<sup>-/+</sup>, and WT) up to an age of 28 weeks when LRep1<sup>-/-</sup> mice become significantly leaner with significantly less total body fat content up to an age of 40 weeks (Fig. 1E and F). This may be due to significantly higher VO<sub>2</sub> consumption and spontaneously higher activity (z-axis day) in LRep1<sup>-/-</sup> mice (Fig. 1G-I). Homozygous deficiency of Repin1 had no significant influence on body length (Supplementary Fig. 4A), daily food intake (Supplementary Fig. 4B), or relative tissue weights of livers (WT, 5.2%; LRep12/2, 5.3%).

### 4.4.3 Repin1 Deficiency in Liver Improves Insulin Sensitivity

To further investigate the role of Repin1 on glucose homeostasis, we characterized the physiological consequences of reduced liver Repin1 expression on insulin action and glucose metabolism. Hyperinsulinemic-euglycemic clamp studies revealed significantly higher whole-body insulin sensitivity in LRep1<sup>-/-</sup> compared with control mice (Fig. 2A). At the steady state, glucose infusion rate (GIR) was ~60% higher in LRep1<sup>-/-</sup> compared with control mice (Fig. 2A). LRep1<sup>-/-</sup> mice showed a higher rate of hepatic glucose production during the basal period as compared with control animals (Fig. 2B), whereas insulin suppressed hepatic glucose production significantly better in LRep1<sup>-/-</sup> (-98%) compared with control mice (-51%) (Fig. 2C). Circulating insulin concentrations achieved in the steady state of the clamp were not significantly different between WT ( $9.1 \pm 1.4$  ng/mL) and LRep1<sup>-/-</sup> ( $8.3 \pm 1.6$  ng/mL) mice.

In addition, we monitored blood glucose, insulin, as well as adiponectin serum concentrations (Table 1) and performed serial GTTs and ITTs over an age range from 12 to 40 weeks (Fig. 2D and E and Supplementary Fig. 4C and D). Independent of age, intraperitoneal GTTs revealed normal glucose tolerance in LRep1<sup>-/-</sup> mice (Fig. 2D). At an age of 24 weeks, LRep1<sup>-/-</sup> mice showed significantly improved insulin sensitivity compared with controls (Fig. 2E), which was even more pronounced at a higher age (Fig. 2F-H). Significantly lower HbA<sub>1c</sub> level confirmed the long-term glucose metabolism in LRep1<sup>-/-</sup> compared with control mice (Fig. 2I). Moreover, insulin secretion in response to the intraperitoneal glucose load in 40-week-old LRep1<sup>-/-</sup> mice showed an improved insulin secretion response to glucose reflected by a higher insulin peak at 15 min and a faster decline in insulin serum concentrations than in controls (Fig. 2G).

Taken together, reduced Repin1 expression in liver results in improved whole-body insulin sensitivity, subsequently contributing to better glycemic control in LRep1<sup>-/-</sup> mice.

#### 4.4.4 Repin1 Affects Insulin Signaling in the Liver

We further sought to investigate the consequences of disrupted Repin1 in the liver and improved insulin sensitivity by analyzing key insulin signaling molecules in livers of LRep1<sup>-/-</sup> and control mice after insulin stimulation. Supporting a role of Repin1 in the regulation of hepatic insulin sensitivity at the molecular level, we find a significant upregulation of phosphorylated Akt and Ppar $\gamma$  expression in LRep1<sup>-/-</sup> compared with control mice (Fig. 3A). These molecular changes may underlie significantly higher Glut2 expression (Fig. 3A), which may explain higher basal glucose uptake in the hyperinsulinemic-euglycemic clamp in LRep1<sup>-/-</sup> compared with control mice.

#### 4.4.5 Liver-Specific Repin1 Deficiency Leads to Dyslipidemia, Altered Liver Lipid Transport/Storage, and Liver Lipidomic Profile

To determine the physiological consequences of reduced liver tissue Repin1 expression, we monitored total serum cholesterol, TG serum concentrations, FFA, and liver function tests such as circulating serum ALT, AST, glutamate dehydrogenase (GLDH), and Alb concentrations. Fasted TGs and FFAs were significantly higher in LRep1<sup>-/-</sup> mice at an age of 32 weeks (Table 1). ALT, AST, and Alb were not affected by Repin1 KO, suggesting that lack of Repin1 has no adverse effect on liver function (Table 1). Also hematoxylin-eosin (H-E) staining of control and LRep1<sup>-/-</sup> mice showed normal hepatic architecture without signs of hepatocyte injury (Fig. 3D and Supplementary Figs. 2 and 3).

Liver lipidomics analyses revealed significantly lower liver content triacylglycerides (TAGs) in LRep1<sup>-/-</sup> compared with control mice (Table 2). The amount of TAGs in liver was significantly decreased in LRep1<sup>-/-</sup> mice by ~40% compared with controls (Table 2 and Fig. 3C). Hepatic cholesterol and cholesterolester were unchanged (Table 2). Lower lipid accumulation in the liver of LRep1<sup>-/-</sup> mice may at least in part explain improved whole-body

insulin sensitivity in these mice.

To identify potential mechanisms underlying reduced TG storage in the liver and elevated circulating TGs and FFAs in LRep1<sup>-/-</sup> mice, we examined hepatic expression of fatty acid transporters *Cd36*, *Fatp1*, *Fatp2*, *Fatp4*, and carnitine palmitoyltransferase 1 (*Ctp1*) as the first component and rate-limiting step in  $\beta$ -oxidation and *Cpt2* (Supplementary Table 3). We performed *in vivo* VLDL production assays, *in vivo* lipogenesis, and oral fat load tests. Injection of p407 resulted in a linear increase in serum TG concentration without significant differences between both experimental groups, which suggests no influence of hepatic VLDL synthesis on altered lipid content in LRep1<sup>-/-</sup> mice (Fig. 3G). Further, to investigate de novo lipogenesis, we injected mice both with tritiated water and [U-<sup>14</sup>C]-glucose (Fig. 3J). Total rate of hepatic fatty acid synthesis was comparable between controls and LRep1<sup>-/-</sup> mice, and the incorporation of [U-<sup>14</sup>C]-glucose into de novo fatty acids was similar as well (Fig. 3I and J). Expression of a key lipogenic enzyme, ACC (pACC), was not changed in livers of LRep1<sup>-/-</sup> mice compared with littermate controls (Fig. 3K). *Cd36* was significantly reduced in LRep1<sup>-/-</sup> mice by ~50% at both protein and mRNA levels (Fig. 3E and F).

#### 4.4.6 LRep1<sup>-/-</sup> Mice Are Protected Against Development of HFD-Induced Adipocyte Hypertrophy

In a subgroup of eight animals of each genotype, we performed an HFD study starting at 6 weeks of age until 16 weeks of age. Weight gain after HFD was not different between all groups (Fig. 4A). Relative liver weight was slightly reduced in LRep1<sup>-/-</sup> mice compared with controls (data not shown). Also ALT and AST as well as Alb levels did not differ among genotypes (data not shown), and Epi mass was comparable between LRep1<sup>-/-</sup> and control mice (data not shown). Despite indistinguishable relative adipose tissue mass, LRep1<sup>-/-</sup> mice showed decreased maximal adipocyte diameters compared with controls in response to HFD (Fig. 4B-F). Maximal epigonadal adipocyte diameter is significantly larger in controls compared with

LRep1<sup>-/-</sup> mice (Fig. 4E and F). Adipocyte frequency size distribution confirmed these findings (Fig. 4C and D). These differences are more pronounced in epigonadal than in SC fat. To elucidate in more detail adipocyte function, we analyzed glucose uptake and glycerol release in isolated adipocytes. Here, we detected a significant elevated glucose uptake and glycerol release under basal conditions in SC adipocytes of LRep1<sup>-/-</sup> mice (Fig. 4I and J). Insulin-stimulated glucose uptake was comparable between the experimental groups (Fig. 4J). To elucidate in more detail elevated basal glycerol release, we performed gene expression analysis in adipose tissue. Here, we detected an elevation of all lipolysis enzymes (*Lpl*, *Atgl*, and *Hsl*) in SC adipose tissue in LRep1<sup>-/-</sup> mice (Supplementary Table 5), indicating enhanced lipolysis. Taken together, LRep1<sup>-/-</sup> mice were protected against HFD-induced adipocyte hypertrophy.

#### 4.4.7 Target Genes of Repin1

To identify Repin1-regulated target genes, we measured mRNA expression in the liver of LRep1<sup>-/-</sup> and control mice using a microarray approach. *Lcn2*, also known as neutrophil gelatinase-associated lipocalin, was the strongest regulated gene in response to reduced Repin1 expression (Supplementary Table 2). We further found reduced levels of clathrin-coated vesicle transport protein (*ap3m2*), vesicle-associated membrane proteins, oxidative stress genes such as *metallothein1* (*Mt1*) and *2* (*Mt2*), as well as *LDL receptor* (*Ldlr*) and *Rarres 2* (chemerin). Exocytosis factor titin, mitochondrial protein *Letm2*, and kallikrein inhibitor (*serpinA4-ps1*) were expressed higher in livers of LRep1<sup>-/-</sup> mice (Supplementary Table 2). In addition to these genes, we detected a number of Repin1-regulated genes including various biological processes and molecular functions (Supplementary Tables 1 and 2). We could confirm the expression microarray data for *Lcn2* and chemerin in a bigger liver tissue cohort (see Supplementary Table 4). Circulating *Lcn2* concentrations and liver *Lcn2* expressions were lower in LRep1<sup>-/-</sup> compared with littermate control mice ( $P = 0.2$  serum;  $P = 0.06$  liver protein) (Supplementary Fig. 5).

#### 4.4.8 Altered Expression of Genes Involved in Accumulation of Cytosolic Lipids and Lipid Droplet Fusion in Liver

Array mRNA expression changes together with the results of the hepatic lipidomic screen indicated an alteration in lipid droplet fusion and formation. We therefore investigated mRNA levels of proteins involved in the fusion process of lipid droplets in more detail. Vesicle-associated membrane protein 4 (*Vamp4*) and synaptosomal-associated protein, 23 kDa (*Snap23*), were significantly decreased in livers of Repin1-deficient mice. *Vamp4* was reduced by 80% and *Snap23* by ~40% in LRep1<sup>-/-</sup> (Supplementary Table 3).

#### 4.4.9 Model for the Role of Repin1 in Insulin Sensitivity

We propose the following model of how liver-restricted knockdown of Repin1 may cause the observed phenotype (Fig. 5). Hepatic Repin1 deficiency causes improved liver and whole-body insulin sensitivity most likely through transcriptional regulation of genes involved in insulin signaling (*Pparγ* and *Akt*), glucose transport (*Glut2*), lipid uptake (*Cd36*), and lipid droplet formation (*Vamp4* and *Snap23*). These changes result in less body weight gain with aging, higher energy expenditure, and reduced liver fat accumulation in LRep1<sup>-/-</sup> compared with controls. Lower liver lipid content may be primarily caused by significantly reduced Cd36 expression in LRep1<sup>-/-</sup> mice. Improved whole-body insulin sensitivity of LRep1<sup>-/-</sup> mice is likely a consequence of reduced liver fat, decreased hepatic glucose production, and eventually lower expression of hepatokines such as Lcn2, which are associated with insulin resistance.

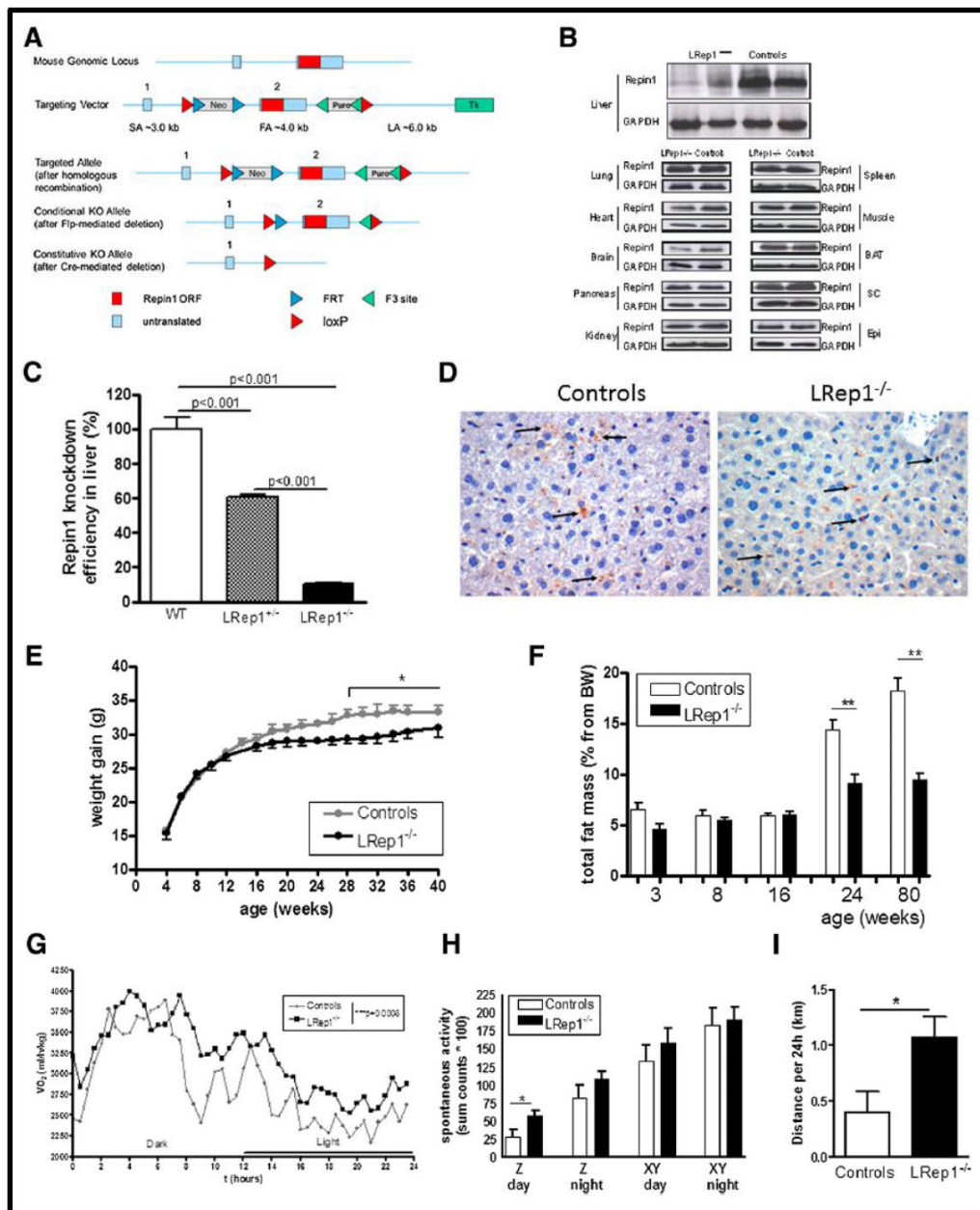


Figure 4.1: Targeting strategy and assessment of *Repin1* recombination and *Repin1* expression. A: Schematic representation of the loxP-flanked *Repin1* allele before and after recombination (Cre expression). The KO allele is shown below the floxed allele, indicating the deletion of exon 2 in the event of recombination of the *Repin1* gene. B: Western blot analysis showing the expression of *Repin1* and GAPDH as loading control of liver, lung, heart, brain, pancreas, kidney, spleen, skeletal muscle, BAT, SC, and Epi of control and LRep1<sup>-/-</sup> mice. C: Knockdown efficiency in liver from WT (controls), heterozygous (LRep1<sup>+/-</sup>), and homozygous (LRep1<sup>-/-</sup>) mice.

Figure 4.1: (Previous page.) D: Representative images (original magnification x 200) of Repin1 immunohistochemistry (positive staining of the Repin1 protein with DAB as chromogen in brown, arrows) of liver tissue (5- $\mu$ m paraffin sections) of WT control (left) and LRep1<sup>-/-</sup> mice (right) at an age of 12 weeks. E: Growth phenotype of LRep1<sup>-/-</sup> mice (n = 12) and controls (n = 12) up to an age of 40 weeks was determined. LRep1<sup>-/-</sup> mice are significant lighter at an age of 28 weeks up to an age of 40 weeks. F: Whole-body fat mass was determined in awake mice by using nuclear magnetic resonance technology with EchoMRI-700 instrument (Echo Medical Systems, Houston, TX) in control and LRep1<sup>-/-</sup> mice at 3, 8, 16, 24, and 80 weeks of age. Data are presented as percentage of total body fat from body weight. Results are expressed as means  $\pm$  SE from at least four animals per genotype and time point. G: VO<sub>2</sub> measured by indirect calorimetry in a calorimetry module (CaloSys V2.1, TSE Systems, Bad Homburg, Germany) at an age of 30 weeks. After 2 h of acclimatization, VO<sub>2</sub> was recorded from LRep1<sup>-/-</sup> (n = 10) and control mice (n = 8) over a period of 72 h (P = 0.0008). Results are expressed as means  $\pm$  SE. H: Spontaneous activity (counts) measured as cage movement (XYZ axis) was determined over 72 h. Data represent means of counts from LRep1<sup>-/-</sup> (n = 10) and control mice (n = 8) of 12 h. I: Mean running distance (km) of LRep1<sup>-/-</sup> (n = 10) mice compared with control (n = 8) animals over a period of 72 h at an age of 30 weeks. Results are expressed as means  $\pm$  SE. The different degrees of significance are indicated as follows in the graphs: \*P < 0.05; \*\*P < 0.01.



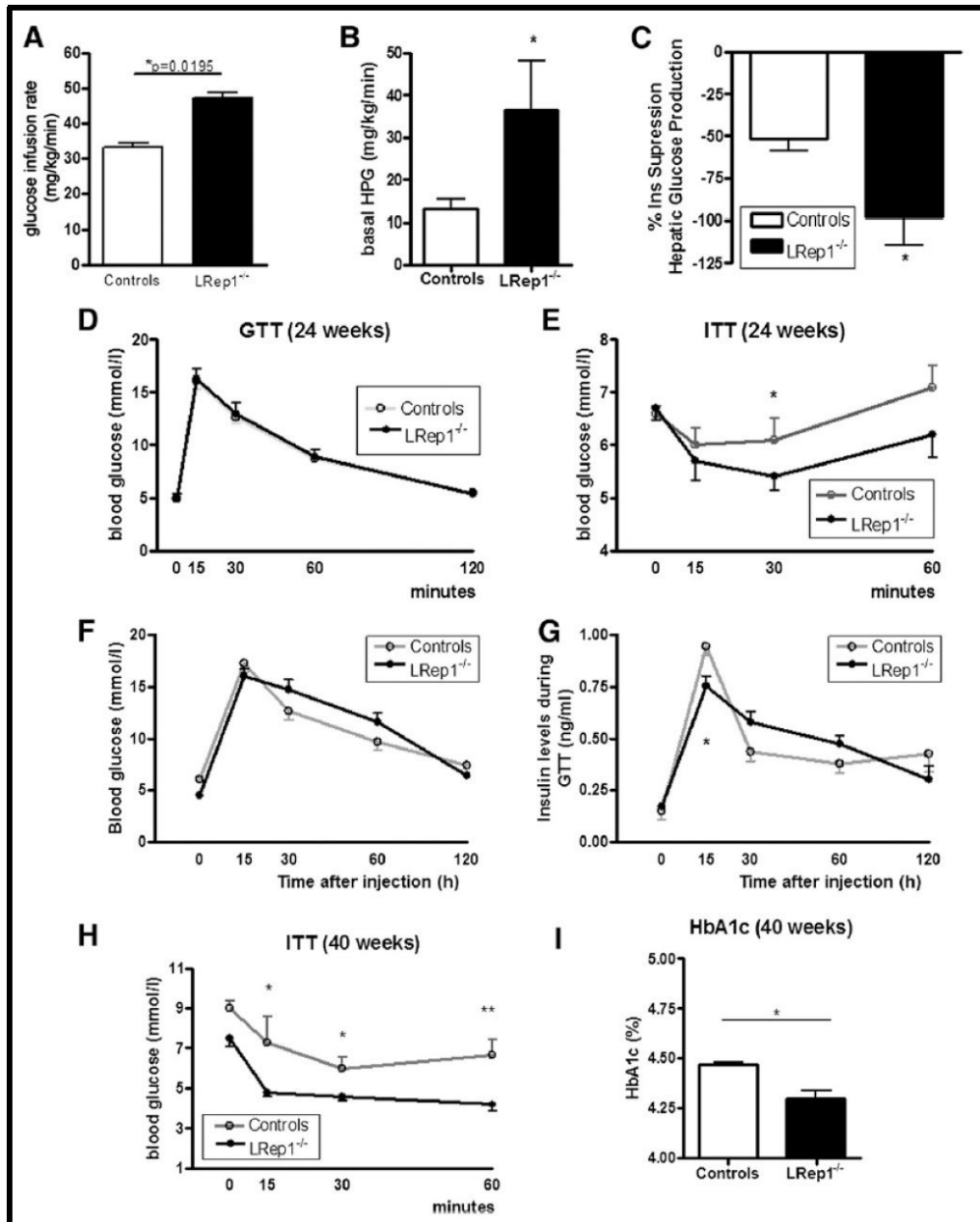


Figure 4.2: Insulin sensitivity, glucose metabolism, and effects in mice with liver-specific Repin1 deficiency. A: GIR during a hyperinsulinemic-euglycemic clamp was increased in LRep1<sup>-/-</sup> mice (n = 8) compared with control mice (n = 6) at an age of 20 weeks. Experiments started after an overnight fast. A 120-min hyperinsulinemic-euglycemic clamp was conducted with a continuous infusion of human insulin at a rate of 20 mU/kg/min. Insulin is infused at a constant rate, resulting in a drop in blood glucose. To maintain blood glucose at a constant level, exogenous glucose (D20%) is infused into the circulation. Variable GIR is determined by measuring blood glucose at brief intervals throughout the experiment and adjusting the GIR accordingly. GIR was calculated as mg/kg/min. Results are expressed as means  $\pm$  SE.

Figure 4.2: (Previous page.) B: Basal hepatic glucose production (HPG) during the clamp in LRep1<sup>-/-</sup> mice is upregulated compared with littermate controls (n = 8). Hepatic glucose production (mg x kg<sup>-1</sup> x min<sup>-1</sup>) was calculated as the difference between the rate of glucose appearance and GIR. Results are expressed as means ± SE from at least six animals per genotype. C: Percentage suppression of hepatic glucose production by insulin (Ins) during the clamp in control (n = 6) and LRep1<sup>-/-</sup> mice (n = 8). Results are expressed as means ± SE from at least six animals per genotype. D: Intraperitoneal GTTs performed on 12 h-fasted 24-week-old control (n = 12) and LRep1<sup>-/-</sup> mice (n = 12) on a chow diet. LRep1<sup>-/-</sup> mice have normal glucose tolerance. E: ITT of LRep1<sup>-/-</sup> showed improved insulin sensitivity at an age of 24 weeks. ITTs were performed in a fed state. Results are expressed as means ± SE from 12 animals per genotype. F: GTT in LRep1<sup>-/-</sup> mice compared with control animals at an age of 30 weeks (per genotype eight animals). G: Insulin levels measured during GTT at an age of 40 weeks in male LRep1<sup>-/-</sup> mice. H: ITT in 40-week-old control animals and LRep1<sup>-/-</sup> mice indicating a significant improvement in insulin sensitivity of LRep1<sup>-/-</sup> mice. Results are expressed as means ± SE from six animals per genotype. I: Significantly lower HbA<sub>1c</sub> (%) levels in LRep1<sup>-/-</sup> mice (n = 8) compared with controls (n = 8) at an age of 40 weeks. The different degrees of significance are indicated as follows in the graphs: \**P* < 0.05; \*\**P* < 0.01.

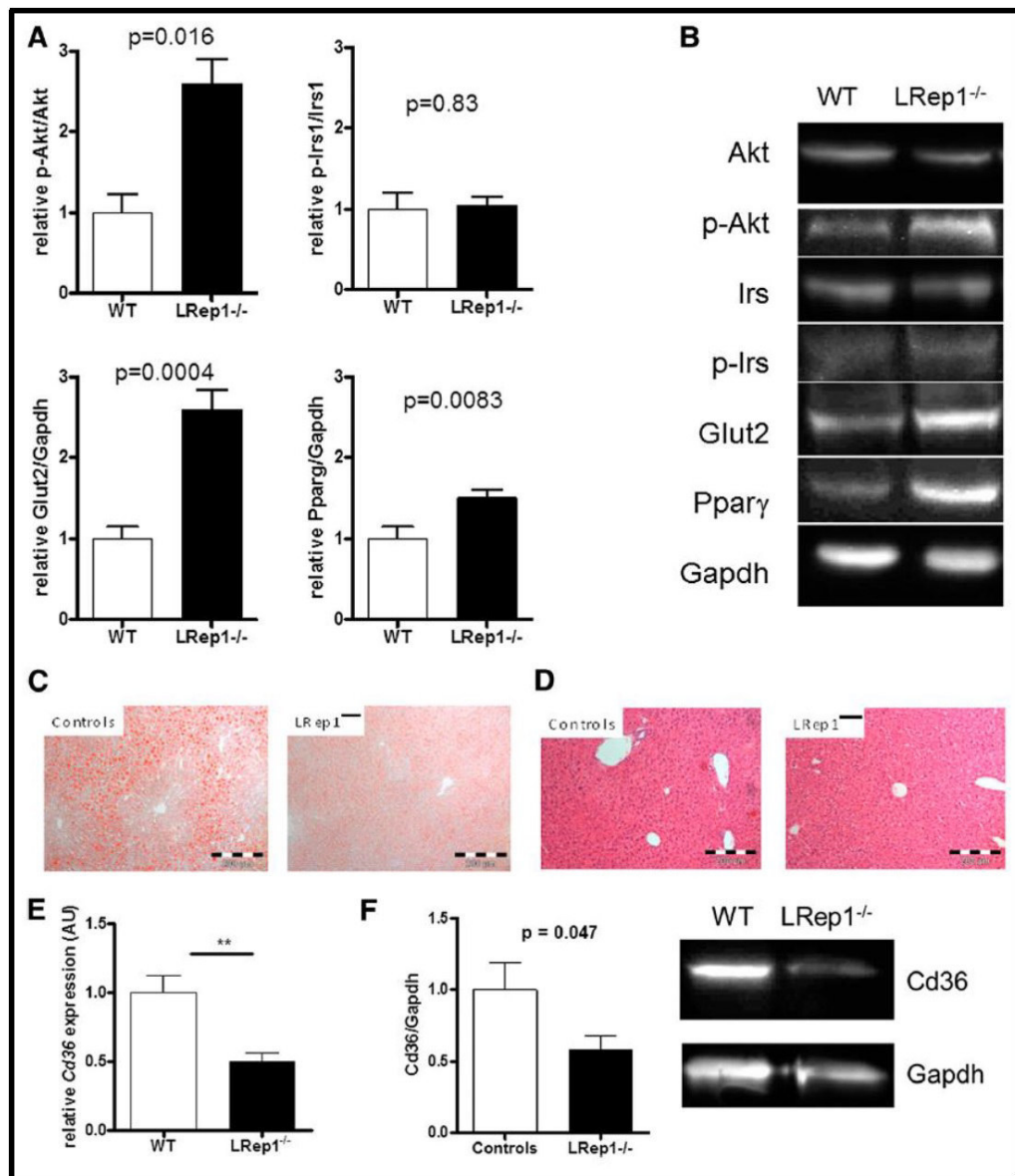


Figure 4.3: Insulin signaling, VLDL TG production, and hepatic de novo lipogenesis in livers of LRep1<sup>-/-</sup> mice. A: Upregulated insulin pathway protein expression measurements with quantification by Western blot analysis (B) in livers of LRep1<sup>-/-</sup> (n = 5) and control (n = 5) animals after injection of 5 units regular insulin into the vena cava inferior. C: Representative images of hepatic tissue fat staining of liver section using sudan-black staining indicates less fat storage in LRep1<sup>-/-</sup> mice compared with control animals. D: Representative images of hepatic tissue for H-E staining of WT and LRep1<sup>-/-</sup> mice showing no morphological changes in livers of LRep1<sup>-/-</sup> mice. Reduction of *Cd36* mRNA expression (E) and representative *Cd36* protein expression (F) and analysis in livers of LRep1<sup>-/-</sup> mice (n = 5) compared with controls (n = 5) at an age of 32 weeks. GAPDH protein served as loading control. Results are expressed as means  $\pm$  SE.

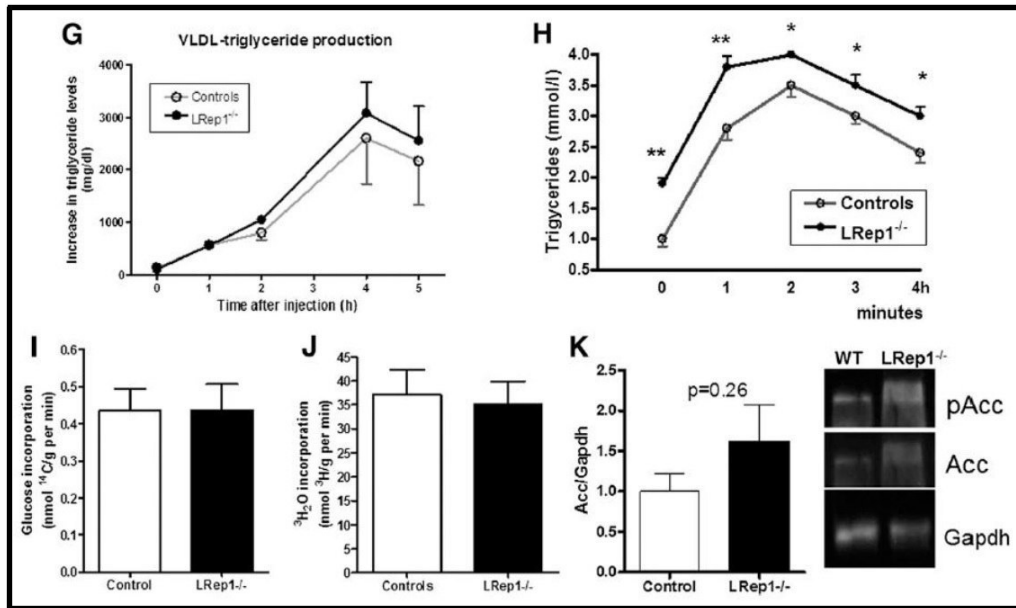


Figure 4.3: (Previous page.) G: Determination of VLDL TG production rates after p407 intraperitoneal treatment and serum samples were taken over a period of 4 h and assay for TGs in LRep1<sup>-/-</sup> (black) and control (gray) littermates (n = 4 per genotype). H: Fat load test after oral application of 200 mL olive oil in LRep1<sup>-/-</sup> (black) and control (gray) littermates (n = 6 per genotype). Rates of <sup>14</sup>C (I) and <sup>3</sup>H<sub>2</sub>O (J) incorporation into liver fatty acids in fed state. n = 6 per genotype. K: ACC and phosphorylated ACC (pACC) protein expression analysis with representative images in livers of control (n = 5) and LRep1<sup>-/-</sup> mice (n = 5). GAPDH protein served as loading control. Western blot analysis results are expressed as means ± SE. The different degrees of significance (Student *t* test with Welch correction) are indicated as follows in the graphs: \**P* < 0.05; \*\**P* < 0.01.

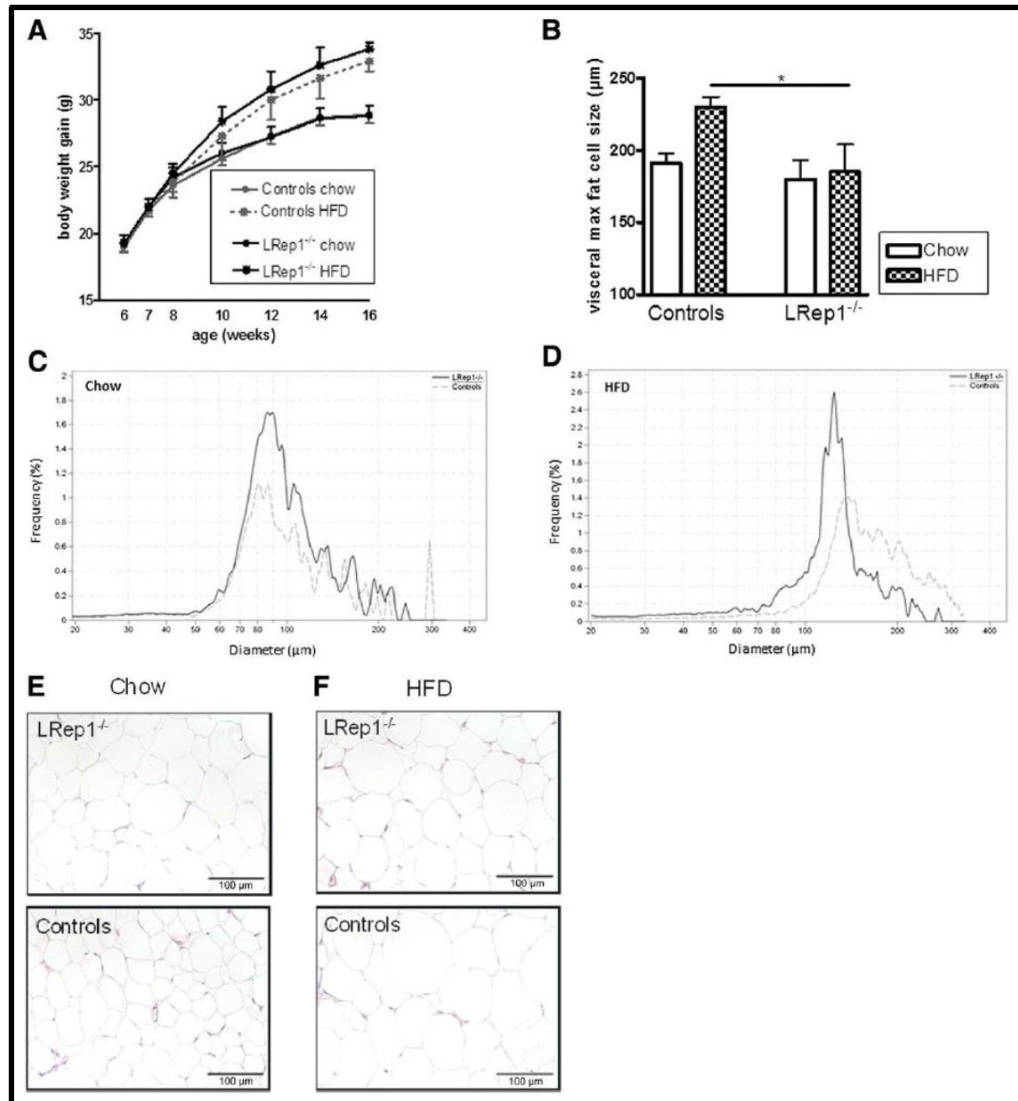


Figure 4.4: Effects of a 10-week HFD on fat accumulation and glucose metabolism in LRep1<sup>-/-</sup> mice. A: Under HFD conditions, LRep1<sup>-/-</sup> mice (n = 8) show identical growth compared with controls (n = 8). B: No hypertrophy of visceral adipocytes in LRep1<sup>-/-</sup> compared with control mice. Maximal adipocyte size measured with multisizer (Beckman Coulter) after 48-h osmium fixation. Data represent means ± SE of eight mice per genotype. C and D: Frequency of adipocyte size distribution after adipocyte isolation and osmium fixation measured with multisizer under chow and HFD conditions indicating a shift in adipocyte size distribution under high-fat feeding conditions. E and F: H-E staining of white adipose tissue (epigonadal) adipocytes after feeding standard chow or HFD from LRep1<sup>-/-</sup> mice. Original magnification X20. Adipocyte size is increased after HFD in control mice only.

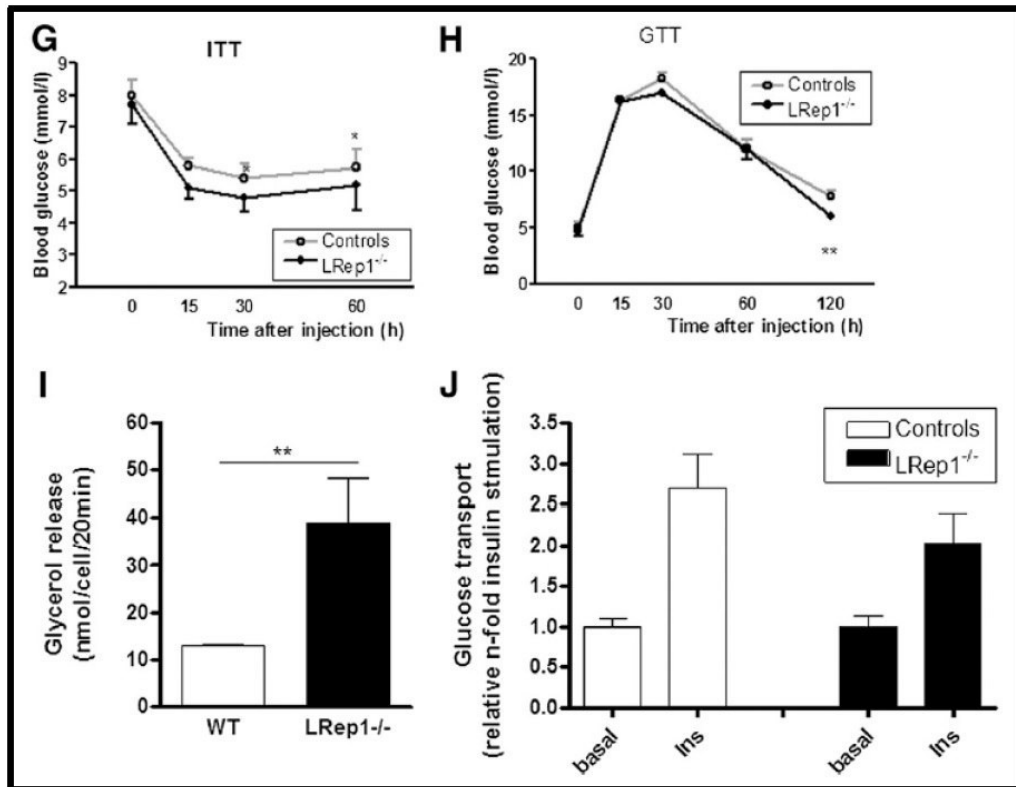


Figure 4.4: (Previous page.) G: ITT in 16-week-old control animals and LRep1<sup>-/-</sup> mice indicating a significant improvement in insulin sensitivity of LRep1<sup>-/-</sup> mice under HFD conditions. Results are expressed as means  $\pm$  SE from six animals per genotype. H: GTT in 16-week-old control animals and LRep1<sup>-/-</sup> male mice under HFD conditions. Results are expressed as means  $\pm$  SE from six animals per genotype. Lipolysis (I) and [U-<sup>14</sup>C]-glucose uptake (J) in isolated adipocytes from SC fat depots of LRep1<sup>-/-</sup> and control mice. I: Lipolysis measured as basal glycerol release assayed over 20 min as an indicator of lipolysis. Results are expressed as nmol of glycerol released per cell in a 20-min period. J: Insulin-stimulated [U-<sup>14</sup>C]-glucose uptake in isolated adipocytes after 20-min incubation in the absence (basal) or presence of 100 nmol/L insulin. Insulin stimulation is presented as n-fold change relative to basal from four animals per genotype. Significant differences between the groups are indicated: \*P < 0.05; \*\*P < 0.01. Values are means  $\pm$  SE.

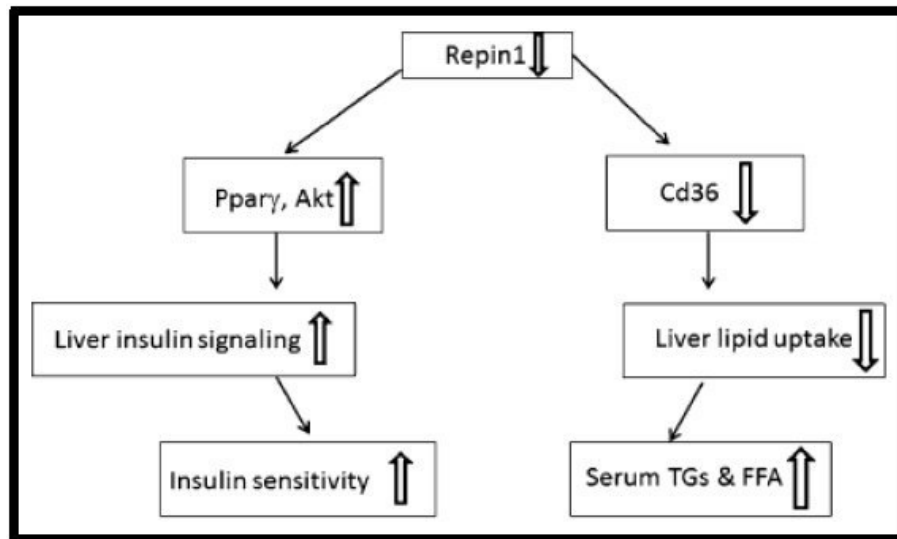


Figure 4.5: Model for the phenotype resulting from hepatic Repin1 deletion. Hepatic Repin1 deficiency leads to expression changes of genes involved in insulin signaling, glucose transport, lipid uptake, and lipid droplet formation. Lower liver lipid content may have caused significantly reduced Cd36 expression and the inability of the liver to take up plasma lipids normally. Reduced liver lipid content leads to improved whole-body insulin sensitivity.

Table 4.1: Serum concentrations of parameters of lipid metabolism, glucose homeostasis, and liver function at an age of 32 weeks (n = 12 per group). All values were obtained after a 14-h overnight fast except for FFA and glycerol levels, which were tested in the fed state (n = 6 per genotype). Significantly different data appear in boldface. \*Significantly different between WT and LRep1<sup>-/-</sup> mice at  $P < 0.05$ . \*\*Significantly different between WT and LRep1<sup>-/-</sup> mice at  $P < 0.01$ .

	WT	LRep1 <sup>-/-</sup>
<b>Serum lipids</b>		
TGs [mmol/l]	<b>1.51 ± 0.34</b>	<b>1.83 ± 0.40*</b>
Cholesterol [mmol/l]	2.44 ± 0.27	2.42 ± 0.28
HDL cholesterol [mmol/l]	1.96 ± 0.16	1.95 ± 0.26
LDL cholesterol [mmol/l]	0.18 ± 0.06	0.14 ± 0.07
FFA [mmol/l], fasted	<b>1.50 ± 0.20</b>	<b>1.68 ± 0.20**</b>
FFA [mmol/l], fed	1.41 ± 0.37	1.33 ± 0.26
Glycerol [nmol/ml], fed	3,184 ± 400	3,020 ± 471
<b>Glucosehomeostasis</b>		
Insulin [ng/ml]	0.15 ± 0.22	0.17 ± 0.23
Adiponectin [μg/ml]	77 ± 25	71 ± 17
Leptin [ng/ml]	139 ± 90	156 ± 50
Fasting glucose [mmol/l]	4.9 ± 1.3	4.9 ± 1.5
Nonfasting glucose [mmol/l]	6.6 ± 0.6	6.7 ± 0.8
<b>Liver function</b>		
ALT [μkat/l]	0.68 ± 0.19	0.86 ± 0.12
AST [μkat/l]	3.86 ± 1.57	5.49 ± 1.15
GLDH [units/l]	60.9 ± 3.5	57.1 ± 2.7
Serum Alb [g/l]	36.80 ± 0.39	36.13 ± 1.55



Table 4.2: Liver lipid profile analysis of male WT and LRep1<sup>-/-</sup> mice at age 32 weeks. Significantly different data appear in boldface. \*Significant difference between WT and LRep1<sup>-/-</sup> mice at 0.05 level.

Parameter [pmol/mg]	WT (n = 5)	LRep1 <sup>-/-</sup> (n = 6)
TAG	<b>22.1 ± 5.3</b>	<b>13.8 ± 2.0*</b>
Diacylglyceride	6.0 ± 2.1	7.0 ± 4.2
Cholesterolester	3.5 ± 1.6	2.4 ± 0.7
Cholesterol	24.8 ± 4.3	26.8 ± 2.8

## 4.5 Discussion

Our data provide the first *in vivo* evidence that Repin1 deletion in liver leads to lower body weight, reduced hepatic steatosis, increased energy expenditure and physical activity, and improved insulin sensitivity both at the organ and whole-body level. Lower body weight in LRep1<sup>-/-</sup> compared with control mice may be due to several mechanisms. LRep1<sup>-/-</sup> mice are characterized by higher VO<sub>2</sub> consumption and, at least in one dimension, higher spontaneous activity with unaltered food intake compared with WT mice. We tested the hypothesis that the increased energy expenditure in LRep1<sup>-/-</sup> compared with WT mice is a result of increased BAT mass or activity. Since mean body temperature, relative and absolute BAT mass, as well as expression of BAT marker genes in white adipose tissue are not different between LRep1<sup>-/-</sup> and control mice, we exclude an effect of liver Repin1 deficiency on BAT or browning of white adipose tissue. Taken together, increased energy expenditure and activity of LRep1<sup>-/-</sup> mice contribute to lower body weight.

Importantly, deletion of Repin1 in liver does not cause an increase in inflammatory marker genes or immune cell infiltration into livers of LRep1<sup>-/-</sup> mice. Moreover, AST, ALT, and GLDH serum concentrations were not significantly different between WT and LRep1<sup>-/-</sup> mice, excluding a hepatotoxic effect of Repin1 deletion.

Reduced liver fat is most likely due to significant changes in the expression of Repin1 target genes such as Cd36 and fatty acid binding proteins (FABPs). In the context of these (beneficial) metabolic consequences of reduced liver-specific Repin1 expression, elevated circulating TGs and FFAs in LRep1<sup>-/-</sup> mice seem to be contradictory to the phenotype. We therefore propose a model (Fig. 5) of how these changes in circulating lipids may be the result of changes in expression of key molecules in fatty acid uptake, transport, and lipid droplet formation in the liver. Elevated TGs and FFAs are most likely due to decreased hepatic lipid uptake capacity as a result of lower Cd36 expression in LRep1<sup>-/-</sup> mice. In addition to reduced Cd36 expression, several mechanisms may contribute to the observed reduction in TG storage

in LRep1<sup>-/-</sup> mice. Both *de novo* lipogenesis and VLDL production were not significantly different between LRep1<sup>-/-</sup> and control mice, suggesting that these processes do not cause reduced TG storage in livers of LRep1<sup>-/-</sup> mice. Moreover, we did not find differences in [<sup>14</sup>C]palmitate oxidation or the expression of key enzymes of  $\beta$ -oxidation between the genotypes, suggesting that Repin1 KO in liver does not significantly affect fatty acid oxidation in liver. Key gene expressions of TG synthesis (*Fasn*, *Scd1*, and *Scd2*) were not altered by Repin1 deletion in liver. However, since we did not directly assess TG synthesis in hepatocytes, we cannot exclude that this mechanism may contribute to reduced TG storage in livers of LRep1<sup>-/-</sup> mice. In accordance with altered liver lipid transporter expression, we detected lower concentrations of TAGs in the liver of LRep1<sup>-/-</sup> mice. These *in vivo* results strongly support our previous data on siRNA-mediated Repin1 knockdown in 3T3-L1 cells, which caused significantly reduced mRNA expression of fatty acid transporter Cd36 and lipid droplet genes (*Snai2* and *Vamp4*) in 3T3-L1 cells [9]. Moreover, the circulating lipid profile of LRep1<sup>-/-</sup> mice closely reflects that of CD36 KO mice, which are also characterized by elevated fasting FFAs and triacylglycerol, as well as cholesterol serum concentrations [26]. Interestingly, both LRep1<sup>-/-</sup> and CD36 KO mice are protected against impaired glucose homeostasis, despite these alterations in lipid metabolism [26]. Therefore, Repin1 deficiency in the liver provides a model to dissect the effects of liver fat accumulation from those of increased circulating lipids on whole-body insulin sensitivity. The insulin-sensitive phenotype of LRep1<sup>-/-</sup> mice further suggests that hepatic steatosis may represent a crucial mechanism in the development of insulin resistance independently of the increased circulating FFAs and TGs. Noteworthy, in mice with liver-specific insulin resistance due to a targeted disruption of the hepatic insulin receptor (LIRKO mice), circulating TGs and FFAs are ~40-50% lower compared with controls [27]. This opposite phenotype further suggests that improved insulin sensitivity in the liver of LRep1<sup>-/-</sup> mice is the primary effect of reduced Repin1 expression and changes in circulating lipids are secondary to that.

Kennedy *et al.* [28] demonstrated that adipose tissue from Cd36 KO mice was more insulin sensitive and had lower levels of inflammatory markers

(i.e., IFN- $\gamma$  and MCP-1) as compared with WT mice.

By several measures, we found beneficial effects of Repin1 deletion in liver on insulin sensitivity both under chow- and HFD-fed conditions. Noteworthy, insulin secretion dynamic in 40-week-old LRep1<sup>-/-</sup> mice suggests that Repin1 KO in the liver may cause secondary changes in islets that are in line with the observed improvements in whole-body insulin sensitivity. Whether the insulin secretion profile of LRep1<sup>-/-</sup> mice is due to improved insulin sensitivity or the result of a hepatic factor directly affecting islets needs to be explored in subsequent studies. Improved insulin sensitivity in LRep1<sup>-/-</sup> mice could be the result of improved activation of the insulin signaling cascade (e.g., Akt phosphorylation), increased Ppar $\gamma$  expression, lower liver fat content mediated by reduced expression of fatty acid transport proteins in LRep1<sup>-/-</sup> mice, lower total body fat content, and lower expression of insulin resistance-associated hepatokines (e.g., Lcn2 and chemerin).

With regard to the latter mechanism, mRNA expression array identified Lcn2 as the strongest potential candidate. Elevated Lcn2 serum concentrations are associated with obesity, dyslipidemia, and insulin resistance [29]. In livers of the LRep1<sup>-/-</sup> mice, we detected a 60-fold reduction of *Lcn2* mRNA level and reduced liver protein levels ( $P = 0.06$ ) compared with controls. There was a trend for lower circulating Lcn2 in LRep1<sup>-/-</sup> mice. Lcn2, also known as neutrophil gelatinase-associated lipocalin, is a lipocalin sub-family member and has been recently identified as an adipose tissue-derived cytokine [30]. Lcn2 is an extracellular lipocalin and has structural similarity with FABPs, and both are members of the multigene family of up and down  $\beta$ -barrel proteins [31]. Both intracellular FABPs and the extracellular lipocalins have a clearly defined  $\beta$ -barrel motif that forms either an interior cavity (FABP) or a deep pit (lipocalin) that constitutes the lipid binding domain [31]. Because of the unique structure, the lipocalins function as efficient transporters for a number of different hydrophobic ligands in extracellular milieus, including a variety of retinoids, fatty acids, biliverdin, pheromones, porphyrins, odorants, steroids, and iron [32]. *In vitro*, it was shown that exogenous Lcn2 promotes insulin resistance in cultured hepatocytes [33]. It is likely that Lcn2 as retinoic acid could potentially be involved

in or mediate lipid storage effects in both liver and adipose tissue. Moreover, reduced *Lcn2* in *LRep1*<sup>-/-</sup> mice may contribute to the observed alterations in adipose tissue with a higher number of smaller adipocytes in *LRep1*<sup>-/-</sup> compared with control mice upon HFD. Liver *Repin1* deficiency leads to secondary changes in adipose tissue with a reduction in adipocyte size under HFD in homozygous *LRep1*<sup>-/-</sup> mice, indicating a protection against hypertrophy of adipocytes. However, since we did not biopsy adipose tissue during HFD, we do not provide direct evidence for increased adipogenesis in *LRep1*<sup>-/-</sup> mice. Protection of *LRep1*<sup>-/-</sup> mice against adipocyte hypertrophy could contribute to significantly better insulin sensitivity as measured by ITT after 10 weeks of HFD.

Our previous *in vitro* studies demonstrated that *Repin1* expression increases during adipogenesis and that RNA interference-based *Repin1* downregulation in mature adipocytes significantly reduces adipocyte size [9]. We found significant correlations between *Repin1* mRNA expression and total body fat mass as well as adipocyte size in human paired visceral and SC adipose tissue, suggesting a potential role for *Repin1* in the regulation of adipocyte size [9]. However, it is not clear how a lack of *Repin1* in liver might influence adipocyte size. One possibility is that absence of *Repin1* in liver generates signals that either restrict adipocyte lipid load or increase adipogenesis. For the latter mechanism, we consider reduced *Lcn2* expression in livers of *LRep1*<sup>-/-</sup> mice as a candidate molecule.

This hypothesis is supported by data that *Lcn2* deficiency protects mice from developing aging- and obesity-induced insulin resistance by modulating insulin resistance factors in adipose tissue [34]. *Lcn2*-disrupted mice are partly protected from HFD-induced insulin resistance. In this context, it has been shown that other members of the lipocalin family, in particular lipocalin-type prostaglandin D synthase, may impair the adipogenesis program [35]. Although we do not have direct evidence for increased adipogenesis in *LRep1*<sup>-/-</sup> mice, we speculate that changes in adipose tissue morphology may be due to reduced *Lcn2* levels with subsequent disinhibition of adipogenesis.

In contrast to our observation marked *Lcn2* deficiency leads to enlarged

adipocytes and improved adipose tissue function, which has been related to reduced inflammation in adipose tissue of these mice [34]. We cannot exclude that changes in adipose tissue of LRep1<sup>-/-</sup> mice are at least in part mediated by reduced inflammatory activation in adipose tissue. In addition, reduced chemerin expression may lead to smaller adipocyte size. Indirect evidence from insulin-sensitive obese individuals supports the hypothesis that lower circulating chemerin (in insulinsensitive, healthy obese) is associated with smaller adipocyte size [36]. Whether additional mediators contribute to the specific response to HFD in adipose tissue of LRep1<sup>-/-</sup> mice should be further studied. Adipocyte-specific insulin sensitivity was not altered in LRep1<sup>-/-</sup> mice. Hepatocyte-derived factors may have further contributed to increased lipolysis in adipocytes of LRep1<sup>-/-</sup> mice, which has been suggested by higher basal glycerol release and higher expression of key lipolysis enzymes (*Hsl*, *Atgl*, and *Lpl*) in LRep1<sup>-/-</sup> adipocytes.

To further elucidate potential mechanisms for improved liver insulin sensitivity and reduced liver fat content in LRep1<sup>-/-</sup> mice, we performed a hepatic lipidomics screen as well as mRNA expression array analysis in liver samples. The liver lipidomics data demonstrate that Repin1 modulates the overall profile of liver lipid species. Here, the main finding of the screen was that hepatic deletion of Repin1 had a significant effect on TAG amount in livers, suggesting altered lipid storage in liver. Thus, reduced liver lipid storage ability could explain significantly higher serum TG levels in LRep1<sup>-/-</sup> mice. Since LRep1<sup>-/-</sup> hepatocytes did not undergo typical ballooning under HFD conditions, we examined whether genes involved in lipid droplet fusion as well as lipid transport proteins are regulated by Repin1 deficiency. We detected significantly reduced levels of *Vamp4* and *Snap23* in livers of Repin1-deficient mice, suggesting a disturbance in lipid vesicle formation and hepatic lipid upload. Boström *et al.* [37] demonstrated that Snap23 and Vamp4 are functional in the fusion between lipid droplets and are essential for the growth of lipid droplets. Our results are in accordance with our previous finding that downregulation of Repin1 in 3T3-L1 adipocytes by siRNA leads to significantly reduced lipid droplet size [9]. In parallel to the mRNA expression data in the liver of Repin1-deficient mice, we found reduced *Snap23*

and *Vamp4* expression in 3T3-L1 cells upon downregulation of Repin1 [9]. Knockdown of VAMP4 and SNAP23 has been recently shown to decrease the rate of lipid droplet fusion and the size of the lipid droplets [33]. Noteworthy, decreased VAMP4 and SNAP23 gene expression in response to Repin1 knockdown seems to be specific, since other lipid droplet proteins, including perilipin and syntaxin5, were not regulated by Repin1 [9].

In conclusion, we provide a model of how Repin1 may, through regulation of gene expression, lead to lower body weight, improved liver and whole-body insulin sensitivity, and alterations in lipid metabolism. We propose that hepatic Repin1 deficiency primarily leads to improved insulin sensitivity and reduced liver fat content with secondary changes in serum lipid profile due to alterations in hepatic lipid transport. Furthermore, hepatic deletion of Repin1 causes altered expression of molecules, including *Lcn2* and chemerin, which may contribute to reduced adipocyte size in response to HFD, which may subsequently further contribute to beneficial effects on whole-body insulin sensitivity in *LRep1<sup>-/-</sup>* mice.

Our findings indicate that Repin1 contributes to insulin sensitivity and glucose and lipid metabolism by regulating the expression of key molecules of these processes. Therefore, alterations in Repin1 expression may contribute to the pathogenesis of insulin resistance and dyslipidemia and subsequent impairment of glucose homeostasis.

## 4.6 Acknowledgments

The authors thank Eva Böge, Manuela Prellberg, Viola Döbel, Anne Kunath, and Daniela Kern (University of Leipzig) for technical assistance. Furthermore, the authors thank Professor Fitzl (Institute of Anatomy, University of Leipzig) for help with liver staining.

## 4.7 Funding

This work was supported by the clinical research group “Atherobesity“ (KFO 152, project KL-2346) and the SFB 1052: B1 (to M.B.), B3 (to P.K.), and B4 (to N.K.) founded by Deutsche Forschungsgemeinschaft, formell program, and the Federal Ministry of Education and Research, Germany, FKZ: 01EO1001 (N.K.). J.T.H. is funded by the European Union and the Free State of Saxony.

## 4.8 Duality of Interest

No potential conflicts of interest relevant to this article were reported.

## 4.9 Author Contributions

M.K. researched data and wrote the manuscript. J.K., N.H., and I.K. researched data and performed Western blots. J.B. and J.T.H. performed Western blots and histological experiments. G.F. measured serum concentrations. P.K. reviewed the manuscript and contributed to discussion. M.M.-S., R.G., S.S., and A.S. performed lipidomics studies. K.K. performed Affymetrix GeneChip analysis. K.A. researched data and performed immunostaining. M.S. conceived the research ideas and reviewed and edited the manuscript. M.B. reviewed and edited the manuscript. N.K. conceived the research ideas, supervised the project, and wrote the manuscript. N.K. is the guarantor of this work and, as such, had full access to all the data in the study and takes responsibility for the integrity of the data and the accuracy of the data analysis.

## 4.10 References

- [1] N. Klöting, B. Wilke, and I. Klöting. Phenotypic and genetic analyses of subcongenic BB.SHR rat lines shorten the region on chromosome 4



- bearing gene(s) for underlying facets of metabolic syndrome. *Physiol. Genomics*, 18(3):325–330, Aug 2004.
- [2] I. Kloting, P. Kovacs, and J. van den Brandt. Sex-specific and sex-independent quantitative trait loci for facets of the metabolic syndrome in WOKW rats. *Biochem. Biophys. Res. Commun.*, 284(1):150–156, Jun 2001.
- [3] P. Kovacs, J. van den Brandt, A. C. Bonne, L. F. van Zutphen, H. A. van Lith, and I. Kloting. Congenic BB.SHR rat provides evidence for effects of a chromosome 4 segment (D4Mit6-Npy approximately 1 cm) on total serum and lipoprotein lipid concentration and composition after feeding a high-fat, high-cholesterol diet. *Metab. Clin. Exp.*, 50(4):458–462, Apr 2001.
- [4] N. Kloting, B. Wilke, and I. Kloting. Triplet repeat in the Repin1 3'-untranslated region on rat chromosome 4 correlates with facets of the metabolic syndrome. *Diabetes Metab. Res. Rev.*, 23(5):406–410, Jul 2007.
- [5] L. Dailey, M. S. Caddle, N. Heintz, and N. H. Heintz. Purification of RIP60 and RIP100, mammalian proteins with origin-specific DNA-binding and ATP-dependent DNA helicase activities. *Mol. Cell. Biol.*, 10(12):6225–6235, Dec 1990.
- [6] M. S. Caddle, L. Dailey, and N. H. Heintz. RIP60, a mammalian origin-binding protein, enhances DNA bending near the dihydrofolate reductase origin of replication. *Mol. Cell. Biol.*, 10(12):6236–6243, Dec 1990.
- [7] A. L. Schroll and N. H. Heintz. Chemical footprinting of structural and functional elements of dhfr oribeta during the CHO 400 cell cycle. *Gene*, 332:139–147, May 2004.
- [8] C. R. Houchens, W. Montigny, L. Zeltser, L. Dailey, J. M. Gilbert, and N. H. Heintz. The dhfr oribeta-binding protein RIP60 contains 15 zinc fingers: DNA binding and looping by the central three fingers and an

- associated proline-rich region. *Nucleic Acids Res.*, 28(2):570–581, Jan 2000.
- [9] K. Ruschke, M. Illes, M. Kern, I. Kloting, M. Fasshauer, M. R. Schon, J. Kosacka, G. Fitzl, P. Kovacs, M. Stumvoll, M. Bluher, and N. Kloting. Repin1 maybe involved in the regulation of cell size and glucose transport in adipocytes. *Biochem. Biophys. Res. Commun.*, 400(2):246–251, Sep 2010.
- [10] A. R. Saltiel and C. R. Kahn. Insulin signalling and the regulation of glucose and lipid metabolism. *Nature*, 414(6865):799–806, Dec 2001.
- [11] N. Kloting, L. Koch, T. Wunderlich, M. Kern, K. Ruschke, W. Krone, J. C. Bruning, and M. Bluher. Autocrine IGF-1 action in adipocytes controls systemic IGF-1 concentrations and growth. *Diabetes*, 57(8):2074–2082, Aug 2008.
- [12] S. J. Fisher and C. R. Kahn. Insulin signaling is required for insulin’s direct and indirect action on hepatic glucose production. *J. Clin. Invest.*, 111(4):463–468, Feb 2003.
- [13] J. H. Youn and T. A. Buchanan. Fasting does not impair insulin-stimulated glucose uptake but alters intracellular glucose metabolism in conscious rats. *Diabetes*, 42(5):757–763, May 1993.
- [14] M. Kern, N. Kloting, H. G. Niessen, L. Thomas, D. Stiller, M. Mark, T. Klein, and M. Bluher. Linagliptin improves insulin sensitivity and hepatic steatosis in diet-induced obesity. *PLoS ONE*, 7(6):e38744, 2012.
- [15] J. FOLCH, M. LEES, and G. H. SLOANE STANLEY. A simple method for the isolation and purification of total lipides from animal tissues. *J. Biol. Chem.*, 226(1):497–509, May 1957.
- [16] M. Carvalho, J. L. Sampaio, W. Palm, M. Brankatschk, S. Eaton, and A. Shevchenko. Effects of diet and development on the *Drosophila* lipidome. *Mol. Syst. Biol.*, 8:600, 2012.

- 
- [17] R. Herzog, D. Schwudke, K. Schuhmann, J. L. Sampaio, S. R. Bornstein, M. Schroeder, and A. Shevchenko. A novel informatics concept for high-throughput shotgun lipidomics based on the molecular fragmentation query language. *Genome Biol.*, 12(1):R8, 2011.
- [18] R. Sandhoff, B. Brugger, D. Jeckel, W. D. Lehmann, and F. T. Wieland. Determination of cholesterol at the low picomole level by nano-electrospray ionization tandem mass spectrometry. *J. Lipid Res.*, 40(1):126–132, Jan 1999.
- [19] A. M. Krowczynska, M. Coutts, S. Makrides, and G. Brawerman. The mouse homologue of the human acidic ribosomal phosphoprotein PO: a highly conserved polypeptide that is under translational control. *Nucleic Acids Res.*, 17(15):6408, Aug 1989.
- [20] K. Kotani, O. D. Peroni, Y. Minokoshi, O. Boss, and B. B. Kahn. GLUT4 glucose transporter deficiency increases hepatic lipid production and peripheral lipid utilization. *J. Clin. Invest.*, 114(11):1666–1675, Dec 2004.
- [21] Y. Minokoshi, M. Saito, and T. Shimazu. Sympathetic denervation impairs responses of brown adipose tissue to VMH stimulation. *Am. J. Physiol.*, 251(5 Pt 2):R1005–1008, 1986.
- [22] J. S. Millar, D. A. Cromley, M. G. McCoy, D. J. Rader, and J. T. Billheimer. Determining hepatic triglyceride production in mice: comparison of poloxamer 407 with Triton WR-1339. *J. Lipid Res.*, 46(9):2023–2028, Sep 2005.
- [23] N. Kloting, M. Bluher, and I. Kloting. The polygenetically inherited metabolic syndrome of WOKW rats is associated with insulin resistance and altered gene expression in adipose tissue. *Diabetes Metab. Res. Rev.*, 22(2):146–154, 2006.
- [24] S. Lorenz, M. Eszlinger, R. Paschke, G. Aust, M. Weick, D. Fuhrer, and K. Krohn. Calcium signaling of thyrocytes is modulated by TSH

- through calcium binding protein expression. *Biochim. Biophys. Acta*, 1803(3):352–360, Mar 2010.
- [25] K. Le Minh, K. Klemm, K. Abshagen, C. Eipel, M. D. Menger, and B. Vollmar. Attenuation of inflammation and apoptosis by pre- and posttreatment of darbepoetin-alpha in acute liver failure of mice. *Am. J. Pathol.*, 170(6):1954–1963, Jun 2007.
- [26] M. Febbraio, N. A. Abumrad, D. P. Hajjar, K. Sharma, W. Cheng, S. F. Pearce, and R. L. Silverstein. A null mutation in murine CD36 reveals an important role in fatty acid and lipoprotein metabolism. *J. Biol. Chem.*, 274(27):19055–19062, Jul 1999.
- [27] M. D. Michael, R. N. Kulkarni, C. Postic, S. F. Previs, G. I. Shulman, M. A. Magnuson, and C. R. Kahn. Loss of insulin signaling in hepatocytes leads to severe insulin resistance and progressive hepatic dysfunction. *Mol. Cell*, 6(1):87–97, Jul 2000.
- [28] D. J. Kennedy, S. D. Kuchibhotla, E. Guy, Y. M. Park, G. Nimako, D. Vanegas, R. E. Morton, and M. Febbraio. Dietary cholesterol plays a role in CD36-mediated atherogenesis in LDLR-knockout mice. *Arterioscler. Thromb. Vasc. Biol.*, 29(10):1481–1487, Oct 2009.
- [29] Y. Wang, K. S. Lam, E. W. Kraegen, G. Sweeney, J. Zhang, A. W. Tso, W. S. Chow, N. M. Wat, J. Y. Xu, R. L. Hoo, and A. Xu. Lipocalin-2 is an inflammatory marker closely associated with obesity, insulin resistance, and hyperglycemia in humans. *Clin. Chem.*, 53(1):34–41, Jan 2007.
- [30] H. Guo, D. Jin, Y. Zhang, W. Wright, M. Bazuine, D. A. Brockman, D. A. Bernlohr, and X. Chen. Lipocalin-2 deficiency impairs thermogenesis and potentiates diet-induced insulin resistance in mice. *Diabetes*, 59(6):1376–1385, Jun 2010.
- [31] J. M. LaLonde, D. A. Bernlohr, and L. J. Banaszak. The up-and-down beta-barrel proteins. *FASEB J.*, 8(15):1240–1247, Dec 1994.

- 
- [32] Q. Yang, T. E. Graham, N. Mody, F. Preitner, O. D. Peroni, J. M. Zabolotny, K. Kotani, L. Quadro, and B. B. Kahn. Serum retinol binding protein 4 contributes to insulin resistance in obesity and type 2 diabetes. *Nature*, 436(7049):356–362, Jul 2005.
- [33] Q. W. Yan, Q. Yang, N. Mody, T. E. Graham, C. H. Hsu, Z. Xu, N. E. Houstis, B. B. Kahn, and E. D. Rosen. The adipokine lipocalin 2 is regulated by obesity and promotes insulin resistance. *Diabetes*, 56(10):2533–2540, Oct 2007.
- [34] I. K. Law, A. Xu, K. S. Lam, T. Berger, T. W. Mak, P. M. Vanhoutte, J. T. Liu, G. Sweeney, M. Zhou, B. Yang, and Y. Wang. Lipocalin-2 deficiency attenuates insulin resistance associated with aging and obesity. *Diabetes*, 59(4):872–882, Apr 2010.
- [35] M. S. Hossain, A. A. Chowdhury, M. S. Rahman, K. Nishimura, M. Jisaka, T. Nagaya, F. Shono, and K. Yokota. Stable expression of lipocalin-type prostaglandin D synthase in cultured preadipocytes impairs adipogenesis program independently of endogenous prostanoids. *Exp. Cell Res.*, 318(4):408–415, Feb 2012.
- [36] N. Kloting, M. Fasshauer, A. Dietrich, P. Kovacs, M. R. Schon, M. Kern, M. Stumvoll, and M. Bluher. Insulin-sensitive obesity. *Am. J. Physiol. Endocrinol. Metab.*, 299(3):E506–515, Sep 2010.
- [37] P. Bostrom, L. Andersson, M. Rutberg, J. Perman, U. Lidberg, B. R. Johansson, J. Fernandez-Rodriguez, J. Ericson, T. Nilsson, J. Boren, and S. O. Olofsson. SNARE proteins mediate fusion between cytosolic lipid droplets and are implicated in insulin sensitivity. *Nat. Cell Biol.*, 9(11):1286–1293, Nov 2007.

## 4.11 Supplementary Data

GOTERM BP_FAT	biological process				
Category	Term	Gene count	%	PValue	
GOTERM BP_FAT	GO:0006412-translation	66	4.00728597	9.73E-13	
GOTERM BP_FAT	GO:0006091-generation of precursor metabolites and energy	46	2.79295689	5.69E-07	
GOTERM CC_FAT	cellular component				
Category	Term	Gene count	%	PValue	
GOTERM CC_FAT	GO:0005840-ribosome	52	3.15725562	3.15E-15	
GOTERM CC_FAT	GO:0030529-ribonucleoprotein complex	85	5.1608986	1.52E-13	
GOTERM CC_FAT	GO:0043228-non-membrane-bounded organelle	227	13.7826351	2.53E-11	
GOTERM CC_FAT	GO:0043232-intracellular non-membrane-bounded organelle	227	13.7826351	2.53E-11	
GOTERM CC_FAT	GO:0005743-mitochondrial inner membrane	59	3.5822708	4.90E-11	
GOTERM CC_FAT	GO:0044429-mitochondrial part	86	5.22161506	5.99E-11	
GOTERM CC_FAT	GO:0031966-mitochondrial membrane	67	4.06800243	1.29E-10	
GOTERM CC_FAT	GO:0019866-organelle inner membrane	60	3.64298725	1.47E-10	
GOTERM CC_FAT	GO:0031090-organelle membrane	115	6.98239223	2.65E-10	
GOTERM CC_FAT	GO:0005740-mitochondrial envelope	69	4.18943534	2.67E-10	
GOTERM CC_FAT	GO:0031967-organelle envelope	82	4.97874924	7.68E-09	
GOTERM CC_FAT	GO:0031975-envelope	82	4.97874924	9.04E-09	
GOTERM CC_FAT	GO:0005739-mitochondrion	158	9.59319976	3.44E-08	
GOTERM CC_FAT	GO:0045259-proton-transporting ATP synthase complex	10	0.60716454	4.88E-06	
GOTERM CC_FAT	GO:0015629-actin cytoskeleton	35	2.1250759	2.34E-05	

Figure 4.6: Supplementary Table 1. Results of functional annotation tool using Database for Annotation, Visualization and Integrated Discovery (DAVID). For data analysis probe set fluorescence intensities were extracted for approximately 39,000 transcripts with complete Mouse Genome coverage and were scaled in order to normalize data for inter-array comparison using MAS 5.0 software according to instructions of the manufacturer (Affymetrix, Santa Clara, CA, USA).

<b>GOTERM_MF_FAT</b>	molecular function					
Category	Term	Gene count	%	PValue		
GOTERM_MF_FAT	GO:0003735~structural constituent of ribosome	47	2,85367335	2,17E-16		
GOTERM_MF_FAT	GO:0005198~structural molecule activity	71	4,31086825	2,04E-08		
GOTERM_MF_FAT	GO:0015077~monovalent inorganic cation transmembrane transporter activity	23	1,39647845	6,34E-07		
GOTERM_MF_FAT	GO:0015078~hydrogen ion transmembrane transporter activity	22	1,33576199	9,07E-07		
GOTERM_MF_FAT	GO:0022890~inorganic cation transmembrane transporter activity	27	1,63934426	4,84E-06		
GOTERM_MF_FAT	GO:0003779~actin binding	46	2,79295689	6,25E-06		
<b>KEGG_PATHWAY</b>						
Category	Term	Gene count	%	PValue		
KEGG_PATHWAY	mmu03010:Ribosome	47	2,85367335	2,94E-25		
KEGG_PATHWAY	mmu05016:Huntington's disease	39	2,36794171	8,66E-07		
KEGG_PATHWAY	mmu00190:Oxidative phosphorylation	29	1,76077717	1,20E-05		
KEGG_PATHWAY	mmu05012:Parkinson's disease	29	1,76077717	1,88E-05		

Figure 4.6: (Previous Page)

	Genes up-regulated in LRep1 <sup>-/-</sup>	n-fold regulation	Genes down-regulated in LRep1 <sup>-/-</sup>	n-fold regulation
1	RIKEN cDNA 2900092N22 gene	30.1	<b>Lipocalin 2*</b>	68.4
2	NLR family, pyrin domain containing 4F	27.8	Predicted gene, ENSMUSG00000076577	45.2
3	Kelch-like 28 (Drosophila)	23.1	Metallothionein 1 (MT1)	16.4
4	RIKEN cDNA 8430419K02 gene	21.3	Transmembrane protein 109	14.1
5	Ubiquitin specific peptidase 15 (Usp15)	20.9	Necdin	13.5
6	Methionine sulfoxide reductase B3	19.6	Metallothionein 2 (MT2)*	12.8
7	Insulin receptor substrate (Irs3)*	15.3	Serum amyloid A 2 (Saa2)*	9.9
8	Granzyme D	13.3	Phosphatidylinositol 4-kinase (PI4Ka)*	8.8
9	Collagen, type XIX, alpha 1 (Col19a1)	12.6	Monooxygenase, DBH-like 1	8.5
10	Toll like receptor 3 (Tlr3)*	12.5	ADP-ribosyltransferase 2a (Art2a)	8.3
11	Titin (Tnt)*	13.9	Adaptor-related protein complex 3, mu 2 (Ap3m2)	8.0
12	Leucine zipper-EF-hand containing transmembrane protein 2 (Letm2)	13.1	Acsl3 (acyl-CoA synthetase long-chain family member 3)	5.6
13	Serine (or cysteine) peptidase inhibitor, clade A, member 4 (Serpina-ps1)	11.4	Junction adhesion molecule 3 (Jam3)	4.6
14	Calcium-sensing receptor (Casr)	11.9	T-box18	3.8
15	Serine threonine kinase 31 (Stk31)	11.8	Vesicle associated membrane protein (Vamp5)*	3.3
16	Transmembrane protein 190	10.4	Low Density Receptor (Ldlr)*	2.1
17	zinc finger and AT hook domain containing (Zfat)	8.6	Vesicle associated membrane protein (Vamp4)*	1.9
18	Extracellular matrix protein 2, female organ and adipocyte specific (Ecm2)	7.9	<b>Rarres 2 (Chemerin)*</b>	1.6

Figure 4.7: Supplementary Table 2. Regulated genes identified by liver Affymetrix GeneChip analysis. \*liver expression has been validate by qPCR in 10 animals per genotype



<b>Gene</b>	<b>WT</b>	<b>LRep1<sup>-/-</sup></b>
<b><i>Vesicle lipid formation</i></b>		
<i>Snap23</i>	<b>1.00 ± 0.48</b>	<b>0.62 ± 0.42*</b>
<i>Vamp4</i>	<b>1.00 ± 0.55</b>	<b>0.16 ± 0.10***</b>
<i>Caveolin</i>	<b>1.00 ± 0.46</b>	<b>0.60 ± 0.34*</b>
<b><i>Lipolysis enzymes</i></b>		
<i>Hsl iso 1</i>	1.00 ± 0.47	0.84 ± 0.74
<i>Hsl iso 2</i>	1.00 ± 0.46	0.77 ± 0.21
<i>Hsl iso 3</i>	1.00 ± 0.42	0.84 ± 0.21
<i>Lpl</i>	1.00 ± 0.56	0.94 ± 0.34
<i>Ldlr</i>	1.00 ± 0.46	0.97 ± 0.28
<b><i>Synthesis</i></b>		
<i>Fasn</i>	1.00 ± 0.67	0.86 ± 0.54
<i>ApoA1</i>	1.00 ± 0.22	1.03 ± 0.33
<i>ApoD</i>	1.00 ± 1.12	1.30 ± 0.97
<i>Mdr2</i>	1.00 ± 0.19	0.98 ± 0.20
<i>Pemt</i>	1.00 ± 0.34	0.98 ± 0.23
<b><i>Synthesis of unsaturated FA</i></b>		
<i>Scd1</i>	1.00 ± 0.47	1.07 ± 0.47
<i>Scd2</i>	1.00 ± 0.18	1.02 ± 0.36
<i>Alt</i>	1.00 ± 0.36	0.90 ± 0.36
<i>Acs11</i>	1.00 ± 0.63	0.92 ± 0.54
<b><i>Fat transporter and fatty oxidation</i></b>		
<i>Cd36</i>	<b>1.00 ± 0.45</b>	<b>0.50 ± 0.22**</b>
<i>Fatp1</i>	1.00 ± 0.34	0.79 ± 0.21
<i>Fatp2</i>	1.00 ± 0.23	1.04 ± 0.21
<i>Fatp4</i>	1.00 ± 0.37	0.92 ± 0.30
<i>Cpt1</i>	1.00 ± 0.61	0.71 ± 0.29
<i>Cpt2</i>	1.00 ± 0.40	0.79 ± 0.30
<b><i>Gluconeogenesis &amp; Glucosetransporter</i></b>		
<i>Pepck</i>	1.00 ± 0.36	1.08 ± 0.40
<i>Glut2</i>	1.00 ± 0.33	1.20 ± 0.36
<i>Ide</i>	1.00 ± 0.31	1.16 ± 0.63
<b><i>Target genes</i></b>		
<i>Chemerin</i>	<b>1.00 ± 0.36</b>	<b>0.68 ± 0.44*</b>
<i>Lipocalin2</i>	<b>1.00 ± 0.41</b>	<b>0.02 ± 0.02**</b>

Figure 4.8: Supplementary Table 3. Relative gene expression in liver (N=12 per group) at an age of 32 weeks. \*significant different between Controls (WT) and LRep1<sup>-/-</sup> mice at \* 0.05, \*\* 0.01 and \*\*\*0.001 level

Gene	EPI		SC	
	WT (N=7)	LRep1 <sup>-/-</sup> (N=7)	WT (N=7)	LRep1 <sup>-/-</sup> (N=7)
<b>Lipolysis enzymes</b>				
<i>Hsl iso 1</i>	1.00 ± 0.40	0.99 ± 0.61	1.00 ± 0.67	<b>1.38 ± 0.17</b>
<i>Hsl iso 2</i>	1.00 ± 0.51	1.02 ± 0.63	1.00 ± 0.70	<b>1.55 ± 0.32</b>
<i>Hsl iso 3</i>	1.00 ± 0.45	0.99 ± 0.58	1.00 ± 0.63	<b>1.48 ± 0.23</b>
<i>Atgl</i>	1.00 ± 0.52	0.95 ± 0.55	1.00 ± 0.72	<b>1.86 ± 0.33</b>
<i>Lpl</i>	1.00 ± 0.42	1.17 ± 0.72	1.00 ± 0.85	<b>1.56 ± 0.12</b>
<b>Glucosetransporter</b>				
<i>Glut4</i>	1.00 ± 0.44	1.24 ± 0.46	1.00 ± 0.54	1.82 ± 0.56
<i>Glut1</i>	1.00 ± 0.42	0.80 ± 0.85	<b>1.00 ± 0.58</b>	<b>0.57 ± 0.34*</b>
<b>Fat transporter and oxidation enzymes</b>				
<i>Cd36</i>	1.00 ± 0.36	1.07 ± 0.62	<b>1.00 ± 0.88</b>	<b>2.62 ± 0.82**</b>
<i>Fasn</i>	1.00 ± 0.47	1.04 ± 0.74	1.00 ± 0.57	1.69 ± 1.02
<b>BAT genes</b>				
<i>Ucp1</i>	1.00 ± 0.85	0.54 ± 0.22	1.00 ± 0.42	0.90 ± 1.10
<i>Prdm16</i>	1.00 ± 0.49	1.09 ± 0.91	1.00 ± 0.98	0.64 ± 0.32
<b>Target genes</b>				
<i>Chemerin</i>	1.00 ± 0.38	1.29 ± 0.69	<b>1.00 ± 0.38</b>	<b>2.51 ± 0.27*</b>
<i>Lipocalin2</i>	<b>1.00 ± 0.81</b>	<b>0.22 ± 0.14**</b>	<b>1.00 ± 1.11</b>	<b>0.33 ± 0.12*</b>

Figure 4.9: Supplementary Table 4. Genexpression analysis in adipose tissue fat depots, epigonadal (EPI) and subcutaneous (SC) of control and LRep1<sup>-/-</sup> mice.

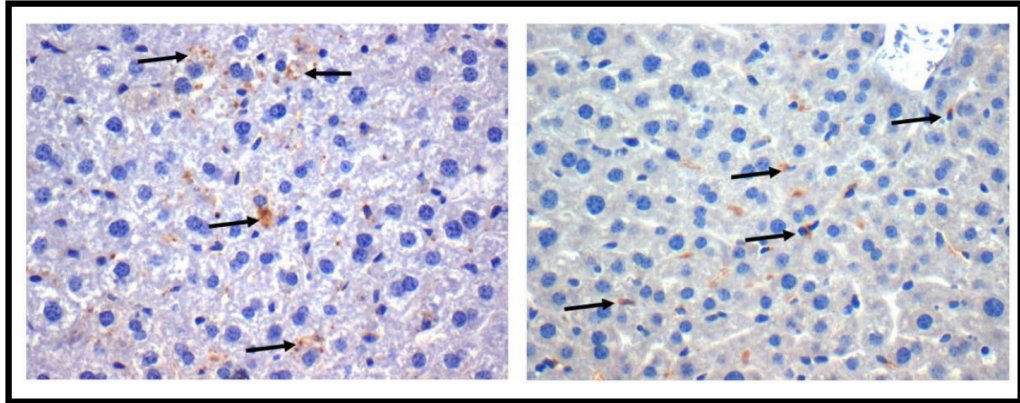


Figure 4.10: Supplementary Figure 1. Representative images (original magnification x200) of Repin1 immunohistochemistry (positive staining of the Repin1 protein with DAB as chromogen in brown, arrows) of liver tissue of wild-type mice (left) and LRep1<sup>-/-</sup> mice (right). Please note the cytoplasmic staining of hepatocytes for Repin1 in wild-type mice, whereas in livers of LRep1<sup>-/-</sup> mice exclusively non-parenchymal cells are Repin1-positive. Sections were stained with hematoxylin and eosin (HE) for routine examination. For immunohistochemical staining of Repin1 sections of liver tissue were incubated with primary antibody overnight at 4 °C (polyclonal anti-Repin1, 1:500, Abcam, Cambridge, UK), followed by horseradish-peroxidase (HRP)-conjugated rabbit anti-mouse immunoglobulin (1:100, Dako Cytomation, Hamburg, Germany) as secondary antibody. Sites of peroxidase-binding were detected by 3,3'-diaminobenzidine (Dako).

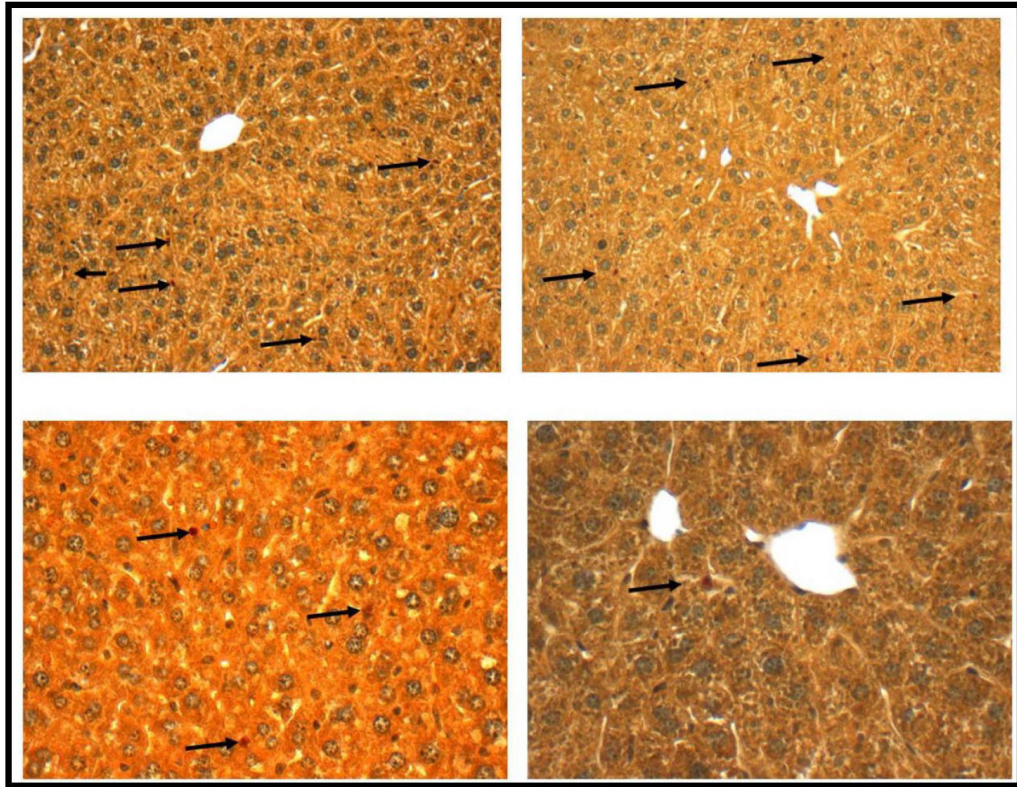


Figure 4.11: Supplementary Figure 2. Representative images of hepatic tissue for F4/80 antigen immunostaining of wild-type (left) and LRep1<sup>-/-</sup> mice (right) (original magnification x200, upper panel; x400, lower panel) (positive staining of the F4/80 extracellular membrane protein with permanent red as chromogen in red). To evaluate the cellular inflammatory response, the numbers of resident liver macrophages were analyzed using the F4/80 antigen (1:10; Serotec, Oxford, UK). Overnight incubation (4 °C) with the first antibody (polyclonal rat anti-F4/80) was followed by conjugated mouse anti-rat immunoglobulin (1:200; Santa Cruz Biotechnology, Santa Cruz, CA, USA). The sites of alkaline phosphatase binding were detected using the chromogen permanent red (Dako). The sections were counterstained with hemalaun and analyzed with a light microscope (Olympus BX51, Hamburg, Germany).

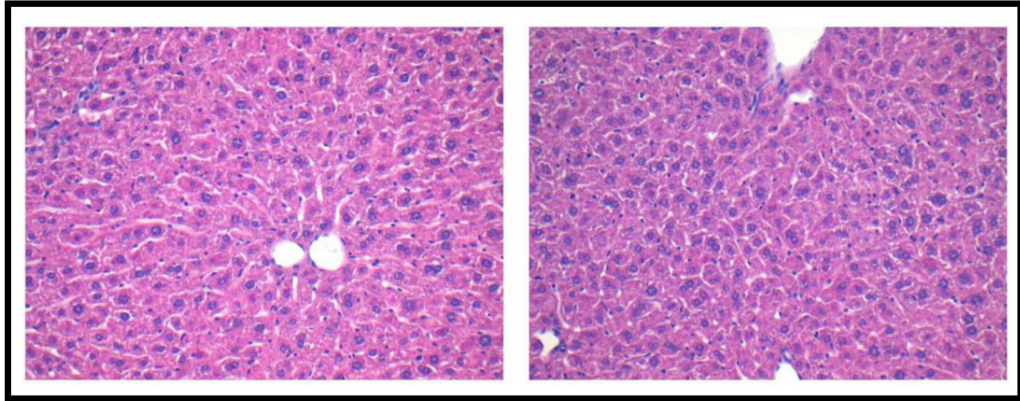


Figure 4.12: Supplementary Figure 3. Representative images of hepatic tissue for CAE-staining of wild-type (left) and LRep1<sup>-/-</sup> mice (right) (original magnification x200, upper panel; x400, lower panel) (CAE-positive cells are in red-brown) showing no increased infiltration of inflammatory cells to the liver of LRep1<sup>-/-</sup> mice. Sections were stained with hematoxylin and eosin (HE) for routine examination and with naphthol AS-D chloroacetate esterase (CAE) for detection of liver tissue-infiltrating leukocytes.

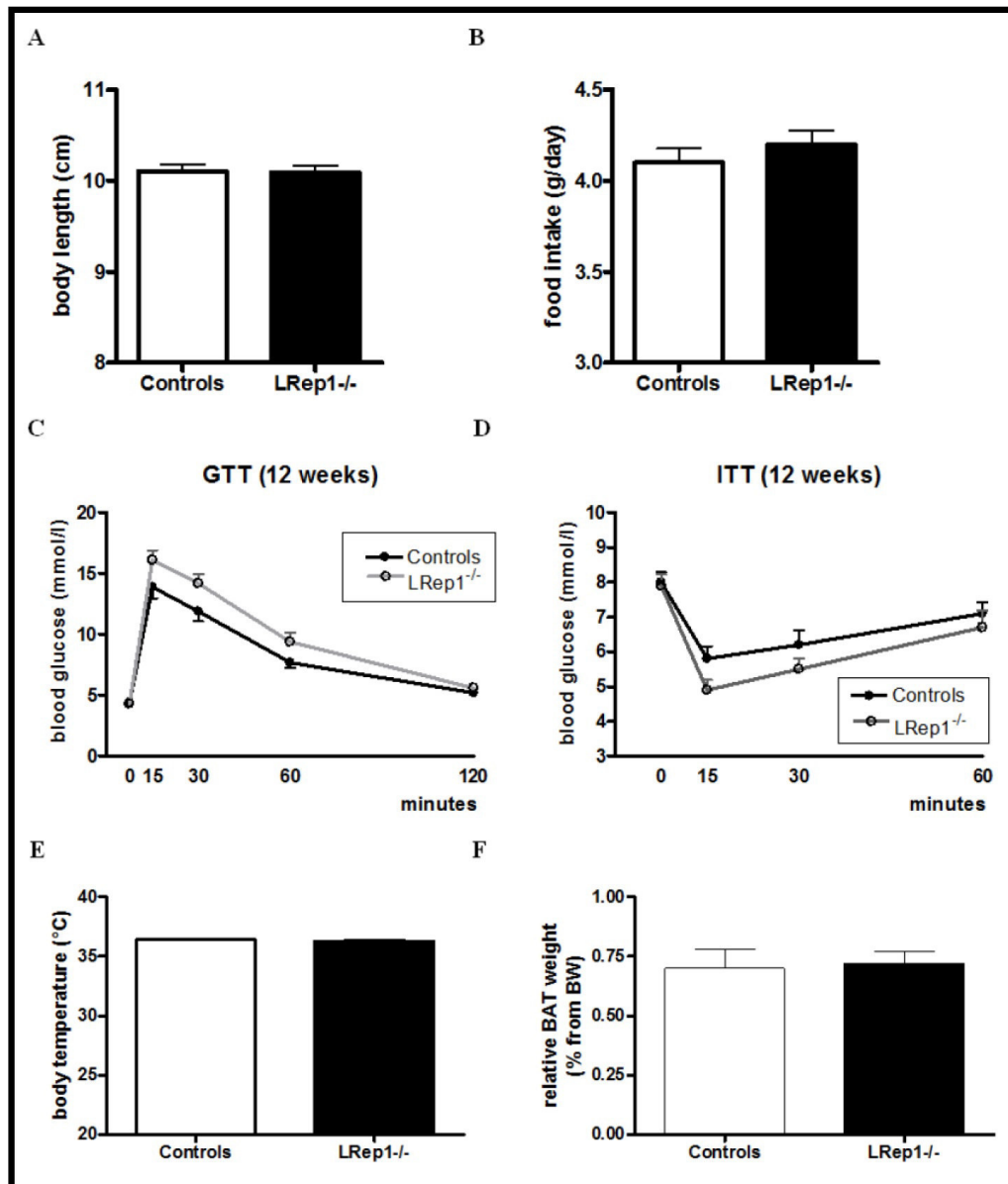


Figure 4.13: Supplementary Figure 4. Body length (A) and food intake (B) as well as ipGTT (C) and ipITT (D) in control and LRep1<sup>-/-</sup> mice. A) Body length (naso-anal length) was measured once at week 32 (per genotype 10 animals). Results are expressed as means  $\pm$  SE from 10 animals per genotype. B) At an age of 16 weeks, in a subgroup of 20 (10 LRep1<sup>-/-</sup> and 10 controls) underwent a food intake measurement over a time period of 1 week. The daily food intake was calculated as the average intake of chow within the time stated. Results are expressed as means  $\pm$  SE from 10 animals per genotype. C) GTTs performed on 12-h-fasted 12-week old male wild-type (control) and LRep1<sup>-/-</sup> mice. Results are expressed as means  $\pm$  SE from 10 animals per genotype. D) ITTs on random fed 12-week-old male wild-type (control) and LRep1<sup>-/-</sup> mic. Results are expressed as means  $\pm$  SE from 10 animals per genotype. (E) Rectal body temperature measures of 32-week old male wild-type (control) and LRep1<sup>-/-</sup> mice. (F) Relative brown adipose tissue weight (BAT) from 6 animals per genotype. Results are expressed as means  $\pm$  SE.

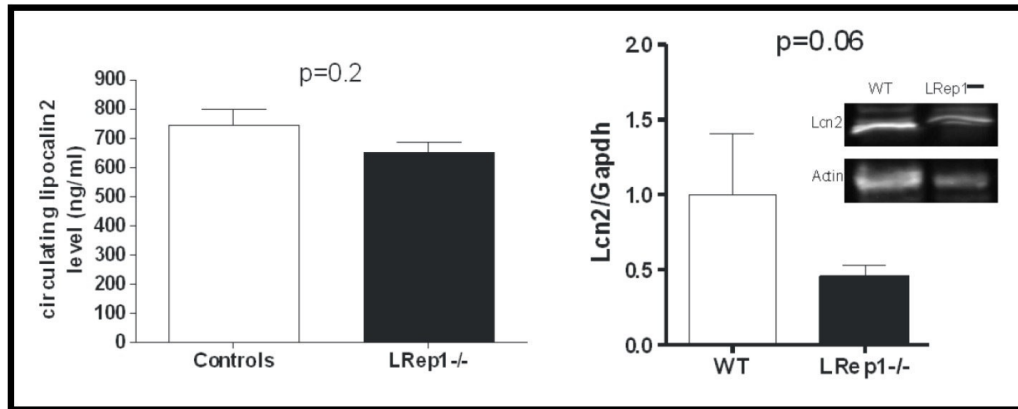


Figure 4.14: Supplementary Figure 5. Lipocalin 2 measurements (A) Serum concentration measured with ELISA (RD Systems) in male LRep1<sup>-/-</sup> mice and controls at an age of 32 weeks (8 animals per genotype). (B) Representative Lcn2 protein expression in liver lysates and quantification in male LRep1<sup>-/-</sup> mice and controls using western blot analysis (5 animals per genotype). Data are given as mean  $\pm$  SE.

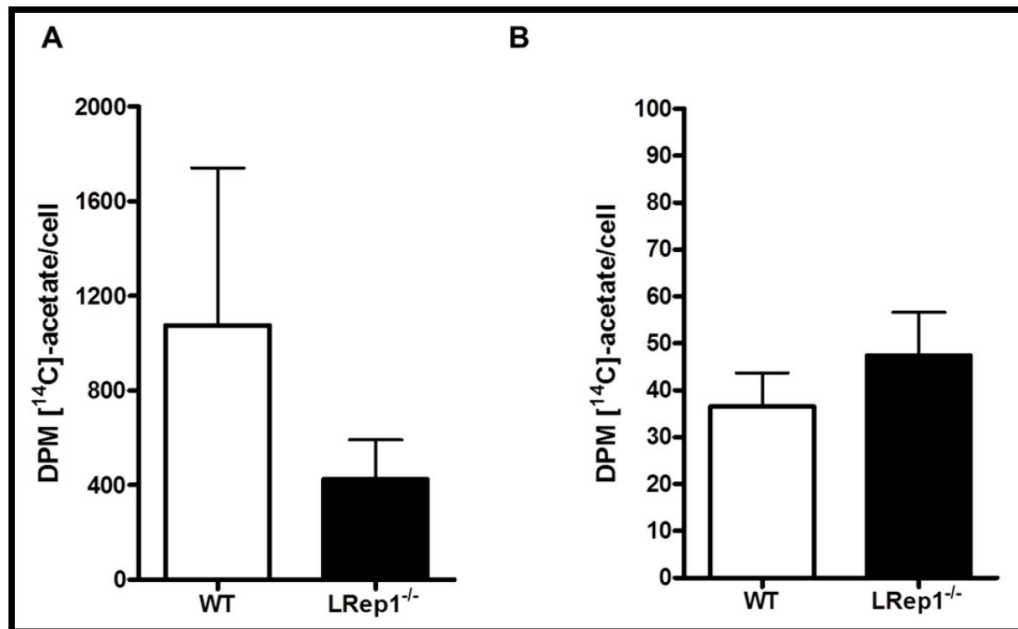


Figure 4.15: Supplementary Figure 6. *Ex-vivo*-<sup>14</sup>C]-acetate loading assay. Mouse adipocytes were isolated and purified immediately after sacrifice as described. 50  $\mu$ l of cell suspension were seeded in 96 well plates in a 5% CO<sub>2</sub> incubator at 37 °C in the presence of 10  $\mu$ M [<sup>14</sup>C]-acetate and left for 4 hours. The cells were disrupted by a standard lysis buffer containing 50 mM TRIS, 1% Triton X-100. The lipid soluble TAG was extracted by addition of 200  $\mu$ l heptane and [<sup>14</sup>C]-incorporation was measured by liquid scintillation. (A) [<sup>14</sup>C]-acetate load into SC adipocytes and (B) epigonadal adipocytes. Data represents DPM per cell as mean  $\pm$  SE from 6 animals per experimental group.

# Chapter 5



## Repin1 Deficiency in Adipose Tissue Improves Whole-body Insulin Sensitivity, and Lipid Metabolism

Nico Hesselbarth<sup>1</sup>, Anne Kunath<sup>1,2</sup>, Matthias Kern<sup>2</sup>, Martin Gericke<sup>3</sup>,  
Niklas Mejhert<sup>4</sup>, Mikael Rydén<sup>4</sup>, Michael Stumvoll<sup>1</sup>, Matthias Blüher<sup>1</sup> and  
Nora Klöting<sup>5</sup>

<sup>1</sup> Department of Internal Medicine III, Leipzig University, D-04103 Leipzig, Germany

<sup>2</sup> German Center for Diabetes Research (DZD), Munich, Germany

<sup>3</sup> Institute of Anatomy, Leipzig University, D-04317 Leipzig, Germany

<sup>4</sup> Department of Medicine (H7), Karolinska Institutet University Hospital, Huddinge, 141 86, Stockholm, Sweden

<sup>5</sup> IFB Adiposity Disease, Junior Research Group 2, Leipzig University, D-04103 Leipzig, Germany

*International Journal of Obesity* (2017) submitted

## 5.1 Abstract

### Background/Objectives:

Replication initiator 1 (Repin1) gene encodes for a zinc-finger protein and has been implicated in the regulation of adipocyte cell size and glucose transport *in vitro*. Here, we investigate the consequences of reduced adipose tissue (AT) Repin1 expression *in vivo*.

### Subjects/Methods:

We have inactivated the Repin1 gene in adipose tissue (iARep<sup>-/-</sup>) at an age of four weeks using tamoxifen-inducible gene targeting strategies on the background of C57BL/6NTac mice. Furthermore, we differentiated human primary adipocytes derived from subcutaneous AT *in vitro* and knocked down *REPIN1* using siRNA technique to measure glycerol release.

### Results:

Conditional Repin1 inactivation results in decreased AT mass, smaller adipocytes in both, subcutaneous and epigonadal AT compared to controls. Compared to controls, iARep<sup>-/-</sup> mice were more insulin sensitive, had better glucose tolerance and lower LDL-, HDL- and total cholesterol. Significantly lower AT expression of the Repin1 target genes *Cd36* and *Lcn2* may contribute to the phenotype of iARep<sup>-/-</sup> mice. Knockdown of *REPIN1* in human *in vitro* differentiated adipocytes revealed an increased glycerol release.

### Conclusion:

In conclusion, deficiency of Repin1 in AT causes alterations in AT morphology and function, which may underlay lower body weight and improved parameters of insulin sensitivity, glucose and lipid metabolism.

## 5.2 Introduction

Replication initiator 1 (Repin1) is a polydactyl zinc finger protein organized in three clusters with a mass of 60 kDa [1], [2], [3]. The gene maps on human chromosome 7, in mice on chromosome 6 and on chromosome 4 in rats [4].

Repin1 was first described as an origin specific DNA binding protein, which acts as an enhancer of DNA bending of the Chinese hamster dihydrofolate reductase (*dhfr*) gene due to replication. It binds to two ATT-rich sites in *oriβ*, a short region 3' to the *dhfr* gene [2], [3]. As for many other zinc finger proteins, the cellular localization and function of Repin1 remains elusive.

Previous studies showed that Repin1 maps to a quantitative trait locus (QTL) associated with obesity and elevated triglyceride levels in congenic and subcongenic rat strains [5], establishing Repin1 as candidate gene for obesity and the metabolic syndrome. In line with these studies, genetic variation in the *Repin1* gene, in particular a coding region SNP (C/T 449) and a triplet repeat (TTT) in the 3'UTR is associated with facets of the metabolic syndrome, including body weight, serum insulin, leptin, triglyceride and cholesterol levels in rats [4].

Repin1 is ubiquitously expressed, but is enriched in liver and adipose tissue (AT) indicating a role in glucose and lipid metabolism. Own *in vitro* studies in 3T3-L1 cells revealed that Repin1 regulates adipocyte size and glucose transport [6]. Small interfering RNA (siRNA) mediated knockdown of Repin1 led to altered *Cd36* expression, reduced palmitate uptake and changes in gene expression involved in lipid droplet formation such as *Vamp4* and *Snap23* [6]. We have demonstrated that hepatocyte specific Repin1 knockout mice exhibit significantly improved whole-body insulin sensitivity and changes in downstream targets such as *Cd36*, *Pparγ*, *Glut2*, *Akt* and *lipocalin*. Repin1 deficiency in the liver also leads to lower body weight and body fat compared to littermate controls [7].

In an attempt to rescue the deteriorated glucose metabolism in *db/db* mice, we have demonstrated that whole body Repin1 deficient *db/db* double knockout mice (*Repin1*<sup>-/-</sup> x *db/db*) are more insulin sensitive, have reduced chronic hyperglycemia and lower AT mass and infiltration compared to the pure *db/db* mice [8].

Taken together, these data indicate an important role for Repin1 in the regulation of AT function, insulin sensitivity, lipid and glucose metabolism. Since AT is one of the major organs of Repin1 expression, we generated inducible adipocyte specific Repin1 knockout mice to further investigate the

function of Repin1 in AT. We induced lower Repin1 expression by tamoxifen at an age of four weeks to avoid any potential developmental effects caused by an earlier (aP2-mediated) disruption of the Repin1 gene.

## 5.3 Materials and Methods

### 5.3.1 Animal Care and Research diets

All animal studies were approved by the local authorities of the state of Saxony, Germany as recommended by the responsible local animal ethics review board (Landesdirektion Leipzig, TVV21/13, T01/13, T08/16, Germany). All mice were housed in pathogen-free facilities in groups of three to five mice at  $22 \pm 2$  °C on a 12-h light/dark cycle. Animals were bred in laboratories at University of Leipzig and were fed a standard chow diet (Sniff Spezialdiäten, Soest, Germany). All animals had *ad libitum* access to food and water at all times, except for experiments where a fasting state was required. Fasted experimental animals were euthanized at 34 weeks of age for tissue and serum collection for further analysis.

### 5.3.2 Generation and Genotyping of iARep<sup>-/-</sup> Mice

Generation of Repin1 floxed mice have been previously described [9]. Repin1 expression was reduced specifically in AT using Cre recombinase-mediated excision of *loxP*-flanked ('floxed') gene sequences. Mice homozygous for floxed alleles of Repin1 (*Repin1*<sup>*loxP/loxP*</sup>) were interbred with mice expressing Cre recombinase under control of the Adipoq promoter (*Adipoq*-Cre<sup>+/-</sup> mice) [10]. Repin1 deficiency was achieved by activating Cre recombinase by intraperitoneal injection of tamoxifen (1 mg per day in five consecutive days) in four weeks old animals. Control animals were also treated with tamoxifen. Animals were maintained on C57BL/6NTac background. All mice were genotyped by isolation of DNA from ear stamp using DNA extraction kit DNeasy (Qiagen, Hilden, Germany). PCR was performed with following two primer pairs: *loxP* sites: 5'-CCCAACACTGATTACAGATCC-3'

(forward) and 5'-GTGGGATCAGATAGA AACTTAGC-3' (reverse) and Cre: 5'-TGGTGCATCTGAAGACACTACA-3' (forward) 5'-TGCTGTTGGATGGTCTTTCACAG-3' (reverse) and ran in 35 cycles under following conditions: 95 °C-15 min, denaturation 95 °C-30 sec, annealing 56 °C-30 sec (*loxP*-sites) 60 °C -30 sec (Repin1), elongation 72 °C-10 min, 72 °C-10 min using Fermentas DreamTaq Polymerase (FastStart PCR Master Roche, Basel, CH; dNTP Mix 10 mM ThermoFisher Scientific, Cambridge, MA, USA; Primer biomers.net, Ulm, Germany) and Peltier Thermal Cycler PTC-200 (Bio-Rad, Hercules, CA, USA). Control mice showed a 292-bp band whereas *iARep*<sup>-/-</sup> mice produced a 484-bp *loxP* band.

### 5.3.3 Phenotypic Characterization

All experimental procedures were conducted using male mice. In this study 13 mice were obtained and compared to 13 control littermates [*Rep1*<sup>*lox/lox*</sup>, *Rep1*<sup>*lox/+*</sup>, *Cre*<sup>+</sup> and WT]. Because these different control genotypes are not significantly different in the key parameters of our study, we studied them together as controls. Body weight was measured weekly starting at 5 until 34 weeks of age. Food intake was evaluated for a period of one week at an age of 30 weeks and calculated as average of daily food consumption. Whole body composition (fat mass and lean mass) was determined in awake mice by using nuclear magnetic resonance technology with EchoMRI700<sup>TM</sup> instrument (Echo Medical Systems, Houston, TX, USA) at an age of 10 and 20 weeks. Body length (naso-anal length) and rectal body temperature was measured at the end of observation period at an age of 34 weeks (TH-5 Thermalert Monitoring Thermometer Physitemp, Clifton, NJ, USA). Intraperitoneal insulin tolerance tests (i.p. ITTs) and glucose tolerance tests (i.p. GTTs) were performed at the age of 14 and 24 weeks as previously described [11]. At an age of 30 weeks, four mice of each genotype were housed for 72 h in metabolic chambers (CaloSys V2.1, TSE Systems, Bad Homburg, Germany) to measure indirect calorimetry (mean oxygen consumption (VO<sub>2</sub>) as well as spontaneous activity (XYZ cage movement) and ability to run on a treadmill). Analyses and calculations for energy expenditure were performed as

previously described [12].

Mice were euthanized at the age of 34 weeks by an overdose of anesthetic (Isofluran, Baxter, Unterschleißheim, Germany). Liver, brown (BAT), subcutaneous (scAT) and epigonadal adipose tissue (epiAT) were immediately removed. Liver, BAT, scAT and epiAT were weighed and organ mass relative to body weight was calculated. Other organs like heart, lung, brain, kidney, spleen, pancreas and muscle were removed and stored at  $-80^{\circ}\text{C}$  for further investigations.

### 5.3.4 Analytical Procedures

Blood glucose was determined in whole venous blood samples using an automated glucose monitor (FreeStyle mini, Abbott GmbH, Ludwigshafen, Germany). Insulin, leptin and adiponectin serum concentrations and hepatic triglycerides were measured by ELISAs using mouse standards according to the manufacturers' guidelines (Insulin/Leptin ELISA; CrystalChem. Inc, Downers Grove, IL; Mouse Adiponectin ELISA; AdipoGen Inc, Incheon, Korea; LabAssay Triglyceride, Wako Pure Chemicals industries Ltd., Osaka, Japan). Serum concentrations of free fatty acids (FFA), triglycerides, total cholesterol, low density lipoprotein- (LDL), high density lipoprotein- (HDL) cholesterol and HbA<sub>1c</sub> were analyzed by an automatic chemical analyzer in our Institute of Laboratory Medicine and Clinical Chemistry.

### 5.3.5 Adipocyte Isolation and Size Distribution

Adipocytes were isolated from epigonadal (epiAT) and subcutaneous (scAT) fat pads by 1 mg/ml collagenase digestion. To assess cell size distribution, 200  $\mu\text{l}$  aliquots of adipocytes were fixed with osmic acid, incubated for 48 h at  $37^{\circ}\text{C}$  and counted in a Coulter Counter (Multisizer III; Beckman Coulter, Krefeld, Germany) as described elsewhere [13]. In addition, adipocyte size and distribution in epiAT and scAT was determined on paraffin sections. HE staining of AT was performed following standard procedures. Adipocyte size was quantified as described previously [14].

### 5.3.6 RNA Isolation and Quantitative Real-Time PCR Analysis

RNA isolation and quantitative real-time PCR were performed as previously described [11]. mRNA expression of genes listed in Supplementary Table 1 was determined. Specific mRNA expression was calculated relative to *18S* or *L19* RNA, which were chosen as an internal controls due to their resistance to glucose-dependent regulation.

### 5.3.7 Western Blot Analysis

For Western blot analysis, tissues were removed and homogenized in sucrose buffer with tissue-mill homogenizer (MM 400; Retsch GmbH, Haan, Germany). Proteins were isolated using standard techniques and Western blot analysis was performed with antibodies raised against Repin1 (1:1 000; Abcam; Cambridge, UK), Cd36 (1:1 000; RD Systems; Minneapolis, USA), Lipocalin2 (Lcn2) (1:1 000; Abcam) and Gapdh antibody (1:3 000; Research Diagnostics; Flanders, Netherlands) as loading control.

### 5.3.8 Cell culture

Human in vitro differentiated primary adipocytes were isolated from scWAT obtained from subjects undergoing plastic surgery for non-malignant conditions. Adipocyte precursor cells were isolated, cultured and differentiated to adipocytes using described protocols [15]. Cells were transfected using HiPerfect (Invitrogen, Life Technologies Corporation) and siRNA (Dharmacon, Thermo Fisher Scientific). Glycerol release into the media 48 h after transfection was used to measure lipolysis as described in detail previously [16].

### 5.3.9 Statistical Analysis

Prism 6.0 software (GraphPad Software) was used to assess statistical significance. Data are given as means  $\pm$  SE. Data sets were analyzed for statistical

significance using a two-tailed unpaired Student's  $t$  test or Mann-Whitney  $U$  test.  $P$  values  $< 0.05$  were considered significant.

## 5.4 Results

### 5.4.1 Generation of iARep<sup>-/-</sup> Mice

To create AT specific Repin1 knockout mice, we crossed mice carrying the *loxP*-flanked Repin1 allele with mice expressing the Cre recombinase under control of the adipocyte specific *Adipoq* promoter. Cre recombinase was activated by tamoxifen injection of four weeks old animals. Transgenic animals were fertile and did not display any differences in reproduction rate and litter size compared with control litter mates. Knockout efficiency was confirmed by qPCR demonstrating  $\sim 80\%$  to  $\sim 85\%$  knockdown of Repin1 expression in scAT and epiAT (Fig. 1A). Western Blot analysis confirmed that Repin1 knockout only appeared in AT and did not affect other tissues (Fig. 1B).

### 5.4.2 Growth, Organ weights, Food Intake and Energy Expenditure of iARep<sup>-/-</sup> mice

iARep<sup>-/-</sup> mice have significantly lower body weight compared to littermate controls from week six up to week 34 (Fig. 1C) and lower body fat mass (Tab. 1). Daily food intake was indistinguishable between iARep<sup>-/-</sup> and control mice (Fig. 1D, Tab. 1). Relative epiAT and scAT weights are  $\sim 50\%$  lower in iARep<sup>-/-</sup> compared to control mice (Fig. 1F). Although relative liver mass is significantly higher in iARep<sup>-/-</sup> mice, there is no evidence for higher liver fat content (Tab. 1). iARep<sup>-/-</sup> mice have significantly smaller adipocytes in both fat depots compared to control animals (Fig. 1H-J, Tab. 1). Adipocyte size distribution analyses in both AT regions revealed a left shift of the curves with a reduction in the number of larger adipocytes in iARep<sup>-/-</sup> mice (Fig. 1I). Circulating leptin and adiponectin are significantly lower in iARep<sup>-/-</sup> mice compared to controls (Fig. 2 G,



Tab. 1). Studies on whole body energy metabolism revealed that carbon dioxide production (Fig. 1E) and oxygen consumption (Fig. 1E) were significantly elevated in  $iARep^{-/-}$  compared to control animals, most likely contributing to leaner phenotype, whereas spontaneous activity is not affected in  $iARep^{-/-}$  (Fig. 1E).

### 5.4.3 Repin1 deficiency in AT improves insulin sensitivity

To investigate the influence of Repin1 depletion in AT on glucose homeostasis, we performed GTTs and ITTs at an age of 14 and 24 weeks. At an age of 14 weeks, insulin sensitivity was not affected in  $iARep^{-/-}$  mice compared to controls (data not shown), whereas at an age of 24 weeks  $iARep^{-/-}$  showed an increased insulin sensitivity compared to control mice (Fig. 2A). Intraperitoneal GTTs revealed improved glucose tolerance at an age of 24 weeks in  $iARep^{-/-}$  mice compared to controls (Fig. 2B). HbA<sub>1c</sub> levels are significantly lower in  $iARep^{-/-}$  mice compared to controls (Tab. 1). It is noteworthy that fasted blood glucose and insulin serum concentrations did not show significant differences between the genotypes (Tab. 1).

### 5.4.4 Deficiency of Repin1 in AT or knockdown in human *in vitro* differentiated adipocytes leads to altered Lipid Metabolism

To determine the consequences of reduced Repin1 expression in AT on lipid metabolism, we assessed total serum HDL-, LDL- and total cholesterol, triglycerides and FFA concentrations. All lipid parameter showed decreased serum concentrations in  $iARep^{-/-}$  mice compared to controls, but only total cholesterol, HDL- and LDL-cholesterol were significantly decreased (Tab. 1).

Liver histology revealed significantly elevated relative liver weights in  $iARep^{-/-}$  mice compared to controls (Tab. 1), but HE staining (Fig. 1K) and hepatic triglyceride measurements (Tab. 1) did not show significant differences between the genotypes.

Furthermore, we isolated human adipocytes from scAT and differentiated them *in vitro* to knockdown *REPIN1* using siRNA to check differential glycerol release of those cells. Adipocytes of *REPIN1* knockdown show significantly higher glycerol release compared to control cells (Fig. 1L), suggesting that reduced Repin1 expression in adipocytes causes increased basal lipolysis.

#### 5.4.5 Target Genes of Repin1

Previous *in vitro* studies of Repin1 knockdown in 3T3-L1 cells and *in vivo* studies of a liver-specific Repin1 knockout mouse suggested fatty acid transporter *Cd36* and the cytokine *Lcn2* as Repin1 target genes. Indeed, *Cd36* and *Lcn2* expression is significantly lower in both AT depots in iARep<sup>-/-</sup> mice compared to controls. *Cd36* expression levels were ~20% reduced (Fig. 3A), whereas *Lcn2* expression levels were ~80% reduced in both fat depots (Fig. 3B). To validate these findings on the protein level, we also performed Western Blot and could confirm a downregulation of ~20-30% in epiAT and scAT of Cd36 and Lcn2 in iARep<sup>-/-</sup> compared to controls (Fig. 3C-D).

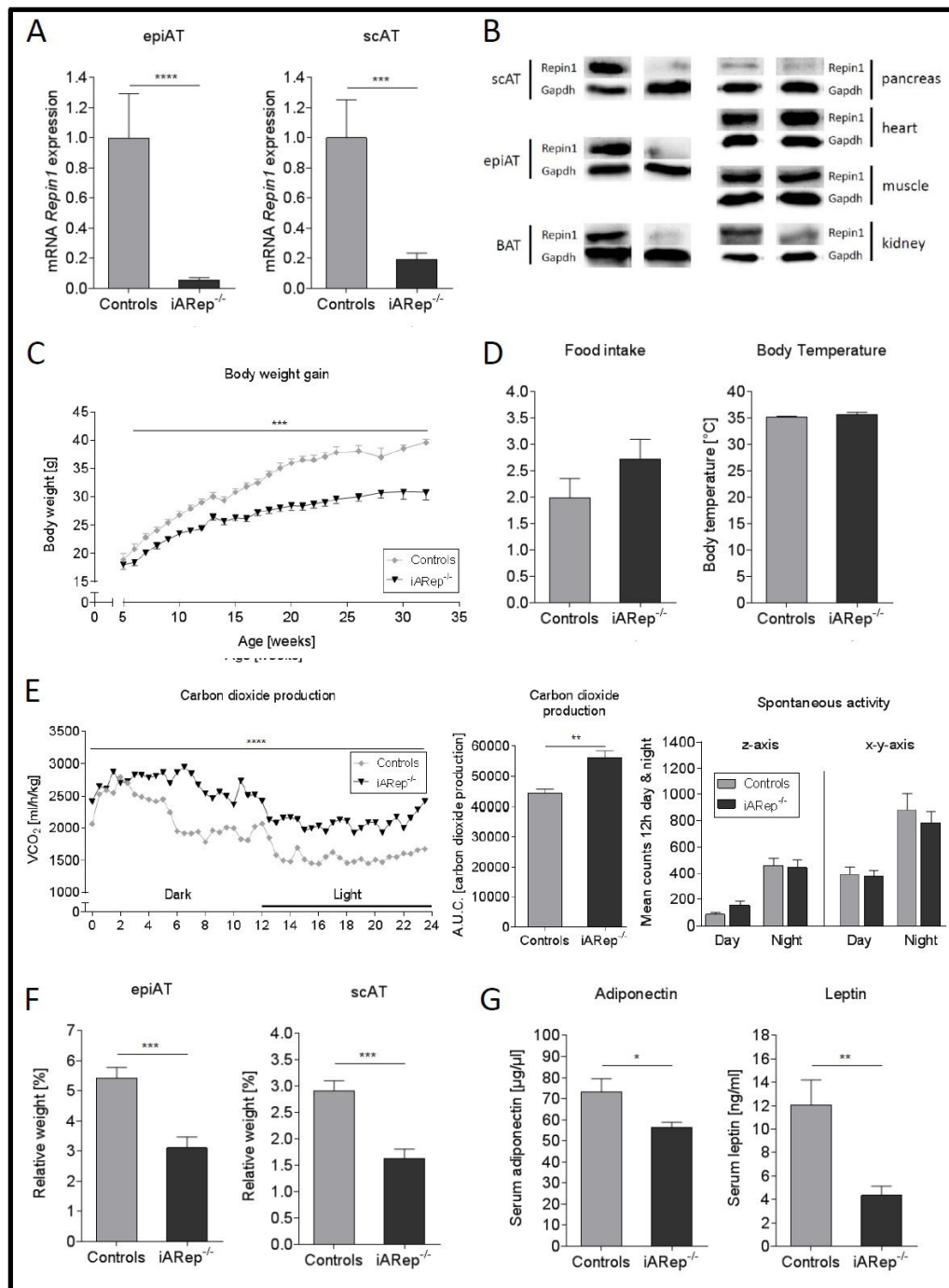


Figure 5.1: Repin1 expression, body composition, adipocyte characterization and energy expenditure in iAREp<sup>-/-</sup> and control mice. A: Knockdown efficiency in epiAT and scAT from control and iAREp<sup>-/-</sup> mice (N=14) showing a reduction of Repin1 expression on mRNA level of ~80% in adipose tissue in knockout animals compared to controls (N=14). B: Western Blot analysis in adipose tissue (scAT, epiAT and BAT), pancreas, heart, muscle and kidney showing Repin1 protein expression and Gapdh expression as loading control. iAREp<sup>-/-</sup> mice showing reduced Repin1 expression in adipose tissue compared to control animals, but similar protein expression of Repin1 in other tissues. C: Body weight gain up to an age of 34 weeks of Repin1 deficient mice (N=14) compared to controls (N=12). iAREp<sup>-/-</sup> mice are significant lighter at an age of 6 weeks up to an age of 34 weeks.

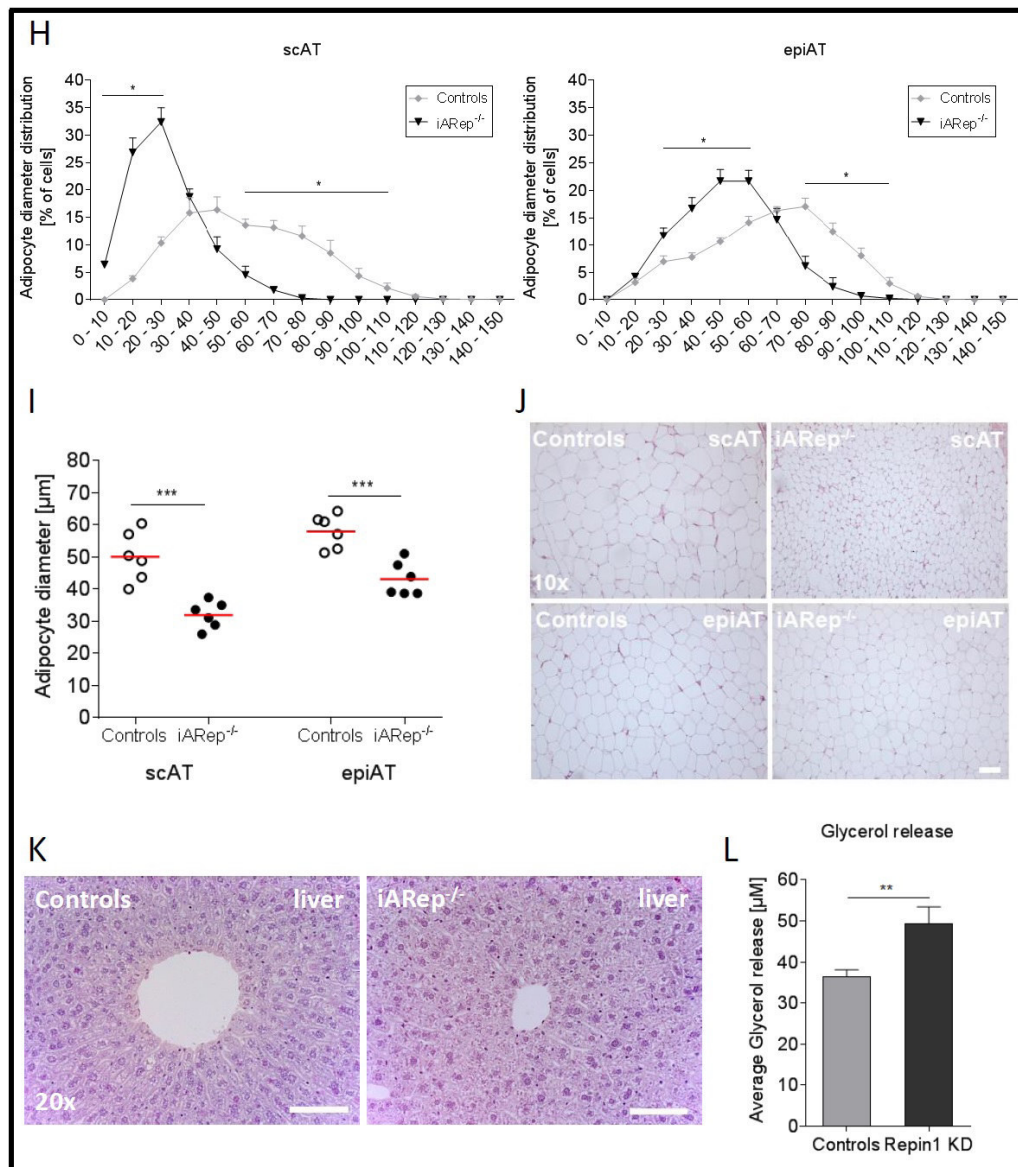


Figure 5.1: (Previous page.) D: Food intake was measured in week 30 for a period of one week and calculated to an average consumption of 24 h. Body temperature was measured at the end of observation period in week 34. Food intake and body temperature show no significant differences between iARep<sup>-/-</sup> mice and controls. E: Mean oxygen consumption (VO<sub>2</sub>) was measured by indirect calorimetry in a Calorimetry Module (CaloSys V2.1, TSE Systems, Bad Homburg, Germany) at an age of 17 weeks. After two hours of acclimatization, mean carbon dioxide production (VCO<sub>2</sub>) was recorded from iARep<sup>-/-</sup> (N=4) and control mice (N=4) over a period of 72 hours. Data reveals significant higher VCO<sub>2</sub> in iARep<sup>-/-</sup> compared to control mice day and night. Spontaneous activity is considered as sit up of the mice on the z-axis and depicted as means over an observation period of overall 72 hours and reveals no significant differences between the two observed groups. F: Relative epiAT and scAT weight was measured in week 34 after scarification and calculated relative to total body weight. Repin1 deficient mice (N=8) in adipose tissue showing ~40-50% reduced relative epiAT and scAT mass compared to control mice (N=8).

Figure 5.1: (Previous page.) G: Adiponectin serum concentration was measured after sacrifice in week 34 using ELISA technique (AdipoGen Inc, Incheon, Korea). Serum concentrations of adiponectin was significantly reduced in  $iARep^{-/-}$  (N=10) compared to control mice (N=10). Leptin serum concentration was measured after sacrifice in week 34 using ELISA technique (CrystalChem Inc, Downers Grove, IL). Mice lacking *Repin1* in adipose tissue (N=10) show significant reduced serum concentrations of leptin compared to controls (N=10). H: Distribution of Adipocyte diameter in scAT and epiAT was measured after HE staining and subsequent evaluation using cellSens Software (Olympus, Hamburg Germany). Adipocyte diameter distribution shows a broader spectrum in a higher range in control mice, whereas  $iARep^{-/-}$  mice show a tighter spectrum in a lower range in scAT and epiAT. I: Adipocyte diameter was measured after HE staining using cellSens Software. In both adipose tissue depots (scAT and epiAT)  $iARep^{-/-}$  mice showed a significant reduction of adipocyte diameter of ~25-40% compared to controls. J: Representative images (HE staining; original magnification X10) of scAT and epiAT of control mice and *Repin1* adipose tissue specific deficient mice. K: Representative images (HE staining; original magnification X20) of liver of control and  $iARep^{-/-}$  mice. L: Glycerol release was performed in vitro on human differentiated adipocytes from scAT, either treated with scrambled (controls) or REPIN1 siRNA (*Repin1* KD). Knockdown of REPIN1 leads to an significant increase of glycerol release compared to control cells. Data are given as means  $\pm$  SEM. Data sets were analyzed for statistical significance using a two-tailed unpaired t test or ANOVA (\*p-value <0.05; \*\* p-value <0.01; \*\*\*p-value <0.001).

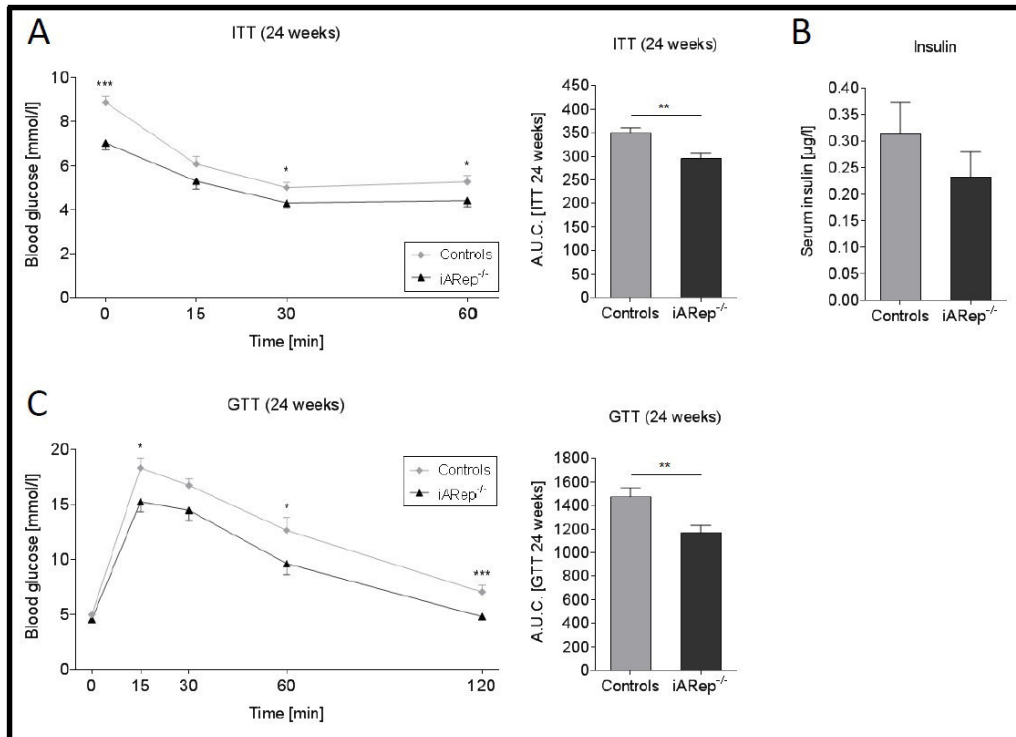


Figure 5.2: Insulin Sensitivity, glucose tolerance and circulating adipokines. A: Intraperitoneal ITT was performed in fed state at week 24. iARep<sup>-/-</sup> (N=13) compared to control mice (N=11) showed improved insulin sensitivity. B: Intraperitoneal GTT was performed in 12 h fasted 24 week old mice. Glucose tolerance was significantly improved in Repin1 deficient adipose tissue specific knockout animals (N=13) compared to controls (N=11). E: Circulating insulin concentration was determined in 34 weeks old mice using ELISA technique (CrystalChem Inc, Downers Grove, IL) and evaluation revealed no significant differences between the two observed groups (each group N=11). Data are given as means  $\pm$  SEM. Data sets were analyzed for statistical significance using a two-tailed unpaired t test or ANOVA (\*p-value <0.05; \*\* p-value <0.01; \*\*\*p-value <0.001).

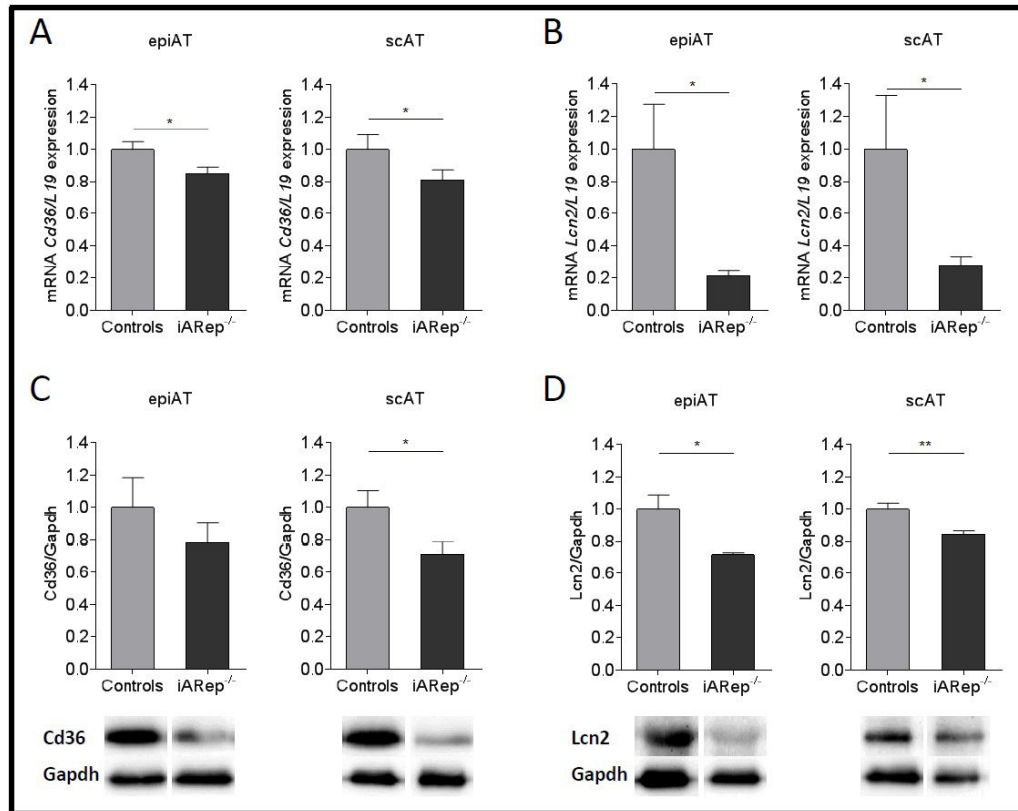


Figure 5.3: Gene and protein expression of Cd36 and Lcn2. A: Expression of Cd36 mRNA in epiAT and scAT normalized to the housekeeping gene L19. Cd36 expression levels were ~20% significantly reduced in iARep<sup>-/-</sup> mice (N=8) compared to littermate controls (N=8). B: Expression of Lcn2 mRNA in epiAT and scAT normalized to the housekeeping gene L19. Mice lacking Repin1 in adipose tissue (N=8) show ~80% significant reduction of Lcn2 mRNA expression in both fat depots compared to control mice (N=8). C: Western Blot analysis of Cd36 protein expression in epiAT and scAT relative to housekeeping protein Gapdh. Protein expression of Cd36 was ~25% significantly downregulated in iARep<sup>-/-</sup> mice (N=4) compared to littermate controls (N=4) in scAT, whereas downregulation in epiAT is not significant. D: Western Blot analysis of Lcn2 protein expression in epiAT and scAT relative to housekeeping protein Gapdh. Expression of Lcn2 was ~20-30% significantly lower in mice lacking Repin1 in adipose tissue (N=4) compared to controls (N=4) in both fat depots. Data are given as means  $\pm$  SEM. Gene expression data were analyzed using 2(-Delta Delta C(T)) method. Protein expression data are given in relation to housekeeping protein (Gapdh). Data sets were analyzed for statistical significance using a two-tailed unpaired t test (\*p-value <0.05; \*\* p-value <0.01).

Table 5.1: Serum concentrations of parameters of glucose homeostasis and lipid metabolism. Phenotypical and histological parameters of body composition and adipocyte size. All values were obtained in week 34 after sacrifice, except for 0-values of GTTs and ITTs. Data are given as means  $\pm$  SE. Significant different data appear in boldface and were considered as \* $p < 0.05$ , \*\* $p < 0.01$  and \*\*\* $p < 0.001$ .

Parameter	Controls	iARep <sup>-/-</sup>	p-value
<b>Phenotyping</b>			
Relative liver weight (%)	3.531 $\pm$ 0.067, n=8	3.873 $\pm$ 0.120, n=8	0.0298*
Hepatic triglycerides (mg/mg tissue)	10.68 $\pm$ 0.450, n=8	8.62 $\pm$ 1.411, n=8	0.1853
Relative hepatic triglycerides (mg x total liver mass/BW)	0.323 $\pm$ 0.015, n=8	0.249 $\pm$ 0.046, n=8	0.1471
Body length (cm)	10.24 $\pm$ 0.078, n=8	10.03 $\pm$ 0.075, n=13	0.0936
Body temp ( $^{\circ}$ C)	35.20 $\pm$ 0.208, n=8	35.77 $\pm$ 0.372, n=13	0.5105
<b>Glucose homeostasis</b>			
Insulin (ng/ml)	0,316 $\pm$ 0.058, n=11	0.232 $\pm$ 0.049, n=11	0.3736
HbA <sub>1c</sub> (%)	4.531 $\pm$ 0.028, n=8	4.225 $\pm$ 0.078, n=13	0.0009***
Fasted blood glucose (mmol/l)	6.700 $\pm$ 0.384, n=8	6.154 $\pm$ 0.402, n=13	0.3635
ITT 0-value week 14 (mmol/l)	7.482 $\pm$ 0.253, n=11	7.877 $\pm$ 0.140, n=13	0.1686
ITT 0-value week 24 (mmol/l)	8.873 $\pm$ 0.299, n=11	7.038 $\pm$ 0.316, n=13	0.0004***
GTT 0-value week 14 (mmol/l)	5.636 $\pm$ 0.278, n=11	4.954 $\pm$ 0.206, n=13	0.0570
GTT 0-value week 24 (mmol/l)	4.982 $\pm$ 0.271, n=11	4.562 $\pm$ 0.212, n=13	0.2285
<b>Characterization adipose tissue</b>			
Relative epi weight (%)	5.438 $\pm$ 0.347, n=8	3.110 $\pm$ 0.365, n=8	0.0006***
Relative sc weight (%)	2.915 $\pm$ 0.192, n=8	1.635 $\pm$ 0,174, n=8	0.0006***
Sc mean ( $\mu$ m)	151.2 $\pm$ 3.009, n=8	132.1 $\pm$ 4.989, n=13	0.0152*
Epi mean ( $\mu$ m)	149.8 $\pm$ 1.099, n=8	134.4 $\pm$ 2.784, n=13	0.0004***
Sc max ( $\mu$ m)	232.1 $\pm$ 3.330, n=8	221.4 $\pm$ 3.618, n=13	0.0920
Epi max ( $\mu$ m)	217.7 $\pm$ 2.626, n=8	217.5 $\pm$ 2.526, n=13	0.9018
Adiponectin ( $\mu$ g/ml)	73.13 $\pm$ 6.424, n=10	56.44 $\pm$ 2.359, n=10	0.0172*
Leptin (ng/ml)	12.04 $\pm$ 2.175, n=9	4.345 $\pm$ 0.775, n=13	0.0033**



Table 5.1: (Previous page.)

Parameter	Controls	iARep <sup>-/-</sup>	p-value
<b>Serum lipids</b>			
Triglyceride (mmol/l)	1.255 ± 0.041, n=10	1.166 ± 0.078, n=13	0.3673
Cholesterol (mmol/l)	2.750 ± 0.165, n=10	2.283 ± 0.067, n=13	0.0079**
HDL-cholesterol (mmol/l)	2.426 ± 0.092, n=9	1.933 ± 0.069, n=13	0.0004***
LDL-cholesterol (mmol/l)	0.388 ± 0.084, n=10	0.216 ± 0.013, n=13	0.0073**
FFA (mmol/l)	1.255 ± 0.065, n=10	1.118 ± 0.056, n=13	0.1703
<b>Energy expenditure</b>			
Distance day (km/12h)	0.455 ± 0.335, n=2	0.524 ± 0.138, n=7	0.9999
Distance night (km/12h)	2.560 ± 0.350, n=2	2.624 ± 0.399, n=7	0.9999
RER day	0.680 ± 0.032, n=4	0.798 ± 0.022, n=8	0.0182*
RER night	0.720 ± 0.033, n=4	0.851 ± 0.031, n=8	0.0424*
Water intake (ml/72h)	5.545 ± 0.894, n=4	10.65 ± 1.581, n=8	0.0485
Food intake (g/72h)	5.983 ± 1.087, n=4	8.184 ± 1.116, n=7	0.2182
VO <sub>2</sub> day (ml/h/kg)	2287 ± 110.7, n=4	2825 ± 141.6, n=8	0.0283*
VO <sub>2</sub> night (ml/h/kg)	2882 ± 186.8, n=4	3497 ± 215.1, n=8	0.1051
VCO <sub>2</sub> day (ml/h/kg)	1551 ± 48.20, n=4	2250 ± 109.2, n=8	0.0081**
VCO <sub>2</sub> night (ml/h/kg)	2083 ± 113.2, n=4	2944 ± 208.9, n=8	0.0485*

## 5.5 Discussion

We show here that adipocyte-specific Repin1 deletion results in leanness, smaller adipocytes and an improved whole body insulin sensitivity *in vivo*.

We propose that these beneficial effects of reduced Repin1 maybe mediated by significant changes in key molecules linking glucose and lipid metabolism such as Cd36 and lipocalin, but also through increased basal lipolysis in adipocytes.

Repin1 is ubiquitously expressed with highest expression levels in liver and AT. Repin1 has been implicated as an important regulator of adipocyte cell size and glucose transport into 3T3L1 adipocytes *in vitro*. Moreover, *Repin1* mRNA expression was shown to be associated with adipocyte size in humans [6], [17]. Therefore, Repin1 has been suggested as a candidate gene for obesity and its related metabolic disorders. However, the physiological role of the Repin1 signaling in AT *in vivo* has not been systematically studied. We therefore created mice lacking the Repin1 gene in AT (iARep<sup>-/-</sup>) using conditional and inducible gene targeting strategies (*Adipoq*-Cre<sup>+/-</sup> mice). To specifically target adipose tissue, we used transgenic mice that express the Cre recombinase cDNA under the control of the Adiponectin promoter [10]. Induction of the knockout was performed by administration of tamoxifen. Tamoxifen has been shown to alter body composition with a lower fat mass one week after treatment and significant higher fat mass five weeks after treatment with tamoxifen [13]. Upon these tamoxifen-related fat mass dynamics, glucose homeostasis and lipid profile showed also significant changes in tamoxifen treated animals as well as browning effects in scAT with higher *Ucp1* expression [13]. To overcome the known problem that tamoxifen per se may influence - at least transiently - the metabolic and AT phenotype, we treated all animals (controls and iARep<sup>-/-</sup>) with tamoxifen. Furthermore, as tamoxifen is washed out within eight weeks [18], all detailed phenotyping was performed at least ten weeks after tamoxifen treatment.

iARep<sup>-/-</sup> mice were viable and fertile and did not exhibit perinatal growth retardation. However, starting from the age of six weeks and onwards, iARep<sup>-/-</sup> mice display a slower body weight gain compared to control mice.

This effect is most likely the result of higher energy expenditure compared to controls (Fig. 1C–E). Several mechanisms could explain this, e.g. increased BAT activity/beige differentiation, alterations in adipokine secretion, which may contribute to this phenotype and/or unrecognized Repin1 target genes regulating energy metabolism. Higher energy expenditure in  $iARep^{-/-}$  mice could be due to higher BAT activity, since previous studies recognized BAT as a regulator of

whole-body energy expenditure in humans and small rodents [19], [20]. We hypothesized that higher energy expenditure in  $iARep^{-/-}$  could be due to higher BAT mass or activity. We therefore compared  $iARep^{-/-}$  and control mice according to their relative and absolute BAT mass and histological signatures of brite/beige adipocytes in white AT depots. Importantly, we did not find any sign of increased BAT activity, mass or browning/beiging of WAT in  $iARep^{-/-}$  mice. Mean core body temperature and BAT mass was indistinguishable between  $iARep^{-/-}$  and control mice. Reduced body weight in  $iARep^{-/-}$  mice is mainly driven by lower body fat mass. *In vitro* studies of downregulation of Repin1 in 3T3-L1 cells [6] and *in vivo* studies of hepatic Repin1 deficiency [7] revealed a correlation of Repin1 expression with cell and lipid droplet size. Further histological analyses identified significant differences in lipid droplet size, with reduced mean adipocyte size and a left-shift from more larger towards more smaller adipocytes in  $iARep^{-/-}$  compared to control mice. We did not observe any significant differences in food intake or physical activity in  $iARep^{-/-}$  mice suggesting that the attenuated circulating levels of leptin in  $iARep^{-/-}$  mice do not cause hyperphagia. Interestingly, both AT and liver exhibit lower relative organ weights than other organs, including heart, kidney, skeletal muscle, and spleen, which are decreased in size proportionally to the lower body weight of  $iARep^{-/-}$  mice supporting the close correlations between (predominantly visceral) fat stores and liver steatosis.

However circulating metabolism parameters were significantly lower in  $iARep^{-/-}$  compared to control mice. Previous studies on siRNA-mediated Repin1 knockdown in 3T3-L1 cells [6] and hepatic Repin1 deficient mice [7] could demonstrate a relation of Repin1 deficiency and reduced mRNA

expression of fatty acid transporter *Cd36*. In this study we could also confirm a correlation between Repin1 deficiency in AT and decreased *Cd36* expression in epiAT and scAT. Interestingly, *Cd36* deficient mice are characterized by improved insulin sensitivity in AT [21] a phenotype which is also reflected in iARep1<sup>-/-</sup> mice. A previous study on whole body Repin1 deficient *db/db* double knockout mice could already show a correlation of Repin1 deficiency and improved insulin sensitivity [8]. Rep1<sup>-/-</sup> x *db/db* mice show significantly improved insulin sensitivity and chronic hyperglycemia, which is most likely derived by reduced fat mass and lower inflammatory infiltrates in AT [8]. However, mice lacking Repin1 in AT do not reflect all characteristics of *Cd36* knockout mice, in particular the latter model shows increased circulating lipids [22], indicating that impaired *Cd36*-mediated fatty acid transport can be compensated by other lipid transport mechanisms or that the remaining *Cd36* is sufficient to protect against dyslipidemia in iARep<sup>-/-</sup> mice. Fatty acid uptake and storage into the liver might be one possible explanation, because liver weights were significantly increased while still showing normal phenotypes and no signs of NAFLD. siRNA-mediated *REPIN1* knockdown in human *in vitro* differentiated adipocytes revealed significantly increased glycerol release compared to control cells indicating an increased lipolysis mediated by deficiency of Repin1. Therefore increased basal lipolysis may contribute to smaller adipocytes observed in iARep<sup>-/-</sup> mice.

Based on those results, we propose that Repin1, as a zinc-finger protein [3], is one of the regulators of transcription of *Cd36*. Former studies showed that zinc finger proteins, like PRDM16, regulate expression of genes involved in obesity by stimulating brown fat selective gene expression, while suppressing white fat selective gene expression [23], [24]. As proposed in a previous study of hepatic Repin1 deficient mice, improved insulin sensitivity could be attributed to an improved activation of the insulin signaling cascade, lower total body fat, lower fatty acid transport protein and/or lower expression of insulin resistance associated cytokines like Lcn2 or chemerin [7]. The cytokine Lcn2 was already significantly reduced on mRNA and protein level in mice lacking Repin1 in liver [7]. Here, we extend these findings showing that Lcn2 is about 80% lower in epiAT and scAT in iARep<sup>-/-</sup> compared to con-

trol mice. Previous studies revealed that higher Lcn2 serum concentrations are associated with obesity [25] and that Lcn2 derives also from AT [26]. *In vitro* studies in hepatocytes showed that exogenous Lcn2 promotes insulin resistance [27] and that Lcn2 deficient mice are protected against obesity induced insulin resistance [28]. These data together with the insulin sensitive phenotype and the significantly lower Lcn2 levels in iARep<sup>-/-</sup> mice prompt us to propose that improved insulin sensitivity in iARep<sup>-/-</sup> mice could at least in part be mediated by lower Lcn2 serum concentrations. This hypothesis fits well into the concept, that improving adipose tissue function may have beneficial metabolic effects at the whole body level [27].

In conclusion, we show that a deficiency of Repin1 in AT leads to a leaner phenotype, improves insulin sensitivity, glucose and lipid metabolism as well as smaller adipocytes most likely mediated through effects on its target genes Cd36, Lcn2 and increased basal lipolysis.

## 5.6 Acknowledgements

We would like to thank Viola Döbel, Eva Böge, Daniela Kern and Susan Berthold of University of Leipzig for technical assistance. We also want to thank Prof. Dr. Stefan Offermanns and Dr. Antonia Sassmann from Max-Planck-Institute for Heart and Lung Research in Bad Nauheim, Germany, for providing *Adipoq*-Cre<sup>+/-</sup> mice.

This work was supported by the research group “SFB1052/2“, B1 (to MB); B4 (to NK) funded by Deutsche Forschungsgemeinschaft and supported by the Federal Ministry of Education and Research (BMBF), Germany, “IFB AdiposityDiseases“, FKZ: 01EO1501 (N. Klöting), DZD (82DZD00601), DDG (934300-003), by the Helmholtz Alliance ICAMED - Imaging and Curing Environmental Metabolic Diseases, through the Initiative and Networking Fund of the Helmholtz Association, the Swedish Research Council, The Swedish Diabetes Foundation, CIMED, the Diabetes Theme Center at Karolinska Institutet, the Stockholm County Council and the Novo Nordisk Foundation.

## 5.7 References

- [1] M. S. Caddle, L. Dailey, and N. H. Heintz. RIP60, a mammalian origin-binding protein, enhances DNA bending near the dihydrofolate reductase origin of replication. *Mol. Cell. Biol.*, 10(12):6236–6243, Dec 1990.
- [2] L. Dailey, M. S. Caddle, N. Heintz, and N. H. Heintz. Purification of RIP60 and RIP100, mammalian proteins with origin-specific DNA-binding and ATP-dependent DNA helicase activities. *Mol. Cell. Biol.*, 10(12):6225–6235, Dec 1990.
- [3] C. R. Houchens, W. Montigny, L. Zeltser, L. Dailey, J. M. Gilbert, and N. H. Heintz. The dhfr oribeta-binding protein RIP60 contains 15 zinc fingers: DNA binding and looping by the central three fingers and an associated proline-rich region. *Nucleic Acids Res.*, 28(2):570–581, Jan 2000.
- [4] N. Kloting, B. Wilke, and I. Kloting. Triplet repeat in the Repin1 3'-untranslated region on rat chromosome 4 correlates with facets of the metabolic syndrome. *Diabetes Metab. Res. Rev.*, 23(5):406–410, Jul 2007.
- [5] P. Kovacs and I. Kloting. Quantitative trait loci on chromosomes 1 and 4 affect lipid phenotypes in the rat. *Arch. Biochem. Biophys.*, 354(1):139–143, Jun 1998.
- [6] K. Ruschke, M. Illes, M. Kern, I. Kloting, M. Fasshauer, M. R. Schon, J. Kosacka, G. Fitzl, P. Kovacs, M. Stumvoll, M. Bluher, and N. Kloting. Repin1 maybe involved in the regulation of cell size and glucose transport in adipocytes. *Biochem. Biophys. Res. Commun.*, 400(2):246–251, Sep 2010.
- [7] M. Kern, J. Kosacka, N. Hesselbarth, J. Bruckner, J. T. Heiker, G. Flehmig, I. Kloting, P. Kovacs, M. Matz-Soja, R. Gebhardt, K. Krohn, S. Sales, K. Abshagen, A. Shevchenko, M. Stumvoll, M. Bluher, and N. Kloting. Liver-restricted Repin1 deficiency improves

- whole-body insulin sensitivity, alters lipid metabolism, and causes secondary changes in adipose tissue in mice. *Diabetes*, 63(10):3295–3309, Oct 2014.
- [8] A. Kunath, N. Hesselbarth, M. Gericke, M. Kern, S. Dommel, P. Kovacs, M. Stumvoll, M. Bluher, and N. Kloting. Repin1 deficiency improves insulin sensitivity and glucose metabolism in db/db mice by reducing adipose tissue mass and inflammation. *Biochem. Biophys. Res. Commun.*, 478(1):398–402, Sep 2016.
- [9] M. Kern, N. Kloting, H. G. Niessen, L. Thomas, D. Stiller, M. Mark, T. Klein, and M. Bluher. Linagliptin improves insulin sensitivity and hepatic steatosis in diet-induced obesity. *PLoS ONE*, 7(6):e38744, 2012.
- [10] A. Sassmann, S. Offermanns, and N. Wettschureck. Tamoxifen-inducible Cre-mediated recombination in adipocytes. *Genesis*, 48(10):618–625, Oct 2010.
- [11] N. Kloting, L. Koch, T. Wunderlich, M. Kern, K. Ruschke, W. Krone, J. C. Bruning, and M. Bluher. Autocrine IGF-1 action in adipocytes controls systemic IGF-1 concentrations and growth. *Diabetes*, 57(8):2074–2082, Aug 2008.
- [12] M. H. Tschop, J. R. Speakman, J. R. Arch, J. Auwerx, J. C. Bruning, L. Chan, R. H. Eckel, R. V. Farese, J. E. Galgani, C. Hambly, M. A. Herman, T. L. Horvath, B. B. Kahn, S. C. Kozma, E. Maratos-Flier, T. D. Muller, H. Munzberg, P. T. Pfluger, L. Plum, M. L. Reitman, K. Rahmouni, G. I. Shulman, G. Thomas, C. R. Kahn, and E. Ravussin. A guide to analysis of mouse energy metabolism. *Nat. Methods*, 9(1):57–63, Dec 2011.
- [13] N. Hesselbarth, C. Pettinelli, M. Gericke, C. Berger, A. Kunath, M. Stumvoll, M. Bluher, and N. Kloting. Tamoxifen affects glucose and lipid metabolism parameters, causes browning of subcutaneous adipose tissue and transient body composition changes in C57BL/6NTac mice. *Biochem. Biophys. Res. Commun.*, 464(3):724–729, Aug 2015.

- 
- [14] J. du Plessis, J. van Pelt, H. Korf, C. Mathieu, B. van der Schueren, M. Lannoo, T. Oyen, B. Topal, G. Fetter, S. Nayler, T. van der Merwe, P. Windmolders, L. Van Gaal, A. Verrijken, G. Hubens, M. Gericke, D. Cassiman, S. Francque, F. Nevens, and S. van der Merwe. Association of Adipose Tissue Inflammation With Histologic Severity of Non-alcoholic Fatty Liver Disease. *Gastroenterology*, 149(3):635–648, Sep 2015.
- [15] D. Eriksson Hogling, P. Petrus, H. Gao, J. Backdahl, I. Dahlman, J. Laurencikiene, J. Acosta, A. Ehrlund, E. Naslund, A. Kulyte, N. Mejhert, D. P. Andersson, P. Arner, and M. Ryden. Adipose and Circulating CCL18 Levels Associate With Metabolic Risk Factors in Women. *J. Clin. Endocrinol. Metab.*, 101(11):4021–4029, Nov 2016.
- [16] J. Hellmer, C. Marcus, T. Sonnenfeld, and P. Arner. Mechanisms for differences in lipolysis between human subcutaneous and omental fat cells. *J. Clin. Endocrinol. Metab.*, 75(1):15–20, Jul 1992.
- [17] J. T. Heiker and N. Kloting. Replication initiator 1 in adipose tissue function and human obesity. *Vitam. Horm.*, 91:97–105, 2013.
- [18] R. Ye, Q. A. Wang, C. Tao, L. Vishvanath, M. Shao, J. G. McDonald, R. K. Gupta, and P. E. Scherer. Impact of tamoxifen on adipocyte lineage tracing: Inducer of adipogenesis and prolonged nuclear translocation of Cre recombinase. *Mol Metab*, 4(11):771–778, Nov 2015.
- [19] B. Cannon and J. Nedergaard. Brown adipose tissue: function and physiological significance. *Physiol. Rev.*, 84(1):277–359, Jan 2004.
- [20] T. Yoneshiro, S. Aita, M. Matsushita, T. Kameya, K. Nakada, Y. Kawai, and M. Saito. Brown adipose tissue, whole-body energy expenditure, and thermogenesis in healthy adult men. *Obesity (Silver Spring)*, 19(1):13–16, Jan 2011.
- [21] D. J. Kennedy, S. D. Kuchibhotla, E. Guy, Y. M. Park, G. Nimako, D. Vanegas, R. E. Morton, and M. Febbraio. Dietary cholesterol plays



- a role in CD36-mediated atherogenesis in LDLR-knockout mice. *Arterioscler. Thromb. Vasc. Biol.*, 29(10):1481–1487, Oct 2009.
- [22] M. Febbraio, N. A. Abumrad, D. P. Hajjar, K. Sharma, W. Cheng, S. F. Pearce, and R. L. Silverstein. A null mutation in murine CD36 reveals an important role in fatty acid and lipoprotein metabolism. *J. Biol. Chem.*, 274(27):19055–19062, Jul 1999.
- [23] P. Seale, S. Kajimura, W. Yang, S. Chin, L. M. Rohas, M. Uldry, G. Tavernier, D. Langin, and B. M. Spiegelman. Transcriptional control of brown fat determination by PRDM16. *Cell Metab.*, 6(1):38–54, Jul 2007.
- [24] S. Kajimura, P. Seale, T. Tomaru, H. Erdjument-Bromage, M. P. Cooper, J. L. Ruas, S. Chin, P. Tempst, M. A. Lazar, and B. M. Spiegelman. Regulation of the brown and white fat gene programs through a PRDM16/CtBP transcriptional complex. *Genes Dev.*, 22(10):1397–1409, May 2008.
- [25] Y. Wang, K. S. Lam, E. W. Kraegen, G. Sweeney, J. Zhang, A. W. Tso, W. S. Chow, N. M. Wat, J. Y. Xu, R. L. Hoo, and A. Xu. Lipocalin-2 is an inflammatory marker closely associated with obesity, insulin resistance, and hyperglycemia in humans. *Clin. Chem.*, 53(1):34–41, Jan 2007.
- [26] H. Guo, D. Jin, Y. Zhang, W. Wright, M. Bazuine, D. A. Brockman, D. A. Bernlohr, and X. Chen. Lipocalin-2 deficiency impairs thermogenesis and potentiates diet-induced insulin resistance in mice. *Diabetes*, 59(6):1376–1385, Jun 2010.
- [27] Q. W. Yan, Q. Yang, N. Mody, T. E. Graham, C. H. Hsu, Z. Xu, N. E. Houstis, B. B. Kahn, and E. D. Rosen. The adipokine lipocalin 2 is regulated by obesity and promotes insulin resistance. *Diabetes*, 56(10):2533–2540, Oct 2007.
- [28] I. K. Law, A. Xu, K. S. Lam, T. Berger, T. W. Mak, P. M. Vanhoutte, J. T. Liu, G. Sweeney, M. Zhou, B. Yang, and Y. Wang. Lipocalin-2 de-

iciency attenuates insulin resistance associated with aging and obesity.  
*Diabetes*, 59(4):872–882, Apr 2010.

# Appendix

## CURRICULUM VITAE

NICO HESSELBARTH

---

date of birth: 29<sup>th</sup> of November, 1984

place of birth: Leipzig

Federal Republic of Germany Citizen

---

EDUCATION

---

**Ph.D. student in Biology**

– Universität Leipzig –

03/2013 – today with focus on **Mechanisms of Obesity in Animal Models****Ph.D. thesis:** The Role of *Repin1* in Adipose Tissue. supervised by PD Dr. Nora Klötting at University Hospital Leipzig, Department for Endocrinology, Core Unit for Animal Models

reviewed by Prof. Dr. Annette Beck-Sickinger

**Master of Science Biology**

– Universität Leipzig –

2009 – 2011 with focus on **Biodiversity and Evolution of Animals****Master thesis:** Population genetic study of the European Green Lizard in fragmented Habitats of Bulgaria. reviewed by Prof. Dr. Martin Schlegel and Dr. Detlef Bernhard

---

**Bachelor of Science Biology**  
– **Universität Leipzig** –

2006 – 2009      studies of **Biology**  
**Bachelor thesis:** Amplification and Sequencing of H3  
gene of *Amphipholis squamata* (Ophiuroidea, Echino-  
dermata).  
reviewed by Prof. Dr. Martin Schlegel and Dr. Detlef  
Bernhard

---

**GRANTS AND AWARDS**

---

05/2014      **ECO 2014 in Sofia, Bulgaria:** Best Poster Award on Eu-  
ropean Congress of Obesity (ECO)

04/2015      **Keystone Symposium for Beige and Brown Fat in**  
**Snowbird, Utah, USA:** Scholarship

02/2016      **DDG Funding:** general project funding of DDG (Deutsche  
Diabetes Gesellschaft) for "Identification of Repin1 target  
genes" of 8,550.00 €

---

**PUBLICATIONS AND PRESENTATIONS**

---

**First-author publications**

2015      **N. Hesselbarth, C. Pettinelli, M. Gericke, C. Berger, A. Kunath,**  
M. Stumvoll, M. Blüher, N. Klöting. 2015. *Tamoxifen affects glu-*  
*ucose and lipid metabolism parameters, causes browning of subcu-*  
*taneous adipose tissue and transient body composition changes in*  
*C57BL/6NTac mice.* BBRC 464:724-729.

- 2016 A. Kunath\*, **N. Hesselbarth\***, M. Gericke, M. Kern, S. Dommel, P. Kovacs, M. Stumvoll, M. Blüher, N. Klöting. 2016. *Repin1 deficiency improves insulin sensitivity and glucose metabolism in db/db mice by reducing adipose tissue mass and inflammation*. BBRC 478:398-402  
\*equal contribution

### Co-author publications

- 2014 M. Kern, J. Kosacka, **N. Hesselbarth**, J. Brückner, J. T. Heiker, G Flehmig, I. Klöting, P. Kovacs, M. Matz-Soja, R Gebhardt, K. Krohn, S. Sales, K. Abshagen, A. Shevchenko, M. Stumvoll, M. Blüher, N. Klöting. 2014. *Liver-Restricted Repin1 Deficiency Improves Whole-Body Insulin Sensitivity, Alters Lipid Metabolism, and Causes Secondary Changes in Adipose Tissue in Mice*. Diabetes 63:3295-3309.
- 2015 N. Klöting, **N. Hesselbarth**, M. Gericke, A. Kunath, R. Biemann, R. Chakaroun, J. Kosacka, P. Kovacs, M. Kern, M. Stumvoll, B. Fischer, U. Rolle-Kampczyk, R. Feltens, W. Otto, D. K. Wissenbach, M. von Bergen, M. Blüher. 2015. *Di-(2-Ethylhexyl)-Phthalate (DEHP) Causes Impaired Adipocyte Function and Alters Serum Metabolites*. PLoS ONE 10(12):e0143190.

### Oral presentations

- 2013 **EAB-Meeting**, Oppurg, Germany, The Role of Repin1 in Adipose Tissue
- 2014 **EAB-Meeting**, Oppurg, Germany, The Role of Repin1 in Adipose Tissue  
**DAG-Meeting** (Deutsche Diabetis Gesellschaft), Leipzig, Germany, The Role of Repin1 in Adipose Tissue

- 2015 **invited speaker, GRK 1482**, Freising (TU Munich), Germany, Tamoxifen: how it influences adipocyte biology *in vivo*
- 2017 **invited speaker, CRC Malmö**, Lund University, Sweden, The role of Repin1 in Adipose Tissue and Tamoxifen: How it influences adipocyte biology *in vivo*  
**invited speaker, Akershus University Hospital**, Norway, The Role of Repin1 in Adipose Tissue

### Poster presentations

- 2014 **DEG-Meeting**, Dresden, Germany, The Role of Repin1 in Adipose Tissue  
**ECO-Meeting**, Sofia, Bulgaria, The Role of Repin1 in Adipose Tissue
- 2015 **Keystone Symposium** for Beige and Brown Fat in Snowbird, Utah, USA, Tamoxifen: how it influences adipocyte biology *in vivo*  
**ECO-Meeting**, Prague, Czech Republic, Tamoxifen: how it influences adipocyte biology *in vivo*  
**DAG-Meeting**, Berlin, Germany, Tamoxifen: how it influences adipocyte biology *in vivo*
- 2016 **DDG-Meeting**, Berlin, Germany, Repin1 deficiency improves insulin sensitivity and glucose metabolism in *db/db* mice by reducing adipose tissue mass and inflammation  
**DAG-Meeting**, Frankfurt am Main, Germany, Repin1 deficiency improves insulin sensitivity and glucose metabolism in *db/db* mice by reducing adipose tissue mass and inflammation

## SELBSTSTÄNDIGKEITSERKLÄRUNG

### **Erklärung über die eigenständige Abfassung der Arbeit**

Hiermit erkläre ich, Nico Hesselbarth geboren am 29.11.1984 in Leipzig, dass die vorliegende Arbeit selbstständig und ohne unzulässige Hilfe oder Benutzung anderer als der angegebenen Hilfsmittel angefertigt wurde. Ich versichere, dass Dritte von mir weder unmittelbar noch mittelbar geldwerte Leistungen für die Arbeit erhalten haben, die im Zusammenhang mit dem Inhalt der vorgelegten Dissertation stehen, und dass die vorgelegte Arbeit weder im Inland noch im Ausland in gleicher oder ähnlicher Form einer anderen Prüfungsbehörde zum Zwecke einer Promotion oder eines anderen Prüfungsverfahrens vorgelegt wurde. Alles aus anderen Quellen und von anderen Personen übernommene Material, das in der vorliegenden Arbeit verwendet wurde oder auf das direkt Bezug genommen wird, wurde als solches kenntlich gemacht. Insbesondere wurden alle Personen genannt, die direkt an der Entstehung der vorliegenden Arbeit beteiligt waren.

Leipzig, den 23.05.2017

---

Nico Hesselbarth



---

## AUTHOR CONTRIBUTIONS CHAPTER 2

---

Title Tamoxifen affects glucose and lipid metabolism parameters, causes browning of subcutaneous adipose tissue and transient body composition changes in C57BL/6NTac mice

Journal Biochemical and Biophysical Research Communications (published July 2015)

Authors Nico Hesselbarth, Chiara Pettinelli, Martin Gericke, Claudia Berger, Anne Kunath, Michael Stumvoll, Matthias Blüher, Nora Klöting

---

Nico Hesselbarth Mouse treatment and dissections  
Metabolic characterization of mice  
Cell size determination  
Western Blot of Ucp1  
Statistical analysis  
Figure preparation  
First draft of manuscript

Chiara Pettinelli Mouse dissections  
Body weight and food intake measurements  
Performed gene expression analysis  
Western Blot of Era  
Statistical analysis  
First draft of manuscript

Martin Gericke Performed histological experiments  
Contributed to discussion

Claudia Berger	Performed ELISAs Contributed to discussion
Anne Kunath	Mouse treatment Performed Echo-MRI Performed GTT and ITT
Michael Stumvoll	Contributed to discussion
Matthias Blüher	Contributed to discussion Proofreading and editing of manuscript
Nora Klötting	Conceived and designed experiments Supervision Proofreading and editing of manuscript



Nico Hesselbarth



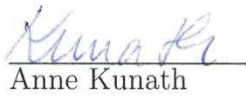
Chiara Pettinelli



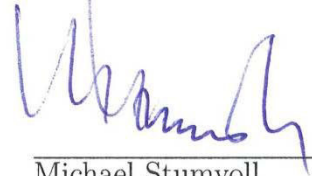
Martin Gericke



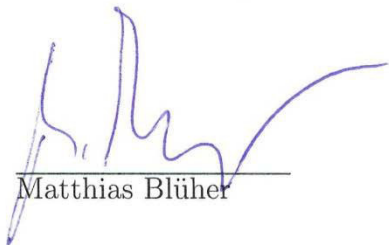
Claudia Berger



Anne Kunath



Michael Stumvoll



Matthias Blüher



Nora Klötting

---

## AUTHOR CONTRIBUTIONS CHAPTER 3

---

Title	Repin1 deficiency improves insulin sensitivity and glucose metabolism in <i>db/db</i> mice by reducing adipose tissue mass and inflammation
Journal	Biochemical and Biophysical Research Communications (published July 2016)
Authors	Anne Kunath*, Nico Hesselbarth*, Martin Gericke, Matthias Kern, Sebastian Dommel, Peter Kovacs, Michael Stumvoll, Matthias Blüher, Nora Klöting
	* these authors contributed equally to this work (first authors)

---

Anne Kunath	Mouse dissections ELISAs Performed gene expression analysis Statistical analysis Figure preparation First draft of manuscript
Nico Hesselbarth	Mouse dissections Western Blots Performed gene expression analysis Statistical analysis Figure preparation First draft of manuscript
Martin Gericke	Performed histological experiments Contributed to discussion

Matthias Kern	Performed Clamps
Sebastian Dommel	Performed Clamps
Peter Kovacs	Statistical analysis Contributed to discussion Proofreading and editing of manuscript
Michael Stumvoll	Contributed to discussion
Matthias Blüher	Contributed to discussion Proofreading and editing of manuscript
Nora Klötting	Conceived and designed experiments Supervision Proofreading and editing of manuscript

  
Anne Kunath

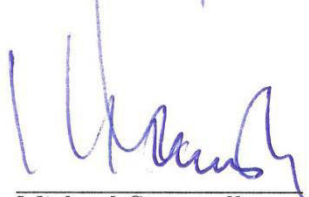
  
Nico Hesselbarth

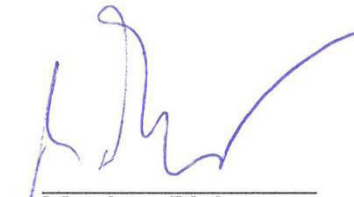
  
Martin Gericke

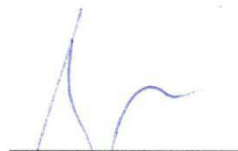
  
Matthias Kern

  
Sebastian Dommel

  
Peter Kovacs

  
Michael Stumvoll

  
Matthias Blüher

  
Nora Klötting

---

## AUTHOR CONTRIBUTIONS CHAPTER 4

---

Title	Liver-Restricted Repin1 Deficiency Improves Whole-Body Insulin Sensitivity, Alters Lipid Metabolism, and Causes Secondary Changes in Adipose Tissue in Mice
Journal	Diabetes (published October 2014)
Authors	Matthias Kern*, Joanna Kosacka*, Nico Hesselbarth, Julia Brückner, John T. Heiker, Gesine Flehmig, Ingrid Klötting, Peter Kovacs, Madlen Matz-Soja, Rolf Gebhardt, Knut Krohn, Susanne Sales, Kerstin Abshagen, Andrej Shevchenko, Michael Stumvoll, Matthias Blüher, Nora Klötting
	* these authors contributed equally to this work (senior authorship)

---

Matthias Kern	Mouse dissections Metabolic characterization of mice Performed Clamps Cell size determination Gene expression analysis
Joanna Kosacka	Immunohistochemistry Histology Statistical analysis Figure preparation

---

Nico Hesselbarth	Performed Western Blots <i>In vivo</i> lipogenesis in liver Palmitat uptake into adipocytes Statistical analysis Figure preparation
Julia Brückner	Liver histology
John T. Heiker	Performed Western Blots Contributed to discussion
Gesine Flehmig	ELISAs
Ingrid Klötting	Contributed to discussion
Peter Kovacs	Statistical analysis Contributed to discussion
Madlen Matz-Soja	Primary hepatocyte isolation Contributed to discussion
Rolf Gebhardt	Contributed to discussion
Knut Krohn	Gene chip analysis Statistical analysis Contributed to discussion
Susanne Sales	Liver lipidomics Statistical analysis Contributed to discussion



Kerstin Abshagen	Liver histology Inflammosome of liver
Andrej Shevchenko	Liver lipidomics Contributed to discussion
Michael Stumvoll	Contributed to discussion
Matthias Blüher	Contributed to discussion Proofreading and editing of manuscript
Nora Klötting	Conceived and designed experiments Supervision First draft of manuscript Proofreading and editing of manuscript

  
Matthias Kern

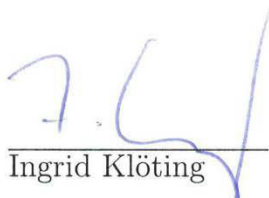
  
Joanna Kosacka

  
Nico Hesselbarth

  
Julia Brückner

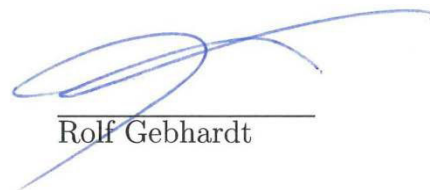
\_\_\_\_\_  
John T. Heiker

  
Gesine Flehmig

  
Ingrid Klötting

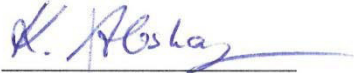
  
Peter Kovacs

  
Madlen Matz-Soja

  
Rolf Gebhardt

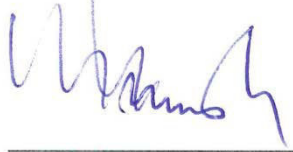
  
Knut Krohn

\_\_\_\_\_  
Susanne Sales



Kerstin Abshagen

Andrej Shevchenko



Michael Stumvoll



Matthias Blüher



Nora Klötting

**Fehlender Nachweis über Anteil einer Co-Autorenschaft**

Hiermit bestätige ich, dass die ausgewiesenen Anteile von Frau Susanne Sales und Herr Andrej Shevchenko in der Publikation "Liver-Restricted Repin1 Deficiency Improves Whole-Body Insulin Sensitivity, Alters Lipid Metabolism, and Causes Secondary Changes in Adipose Tissue in Mice" korrekt sind.

---

Prof. Dr. Annette Beck-Sickinger

---

Nico Hesselbarth

---

## AUTHOR CONTRIBUTIONS CHAPTER 5

---

Title            Repin1 Deficiency in Adipose Tissue Improves Whole-body  
                  Insulin Sensitivity, and Lipid Metabolism

Journal        International Journal of Obesity (submitted February 2017)

Authors        Nico Hesselbarth, Anne Kunath, Matthias Kern, Martin  
                  Gericke, Niklas Mejhert, Mikael Rydén, Michael Stumvoll,  
                  Matthias Blüher, Nora Klöting

---


Nico Hesselbarth	Mouse dissections Metabolic characterization of mice ELISAs Gene expression analysis Western Blots Statistical analysis Figure preparation First draft of manuscript Editing of manuscript
Anne Kunath	Glucose and Insulin tolerance tests Contributed to discussion
Matthias Kern	Mouse dissections Metabolic characterization of mice Performed Clamps
Martin Gericke	Histology Adipocyte size distribution Contributed to discussion

---

Niklas Mejhert	Glycerol release of human adipocytes
Mikael Rydén	Glycerol release of human adipocytes Contributed to discussion
Michael Stumvoll	Contributed to discussion
Matthias Blüher	Contributed to discussion Proofreading of manuscript
Nora Klöting	Conceived and designed experiments Supervision Proofreading of manuscript

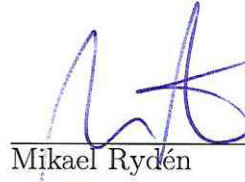
  
Nico Hesselbarth

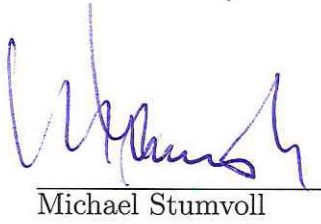
  
Anne Kunath

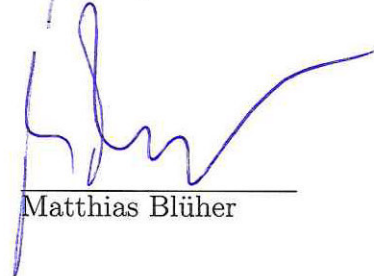
  
Matthias Kern

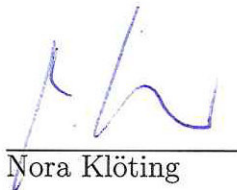
  
Martin Gericke

  
Niklas Mejhert

  
Mikael Rydén

  
Michael Stumvoll

  
Matthias Blüher

  
Nora Klötting

## ACKNOWLEDGEMENT

I am grateful to Professor Dr. Annette Beck-Sickinger for acting as a referee on my PhD thesis.

I am grateful to Professor Dr. Joachim Spranger for acting as a second referee on my PhD thesis.

Furthermore, I am heartily thankful to my supervisors, PD Dr. Nora Klötting and Prof. Dr. Matthias Blüher, who provided me an opportunity to join their team as intern, and who gave access to the laboratory and research facilities. Without their precious support it would not be possible to conduct this research.

Besides my supervisors my sincere thanks goes to the, at least for me, most important person in the lab, Viola Döbel, whose guidance and support from the initial to the final level of my thesis enabled me to develop an understanding of all the lab work. You not only saved my life during lab work, you also made me enjoying time in between such as all the stimulating discussions during lunch break or even after work. A big part of this thesis would never been done without you. Thank you so much!

I also want to thank all the animal keepers, especially Eva Böge, whose diligence and serenity to handle the mice made the projects possible and successful.

In addition I would like to thank the whole work group for the good working atmosphere.

Special thanks goes to all my mates from the office, especially to Gesine, Nicole and Claudi, who developed even beside office times to good friends. It was always a great atmosphere working with you guys in the same room, even if sometimes there was less working and more talking.



Also, very important to mention are Eileen Bösenberg and Susanne Renno, who helped me out to overcome technical or administrative barriers.

Further, I want to thank all the other guys from the basement (Annett, Jule, Suse and Kerstin) and top floor (Maria and Kerstin), who helped me out, not only with laboratory material, but also contributed to endless discussions and good evenings/nights during summer school and other events.

Finally for the research stuff, I want to thank John for getting me on the road with Western Blot analysis and further discussions on either conferences or beyond. Mo for proofreading my thesis and the support he gave me. Your words and opinion after reading meant a lot to me. Thank you very much! My good friend, Gekke, who supported me with all the histological parts, contributed to discussions of work related and not related topics. In football I would never say this, but for science you always serve as a good example for me!

I further would like to thank all my friends and family for supporting me throughout all my studies at University and PhD thesis. Without you this time would not even half of the fun it has been. My sincerest thanks to all those guys who caught me during my tough time, for endless conversations and for distracting my thoughts.

Last but not least I owe a depth of gratitude to my mother. Without her care, support, guidance and encouragement in raising me, I would never been able to reach this goal. She always made things possible for me, even despite her severe illness she gave me so much moral support. Unfortunately, she can't read this words any more, but I still want to say, thank you for everything. I will always love you and keep you in my mind! This work is dedicated to you!